SYNTHESIS OF IMIDAZOPYRIDAZINE AND PYRAZOLOPYRIMIDINE DERIVATIVES AS POTENTIAL INHIBITORS OF *PLASMODIUM* KINASES PI4K AND PKG

BY

MABATAMELA LEBOGANG FRANS

A RESEARCH DISSERTATION SUBMITTED TO THE DEPARTMENT OF CHEMISTRY, SCHOOL OF PHYSICAL AND MINERAL SCIENCES, FACULTY OF SCIENCE AND AGRICULTURE, UNIVERSITY OF LIMPOPO, SOUTH AFRICA, IN COMPLETION OF THE REQUIREMENTS FOR THE DEGREE, MASTER OF SCIENCE.

SUPERVISOR: PROF W NXUMALO

CO-SUPERVISOR: DR TC LEBOHO

2023

DECLARATION

I declare that the dissertation "Synthesis of imidazopyridazine and pyrazolopyrimidine derivatives as potential inhibitors of *Plasmodium* kinases PI4K and PKG" is a product of my own initiative and is being submitted to the University of Limpopo for the Master of Science degree. It has not been submitted to any other university for consideration for a degree or examination, and all sources I have utilized or quoted have been acknowledged with full citations.

26 September 2023

…… ……

Mr Mabatamela LF Date

DEDICATION

The dissertation is dedicated to my family at large.

Mother:

Khekulana Rahab Mabatamela,

Grandparents:

Edward (Late) and Sarah Mabatamela

My siblings:

Samuel and Anna Mabatamela

My daughter:

Sefako Ditebogo

And

Friends at large.

ACKNOWLEDGEMENTS

I would like to thank God for the gift of life and good health throughout this project and to express my sincere gratitude and appreciation to:

1. My supervisor, Prof W Nxumalo for all his guidance throughout the project and during the writing of this report.
2. My co-supervisor, Dr TC Leboho for all his inputs throughout the project and his guidance during the writing of this report.
3. My mentors, LA Raphoko and D Mambwe for their guidance, inputs, and patience.
4. Ms Ramakadi for helping with NMR analysis.
5. The head of the department of Chemistry, Prof RM Mampa.
6. My lab partners, Ursula Ralepelle, Terrine Mokoena, Kerryn Maluleke and other organic chemistry members for making the lab environment friendly and for sharing their knowledge and skills in Chemistry throughout.
7. Koketso Ramoroka for her motivation and support.
8. University of Limpopo and the Department of Chemistry for granting me an opportunity to study with them.
9. University of Cape Town for support.
10. Holistic Drug Discovery and Development (H3D) centre for support and performing the biological assays for my compounds.
11. National Institute of Health (NIH) for financial support.

SCIENTIFIC CONTRIBUTION

Introduction to Drug Discovery workshop

Venue: Western Cape, Cape Town, South Africa

Date: 24-26 October 2021

Conference attended.

Oral presentation.

12th Faculty of Science and Agriculture Postgraduate Research Day, University of Limpopo.

Venue: Limpopo, Polokwane, South Africa

Date: 21-23 September 2022

Synthesis of imidazopyridazine and pyrazolopyrimidine derivatives as potential inhibitors of *plasmodium* kinases PI4K and PKG

Lebogang Mabatamela [1], Winston Nxumalo[1], Tlabo Leboho[1]
[1]*University of Limpopo, Department of Chemistry, Private Bag X1106, Sovenga 0727*
e-mail address: lebogangmabatamela0@gmail.com

Malaria is a disease that is caused by various *Plasmodium* species, with *Plasmodium falciparum* and *vivax* being the most prevalent. The disease is usually most severe in pregnant women and children under the age of five. Emergence of resistance towards previously effective anti-malarial drugs, has resulted in an urgent need for the development of new drugs with new modes of action. A series of imidizopyridazine and pyrazolopyrimidine derivatives have been reported to be potent against *Plasmodium falciparum*. We report on the synthesis of a new library of imidazopyridazine and pyrazolopyrimidine derivatives, with substituents at 3- and 6- positions and 3- and 5- positions respectively, and their activity against *Plasmodium falciparum* through the inhibition of *Plasmodium* phosphatidylinositoil 4-kinase (PI4K) and cGMP-dependent protein kinase (PKG). A library of Imidazopyridazine and pyrazolopyrimidine derivatives were synthesized starting with the iodination of either 6-chloroimidazo[1,2-b]pyridazine or 5-chloropyrazolo[1,5-a]pyrimidine at the 3-position, followed by two successive Suzuki cross coupling reactions, firstly at 3-position of each scaffold, then on the 6- and 5- positions of imidazopyridazine and pyrazolopyrimidine respectively. A total of 25 compounds were synthesized with yields ranging from 30-70%. Characterization was done using NMR and HPLC-MS, and the compounds were submitted for antimalarial biological assays.

Keywords: Malaria, Imidazopyridazine, pyrazolopyrimidine

Poster presentation

H3D symposium "A spectrum of Opportunities in Infectious Disease Drug Discovery to Enhance Global Health."

Venue: Western Cape, Stellenbosch, South Africa

Date: 25-28 October 2022

H3D
PIONEERING WORLD-CLASS DRUG DISCOVERY IN AFRICA

Registration file number: 585
Lebogang Mabatamela
University of Limpopo
South Africa

Dear Lebogang Mabatamela

We appreciate your interest in the H3D 2022 Symposium "A Spectrum of Opportunities in Infectious Disease Drug Discovery to Enhance Global Health" taking place 25 – 28 October 2022 and thank you for submitting your abstract (listed below).

Title	SYNTHESIS OF IMIDAZOPYRIDAZINE AND PYRAZOLOPYRIDINE DERIVATIVES AS POTENTIAL INHIBITORS OF PLASMODIUM KINASES PI4K AND PKG
Paper Number	307

Your abstract has been reviewed by the scientific committee and we are pleased to inform you that it has been selected for **poster presentation**.

Table of Contents

LIST OF ABBREVIATIONS

A

ACT	Artemisinin Combination Therapy
ADME	Absorption, Distribution, Metabolism and Excretion

B

brs	Broad Singlet

C

CLogP	Calculated Logarithm of n-octanol/water partition coefficient.
δ	Chemical shift
CDCl3	Chloroform-d
CQ	Chloroquine

D

℃	Degree Celsius
DMSO-d_6	Deuterated Dimethyl sulfoxide
DCM	Dichloromethane
DMAP	4-Dimethylamino pyridine
DMF	*N,N*-Dimethylformamide
d	Doublet
dd	Doublet of doublets

E

EtOH	Ethanol
EtOAc	Ethyl acetate
Eq.	Equivalence

Et_3N	Triethylamine
G	
g	Gram
H	
H3D	Holistic Drug Discovery and Development Centre
Hz	Hertz
HRMS	High Resolution Mass Spectrometry
H_2O	Water
I	
IC_{50}	Half Maximal Inhibitory Concentration
J	
J	Coupling constant
K	
K_2CO_3	Potassium carbonate
M	
MeOD	Deuterated methanol
m/z	Mass-to-charge ratio
MHz	Megahertz
Mp.	Melting point
MeOH	Methanol
mg	Milli-gram
mL	Milli-liters
mmol	Millimole

min	Minutes
m	Multiplet

N

$NaHCO_3$	Sodium hydrogen carbonate
Na_2SO_4	Sodium sulfate
N_2	Nitrogen molecule
NMR	Nuclear magnetic resonance

P

PKG	cyclic guanidine monophosphate (cGMP)-dependent protein kinase
PI4K	phosphatidylinositol-4-kinase
%	Percentage
$PdCl_2(PPh3)_2$	Bis(triphenylphosphine)palladium(II) dichloride

R

Rf	Retention Factor

T

TACT	Triple Artemisinin Combination Therapy
t	Triplet

W

WHO	World Health Organization

ABSTRACT

Malaria is a disease that is caused by various *Plasmodium* species, with *Plasmodium falciparum* and *vivax* being the most prevalent. The disease is usually mostly severe in pregnant women and children under the age of five. The 2020 World Malaria Report from WHO estimated 241 million new malaria cases and 627000 malaria deaths globally. In comparison to 2019, there has been an increase of approximately 14 million new cases and 69000 deaths. Approximately 47000 of these additional deaths were caused by interruptions in malaria diagnosis, prevention, and treatment during the COVID-19 pandemic. Emergence of resistance towards previously effective anti-malarial drugs, has resulted in an urgent need for the development of new drugs with new modes of action.

A series of imidazopyridazine and pyrazolopyrimidine derivatives have been reported to be potent against sensitive (NF54) strain of the human malaria parasite *Plasmodium falciparum*. In this study we focused on synthesizing a new library of imidazopyridazine and pyrazolopyrimidine derivatives, with substituents at 3- & 6- positions and 3- & 5- positions respectively. The compounds were successfully synthesized and characterized by NMR and HRMS. The imidazopyridazine derivatives percentage yields ranged from 38% to 70%, whereas the percentage yields for the pyrazolopyrimidine derivatives ranged from 41% to 75%. All the imidazopyridazine compounds were evaluated for their *in vitro* antiplasmodial activities against NF54 strain and inhibitory activity against *Plasmodium falciparum* cGMP-dependent protein kinase (*Pf*PKG) and *Plasmodium vivax* phosphatidylinositoil 4-kinase type III beta (*Pv*PI4Kβ). The pyrazolopyrimidine compounds were only evaluated for their *in vitro* antiplasmodial activity against the NF54 strain.

Imidazopyridazine compounds **20B**, **20D**, **20E**, **20F**, **20M** and **20O** demonstrated *in vitro* antiplasmodial activity of below 6 μM against NF54 strain, which was used as a cutoff to determine good activity versus moderate activity. Imidazopyridazine compounds **20A**, **20C**, **20G**, **20H**, **20I**, **20J**, **20K**, **20L** and **20N** demonstrated a moderate activity of greater than 6 μM against NF54 strain. Imidazopyridazine compounds **20H**, **20K**, **20L and 20N** demonstrated good activity against both *Pf*PKG and *Pv*PI4Kβ with IC_{50} values ranging from 0.96 μM to 5.04 μM and 0.006 μM to 0.071 μM, respectively. Imidazopyridazine

compounds **20A**, **20B**, **20C**, **20D**, **20E**, **20F**, **20G**, **20I**, **20J**, **20M** and **20O** demonstrated moderate activity of greater than 10 μM against *Pf*PKG and good activity against *Pv*PI4Kβ with IC_{50} values ranging from 0.006 μM to 0.643 μM.

From the pyrazolopyrimidine scaffold, compounds **39A** (0.013 μM) and **39E** (0.009 μM) demonstrated the highest activities against the NF54 strain. The reduction of the pyrazolopyrimidine scaffold did not improve the potency, as it was seen with compounds **39A** (0.013 μM) reduced to **40A** (0.197 μM), compound **39B** (0.190 μM) reduced to **40B** (1.056 μM) and compound **39C** (1.504 μM) reduced to **40C** (2.113 μM). 3-(Methylsulfonyl) phenyl was a better substituent to have on the left-hand side of the pyrazolopyrimidine core scaffold than 4-(methylsulfonyl) phenyl substituent. Pyrazolopyrimidine compounds demonstrated very good *in vitro* antiplasmodial activity against the sensitive (NF54) strain as compared to the imidazopyridazine compounds. Therefore, pyrazolopyrimidine is a better scaffold to explore to eradicate malaria. Compounds **38A**, **38A**, **39B**, **39D** and **39E** have a selectivity index of more than 100, therefore they will be progressed further for solubility, chemical stability, microsomal stability (m,r,h) and *in vitro Pf*K1, Dd2 assays.

CHAPTER 1: LITERATURE REVIEW

1.1. MALARIA

Malaria is a very dangerous and fatal disease that is caused by a *Plasmodium* parasite that a mosquito carries [1]. The *Plasmodium* species which cause the disease are *P. falciparum, P. vivax, P. malariae, P. ovale and P. knowlesi* [2]. Among the five *Plasmodium* species that cause malaria, the *Plasmodium falciparum* is the most prevalent cause of malaria and the deadliest species [3], and it was responsible for about 500 thousand deaths in 2018 and over 220 million clinical cases, with pregnant women and young children under the age of five being the most affected. *Plasmodium vivax* is the next prevalent cause of malaria, and it was responsible for 64% of malaria cases in the Americas and 30% of the cases in Southeast Asia [4]. The World Health Organization (WHO) 2019 report has recorded above 90% malaria cases in Sub-Saharan Africa alone [5].

The 2020 World Malaria Report from WHO estimated 241 million new malaria cases and 627,000 malaria deaths globally. In comparison to 2019, there has been an increase of approximately 14 million new cases and 69,000 deaths. The interruptions in malaria diagnosis, prevention, and treatment during the COVID-19 pandemic have resulted in approximately 47,000 of these additional deaths [6]. Symptoms of malaria are usually not specific and commonly include high fever, shaking chills, headache, cough, back pain, weakness, malaise, gastrointestinal distress (vomiting, diarrhea, nausea), flu-like illness, neurologic complaints (coma, confusion, dizziness, disorientation) and complications that can lead to death [7]. Fortunately, indoor spraying with insecticides, the use of insecticide-impregnated bed-nets, appropriate drug therapies, vaccines, and global health investments have reduced the mortality rate of malaria by more than 60% between 2000 and 2016 [8].

Resistance to mostly used anti-malarial drugs, most notably chloroquine **1**, mefloquine **2**, and quinine **3**, has been observed in *P. falciparum*, the most dangerous parasite species. Resistance is a problem mostly in Africa and Southeast Asia. For example, chloroquine's treatment failure rates of 70%–80% have been stated, which was previously the most affordable and widely accessible anti-malarial drug [9].

Monotherapy is no longer utilized to treat malaria since *Plasmodium falciparum* has a high level of parasite resistance to most medications. Thus, the World Health Organization (WHO) recommends the use of artemisinin-based combination therapies (ACTs) [10], which are based on the concurrent use of medications with several mechanisms of action to avoid recurrence and delay the emergence of parasite resistance [11]. Despite the efforts that people take to control or prevent malaria, parasite resistance to antimalarial drugs and mosquito resistance to insecticides, has resulted in urgent need for the development and synthesis of new antimalarial drugs with the new mechanism of action [12].

1.1.1. *Plasmodium* life cycle

Malarial Infection commences when an infected female anopheles mosquito injects *Plasmodium* sporozoite when it bites a human being, where they reach the blood stream. The sporozoite will then travel to the liver within 10-15 minutes via blood and take up residence in the liver cells and infect hepatocytes [13]. In the liver, the sporozoites multiply asexually and become merozoites which are collectively known as schizont. The liver cells will then burst, releasing merozoites into the bloodstream. Following erythrocytes invasion, merozoites transform into rings, trophozoites and schizonts, each of which release up to 32 merozoites [8].

Clinical malarial symptoms result after this asexual blood phase. A certain portion of the merozoites develop into gametocytes, which can reach a mosquito after a period of maturation which lasts for 10 days following a blood meal [8]. Once in the mosquito, the gametocytes develop into male and female gametes which will in turn fuse to form a zygote, the zygote will then form an ookinete and finally the oocyst. Multiple asexual replications take place in the oocyst with sporozoites until the oocyst ruptures and releases the sporozoites into the salivary glands of the mosquito, which will in turn be transmitted to the human host during another blood meal, hence completing the cycle as shown in **Figure 1** [14] [15].

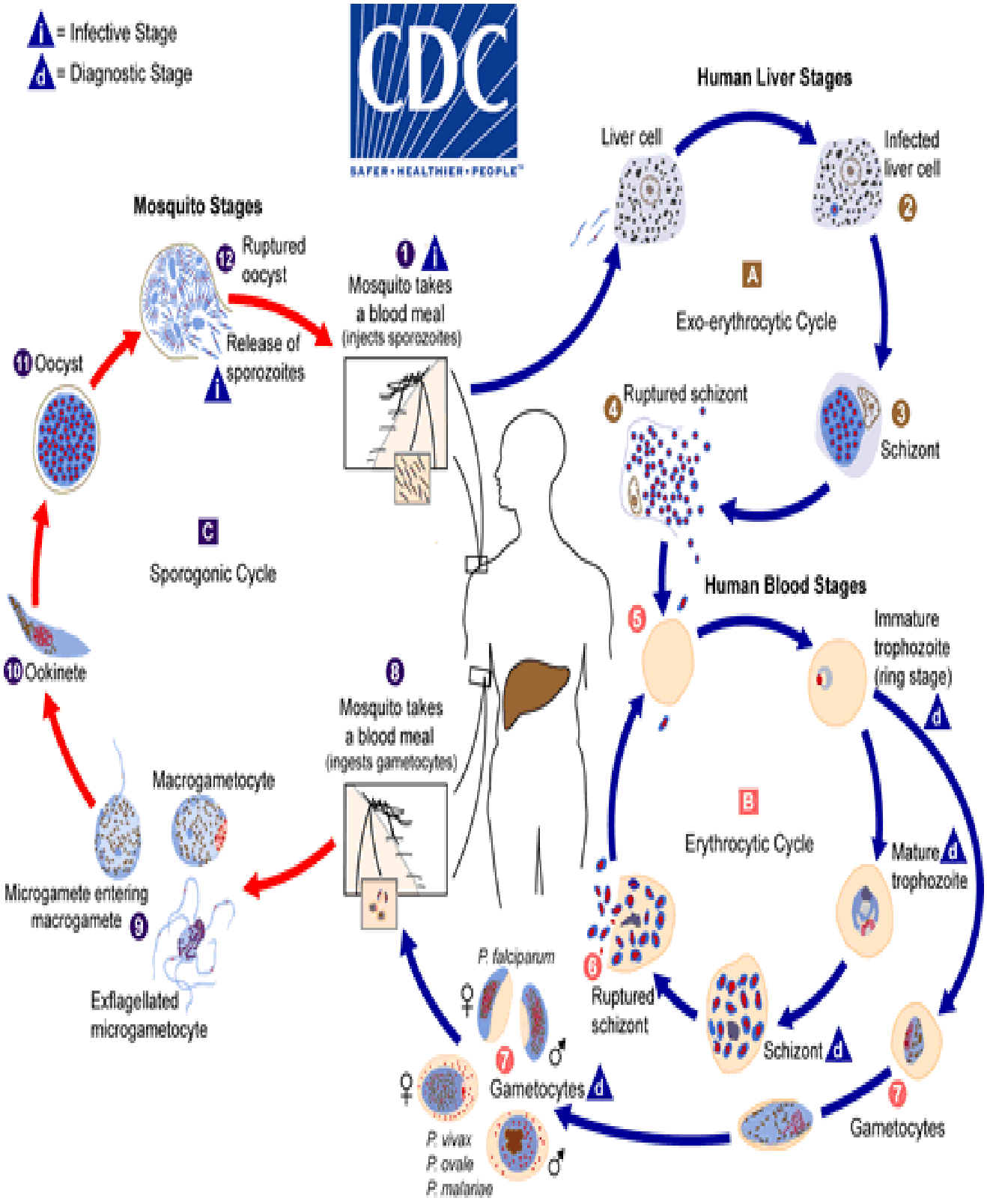

Figure 1: The *Plasmodium* life cycle [14] [15].

1.2. THERAPY

Malaria is a serious, potentially fatal disease that should be treated as soon as possible, more especially when caused by *Plasmodium falciparum*. Malaria treatment should ideally not begin until the diagnosis has been confirmed with laboratory assay results. Once malaria has been diagnosed, appropriate antimalarial treatment must be started immediately [15]. The patient's clinical status, the type of *Plasmodium* species causing infection, the area in which the infection was acquired, pregnancy status, the age of a patient, drug resistance status, and the patient's history of drug allergies are used to determine the drug regime used to treat patients with malaria [16]. Centers for Disease Control and Prevention (CDC) recommends the use of chemoprophylaxis, which involve antimalarial medications, that are taken before, during and after travel to an area or country affected with malaria [16].

Plasmodium drug resistance has emerged, and it is growing worldwide, more especially in endemic areas. Resistance to atovaquone **4**, proguanil **5**, mefloquine **2** and combination therapy with artemisinin has been reported in addition to quinine **3** and chloroquine **1** (**Figure 2**), which were previously effective antimalarial drugs [6]. The two most important aspects of malaria control and elimination are early diagnosis and timely treatment with effective antimalarial drugs [17]. Various antimalarial drugs have been used to treat and control malarial. Here we will discuss the classification of antimalarials based on their anti-plasmodial activity on the *Plasmodium* lifecycle and chemical structure. We will also discuss artemisinin-based combination therapies (ACTs) which are currently recommended by the World Health Organization (WHO).

1.2.1. Classification of antimalarial drugs

1.2.1.1. Classification of antimalarial agents according to their anti-plasmodial activity.

Antimalarial drugs are categorized into gametocidal, blood schizonticides, prophylaxis, sporontocides and tissue schizonticides with respect to their anti-plasmodial activity as shown on **Figure 2** [18].

Gametocidal are used to prevent the spread of malaria from an infected person to an uninfected female Anopheles mosquito. They kill the parasite's female and male

gametocytes in the blood stage of the malaria parasite lifecycle. Artemisinin **6** and chloroquine **1** are two examples of gametocidal.

Blood schizonticides are administered to disrupt asexual red blood cell forms of *Plasmodium* parasites and cease early malaria symptoms. Halofantrine **7**, sulfadoxine **8**, mefloquine **2**, and quinine **3 (Figure 2)** are examples of blood schizonticides.

Prophylactic antimalarial bioactives are used to prevent malaria infections in people traveling from nonmalaria countries to malaria-endemic countries, particularly those with weakened immune systems. Pyrimethamine **9**, proguanil **5**, and primaquine **10 (Figure 2)** are examples of preventative medications.

Sporontocidal antimalarial drugs prevent the development of oocytes in Plasmodium parasites during the mosquito stage of the *Plasmodium* life cycle, thereby preventing disease transmission. Primaquine **10** and pyrimethamine **9** are examples of sporontocidal drugs.

Tissue schizonticides are used to avoid the relapse of *P. ovale* and *P. vivax* parasites caused by hypnozoites in the *Plasmodium* life cycle's liver stage. Tissue schizonticides include pyrimethamine **9** and primaquine **10**.

1.2.1.2. Classification of antimalarial drugs according to their chemical structure

Classes of antimalarials are categorized based on their chemical structure as shown on **Figure 2**. They are categorized into 4-aminoquinolines (amodiaquine **11** and chloroquine **1**), hydroxynaphthoquinones (atovaquone **4**), sulfonamides (sulfadoxine **8**), diaminopyrimidines (pyrimethamine **9**), 8-aminoquinolines (primaquine **10**), biguanides (proguanil **5** and chloroproguanil **14**), 4-quinolinemethanols (mefloquine **2**), artemisinin derivatives (Artemether **12a** and artesunate **12b**) and quinoline-based cinchona alkaloids (quinine **3** and quinidine **13**) [18].

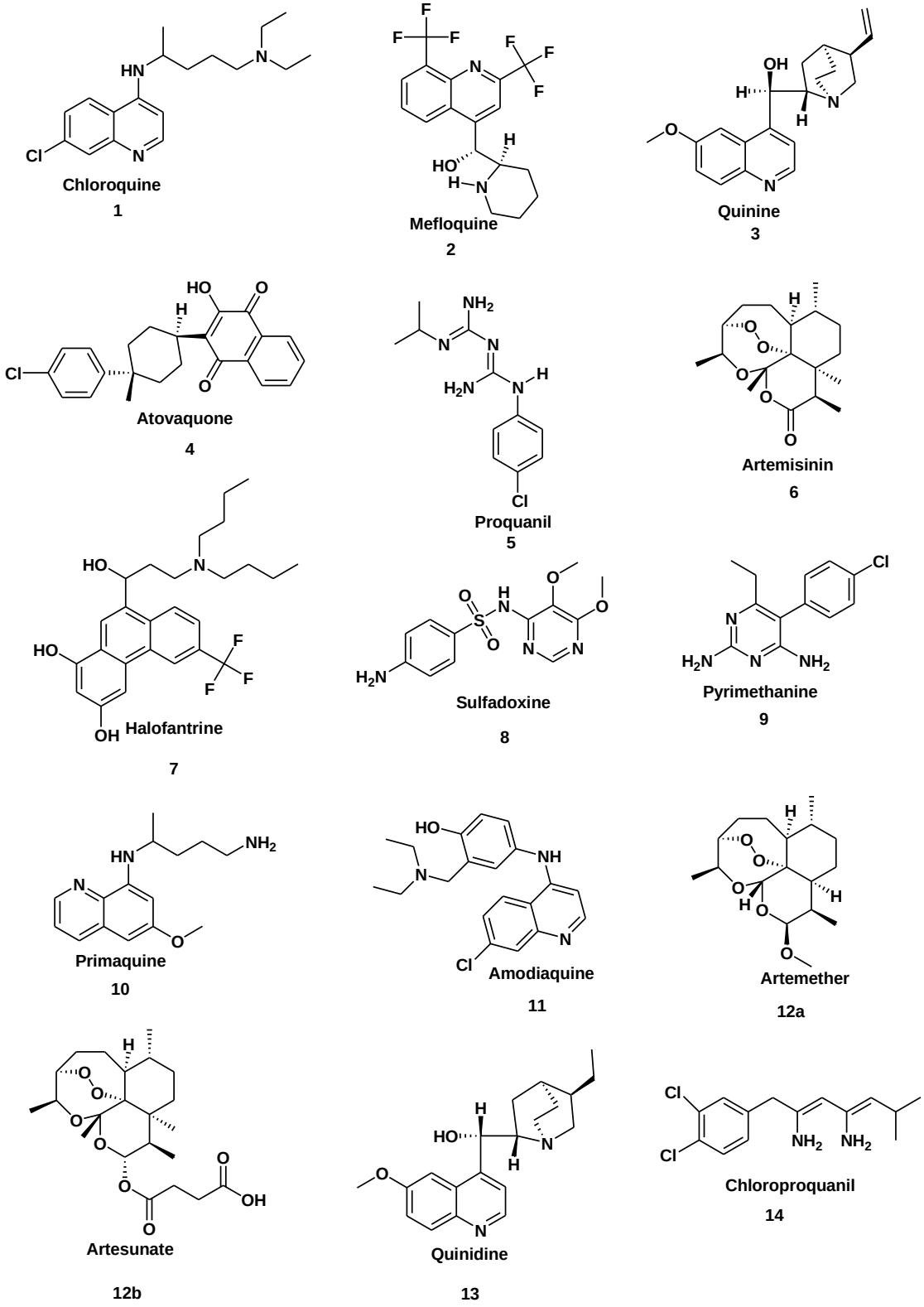

Figure 2: Anti-malarial agents classified based on their anti-plasmodial activity and chemical structure.

1.2.2. Artemisinin

Artemisinin **6**, also known as sweet wormwood, is an antimalarial drug derived from the plant *Artemisia annua L* [19]. The semi-synthetic derivatives of artemisinin are artemether, artesunate and dihydroartemisinin and are potent drugs recognized for their ability to rapidly decrease the number of *Plasmodium* parasites in the blood of malaria patients [20]. Professor Tu Youyou made the discovery in 1972, for which she was awarded the Nobel Prize in Physiology or Medicine in the year 2015 for her contribution to artemisinin extraction, purification, and testing [21]. Artemisinin has been used in traditional Chinese medicine as an antimalarial treatment and to reduce fever, among other things, and this led to Professor Tu Youyou's discovery [22].

The synthesis process of artemisinin is complicated and costly, and the compound's primary commercial source remains the extraction, isolation, and purification of *Artemisia annua* leaves [21]. Artemisinins are unique in that they clear parasitemia faster than any other antimalarial, including quinine. Their effectiveness can be attributed to the fact that these substances target both the early and late erythrocytic parasite stages, in contrast to most antimalarial medications. They enable the parasites to be taken out of the host's red blood cells, thus, eliminating them from blood circulation and avoiding these parasite stages from growing and sequestering in the vessels [20].

1.2.2.1. Artemisinin-based Combination Therapies (ACTs)

The World Health Organization (WHO) recommends that malaria be diagnosed using microscopic or biochemical tests before beginning treatment. In 2016, approximately 409 million ACT treatment courses were administered. ACTs were administered to 70% of the patients [4]. In most endemic countries, ACT which combines artemisinin or its derivatives with other antimalarial drugs which are referred to as partner drugs, is currently used as first and second line treatment for uncomplicated *Plasmodium falciparum* malaria as well as for *Plasmodium vivax* malaria resistant to chloroquine [23], [24]. Although both agents are required for the ACT to be effective, artemisinin is important for minimizing parasite biomass in the first 3 days of treatment. The companion drug then aids in the elimination (cure) of the remaining parasitic infections [25]. As a result, two agents collaborate to achieve effective clinical and parasitological cures and are thought to protect each other

from resistance development. The two agents can be administered together either as a single capsule or co-administered in separate capsules [24].

The World Health Organization (WHO) currently recommends five ACTs for children and adults with uncomplicated *falciparum* malarial from the 2015 and 2021 malaria guideline [26]: Artemether + lumefantrine (AL), artesunate + amodiaquine (ASAQ), artesunate + mefloquine (ASMQ), dihydroartemisinin + piperaquine (DP), artesunate + sulfadoxine-pyrimethamine (ASSP). Artesunate-pyronaridine (ASPY), a sixth ACT, was just added to the 2021 guideline under strict conditions [26]. The introduction of ACTs has been essential in lowering the prevalence of malaria and deaths associated with it over the past ten years, particularly in sub-Saharan Africa, which carries most of the burden of the global malaria burden. This is in addition to widespread distribution of insecticide-treated bed nets and chemoprevention in pregnant women and children [27].

1.2.2.2. Triple Artemisinin-based Combination Therapies (TACTs)

Triple Artemisinin-based Combination Therapies (TACTs) are being developed to address the growing issue of *P. falciparum* resistance to artemisinin and their partner drugs in artemisinin combination therapies (ACTs) [28]. TACTs combine approved artemisinin-based combination therapies (ACTs) with a third commonly utilized antimalarial drug, such as mefloquine and amodiaquine. The primary objective is that incorporating the artemisinin derivative with two different partner drugs that have opposing resistance mechanisms will increase the therapeutic lifetime of drug combinations, since the two partner drugs offers mutual protection against the emergence of resistance [29].

TACTs are potent, well tolerated, safe, efficacious and are available as an alternative to ACT and other antimalarial drugs. TACTs are readily accessible as a new option for uncomplicated *falciparum* malaria treatment. They could potentially improve treatment outcomes in areas like the Greater Mekong Subregion where resistance to artemisinin and partner drugs have been reported. TACTs deployment may delay the development and spread of resistance in areas where such resistance has not yet emerged [30]. The efficacy and safety of Dihydroartemisinin-piperaquine plus mefloquine and artemether-lumefantrine plus amodiaquine have been studied from seventeen sites in Asia and one

site in Africa [31]. These combinations also made use of the counteracting resistance mechanisms between piperaquine versus mefloquine and lumefantrine versus amodiaquine that were discovered in field and laboratory research. Dihydroartemisinin-piperaquine plus mefloquine was 98 percent successful in Thailand, Cambodia, and Vietnam [22].

In an area with multidrug-resistant parasites, the triple ACT artemether-lumefantrine plus amodiaquine is a well-tolerated and successful therapy for uncomplicated *Plasmodium falciparum* malaria. Adding amodiaquine to artemether-lumefantrine roughly halves the risk of reemergence, and this might be the recommended treatment in areas where artemisinin resistance exists. Artemether-lumefantrine plus amodiaquine offers an alternative first-line treatment for *Plasmodium falciparum* malaria in the Southeast of Asia, with an anticipated longer beneficial therapeutic lifetime than currently prescribed ACTs [23].

1.3. KINASES

Protein and lipid kinase are two classes of molecular drug targets that have been extensively studied in a variety of disease areas [9]. Protein kinases catalyze the phosphorylation of amino acids like tyrosine (Y), Serine (S) and Threonine (T) in protein substrates. Protein kinases play an important role in signal transduction pathways in cells [32]. Lipid phosphoinositides are universal signaling molecules that are involved in nearly every aspect of cellular function, which include cell division, growth, membrane trafficking and organelle identity of the parasite [9].

1.3.1. *Plasmodium* kinases

Plasmodium kinases have been reported as viable targets for the new antimalarial generation, due to their involvement in several critical stages in the parasite life cycle and have surfaced as promising antimalarial drug targets [1]. The two targets that have recently received a lot of attention are cyclic guanidine monophosphate (cGMP)-dependent protein kinase (PKG) [12] and phosphatidylinositol-4-kinase (PI4K) [1]. *Plasmodium* PI4K and PKG inhibitors have demonstrated the potential to block transmission and to offer liver stage protection in addition to asexual blood-stage activity. For example, MMV390048 **15**, which targets *Plasmodium* PI4K was the first *Plasmodium*

kinase inhibitor to enter clinical development for malaria treatment [33]. PI4K inhibitors include KDU691 **16** and PKG inhibitors include ML10 **17** and trisubstituted pyrimidine **18 (Figure 3**) [9].

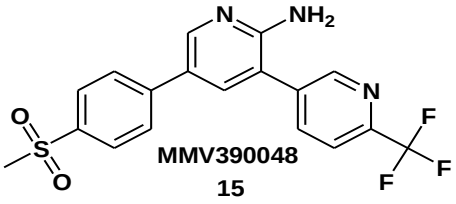

MMV390048

15

*Pv*PI4K IC_{50} = 3.4 nM
EC_{50} = 28 nM

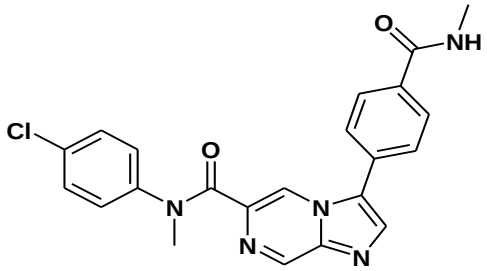

KDU691

16

*Pv*PI4K IC_{50} = 1.5 nM
EC_{50} = 50 nM

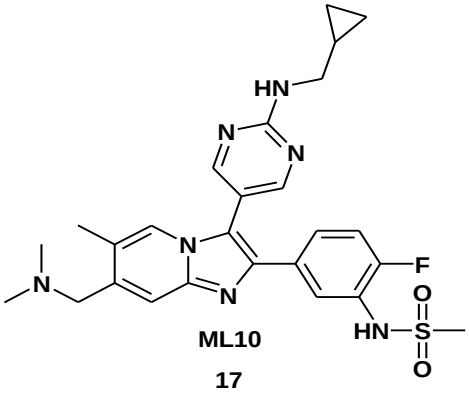

ML10

17

*Pf*PKG IC_{50} = 0.16 nM
EC_{50} = 2.1 nM

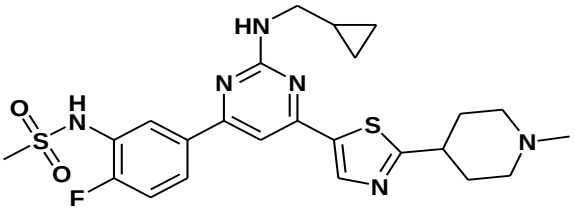

Trisubstituted pyrimidine

18

*P*fPKG IC50 = 2 nM
EC_{50} = 113 nM

Figure 3: *Plasmodium* kinases inhibitors.

1.3.1.1. PKG

PKG is a serine/threonine protein kinase that is activated by the cyclic GMP (cGMP) and has been identified as a potential chemotherapeutic target in *Plasmodium* and related parasites such as *Eimeria tenella* and *Toxoplasma gondii* [34] [35]. *Plasmodium falciparum* PKG (P*f*PKG) activities are critical in various parasite lifecycle stages, where they regulate various biological processes such as merozoite invasion and egress, the liver cell invasion, gametogenesis, ookinete motility and sporozoite motility [36].

In accordance with their activities, inhibiting P*f*PKG prevents parasite pathogenicity and development at various stages of the parasite lifecycle. When compared to human PKG (hPKG), P*f*PKG has a significant different ATP-binding pocket, which can provide selectivity. A threonine (Thr618) occupies the gatekeeper position in P*f*PKG, this threonine has a shorter side chain as compared to methionine, which occupies the same space in hPKG. Therefore, it is projected that the gatekeeper pocket next to the ATP binding pocket will be more accessible in P*f*PKG than in hPKG. Thus, *Plasmodium falciparum* PKG (P*f*PKG) inhibitors that can safely cure and/or prevent infection have been developed because of these properties [34]. A series of various compounds which inhibit *Plasmodium falciparum* PKG (P*f*PKG) as a drug target have been reported in recent years. A library of thiazoles [36], imidazo[4,5-b]pyridines [36], imidazopyridines [8], MMV030084 [37], imidazopyridazine [38] and pyrazolopyridines [11] are amongst compounds that showed potency against P*f*PKG.

1.3.1.2. Phosphoinositide lipid kinases (PIKs)

Phosphoinositide lipid kinases (PIKs) control a variety of cellular functioning including membrane trafficking, survival, and cell proliferation. Three types of phosphoinositide lipid kinases (PIKs) include phosphatidylinositol-4-kinase (PI4K), phosphatidylinositol-3-kinase (PI3K) and phosphatidylinositol phosphate kinase (PIPK) [39].

PIKs play an essential role in the cellular functioning of the parasite. Phosphatidylinositol-3-kinase (PI3K) and phosphatidylinositol-4-kinase (PI4K) are the most widely studied Phosphoinositide lipid kinases (PIKs) in *Plasmodium* species. The lipid kinases play an important role in the survival of the *Plasmodium* parasite. Phosphatidylinositol-4-kinase (PI4K) has been widely studied as a drug target in malaria research as compared to

Phosphatidylinositol-3-kinase (PI3K) and phosphatidylinositol phosphate kinase (PIPK) [40], therefore, our focus will be on PI4K as a potential drug target.

Phosphatidylinositol-4-kinase (PI4K) catalyzes the conversion of phosphatidylinositol (PI) to phosphatidylinositol-4-phosphate (PI4P). *Plasmodium* PI4K is crucial for membrane trafficking and signal transduction, and it has been established as a reliable drug target for the treatment, prevention, and eradication of malaria [1]. The 2-aminopyridine MMV390048 [1], imidazopyrazine [41], imidazopyridazine [38] and pyrazolopyridines [11] have been reported as potential *Plasmodium* PI4K inhibitors.

Recently, the Prof Chibale group reported different compounds that are known to inhibit cyclic guanidine monophosphate (cGMP)-dependent protein kinase (PKG) and Phosphatidylinositol-4-kinase (PI4K). Initially, a series of compounds based on scaffold **19** were designed, with the aryl group at the 3-position fixed as a pyridyl and variations at the 6-position introduced. Based on encouraging preliminary *in vitro* Absorption Distribution Metabolism and Excretion (ADME) data with 4-methylsulfonylphenyl substituent, this encouraged them to set 3-posititon as 4-methylsulfonylphenyl instead of 4-pyridyl as illustrated on scaffold **20,** resulting in the identification of highly potent (IC_{50} <10 nM, against multidrug resistant strain (K1) and sensitive strain (NF54)) and metabolically stable compounds **21** and **22** [2]. Compound **23** was the first compound in the imidazopyridazine series to cure mice from the *Plasmodium berghei* infection and has improved *in vivo* efficacy, solubility, and exposure as compared to compound **22** [42] (**Figure 4**).

Changes were made to the imidazopyridazine heterocycle to improve the previously reported structure activity relationship (SAR) properties, improve *in vivo* efficacy, pharmacokinetics (PK), and selectivity over the human ether-a-go-go-related gene (hERG). Other studies involving imidazopyridines and imidazolopiperazines which showed good pharmacokinetics (PK) and good *in vivo* efficacy influenced their strategy [42]. Hence, the scaffolds based on the imidazopyridazine will be explored even further in this work. The plan is to build on the scaffolds and make more derivations, introducing groups of varying polarities to check the effect of polarity and the effect of the substitution

around the ring. This study focuses on the derivations around imidazolopyridazine and pyrazolopyrimidine scaffolds.

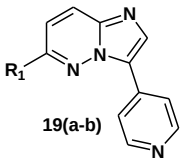

19(a-b)

19a: $R_1 = C_8H_{10}O_2$, *Pf*NF54 IC_{50} = 16 nM
*Pf*K1 IC_{50} = 14 nM
19b: $R_1 = C_7H_9NO_2S$, *Pf*NF54 IC_{50} = 16 nM
*Pf*K1 IC_{50} = 15 nM

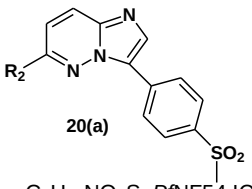

20(a)

20a: $R_2 = C_9H_{11}NO_2S$, *Pf*NF54 IC_{50} = 0.66 nM
*Pf*K1 IC_{50} = 0.58 nM

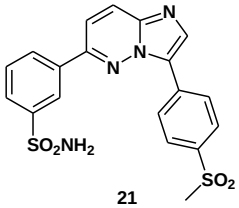

21

*Pf*NF54 IC_{50} = 4.4 nM
*Pf*K1 IC_{50} = 4.4 nM

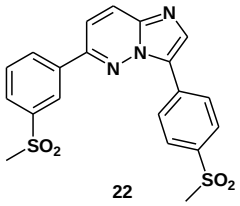

22

*Pf*NF54 IC_{50} = 7.3 nM
*Pf*K1 IC_{50} = 6.3 nM
*Pv*PI4K IC_{50} = 0.8 nM
*Pf*PKG IC_{50} = 120 nM

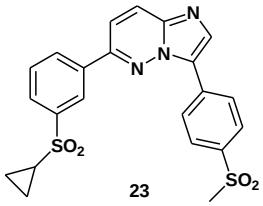

23

*Pf*NF54 IC_{50} = 1.1 nM

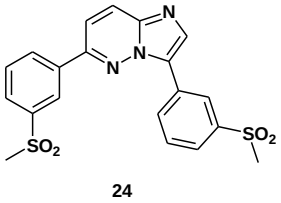

24

*Pf*NF54 IC_{50} = 31 nM

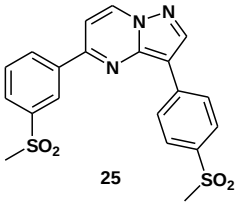

25

*Pf*NF54 IC_{50} = 2.6 nM
*Pf*K1 IC_{50} = 2.2 nM

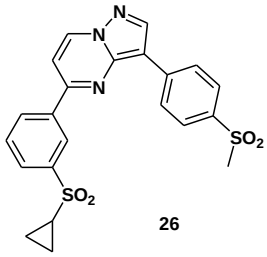

26

*Pf*NF54 IC_{50} = 0.42 nM
*Pf*K1 IC_{50} = 0.37 nM

Figure 4: Antiplasmodium compounds with their respective multidrug resistant strain (K1) and sensitive strain (NF54).

1.4. IMIDAZOPYRIDAZINES

The imidazopyridazine scaffold has been linked to a variety of pharmacological properties, including antimalarial, anticancer, antiviral, antitubercular, antisense and antidiabetic [43]. Imidazopyridazine derivatives have been reported to inhibit Mitogen-activated protein kinase interacting protein kinases (MNKs) which have recently gained interest from research institutions and pharmaceutical companies as a tumor treatment target [44]. Imidazopyridazine scaffolds have demonstrated excellent inhibition of the mammalian target of rapamycin (mTOR) which is known to promote cancer cell growth and play a role in mediating cellular functioning such as autophagy, apoptosis, and cell cycle regulation [45]. The imidazopyridazine is also known to inhibit the *Plasmodium falciparum* calcium-dependent protein kinase 1 (*Pf*CDPK1) enzyme which is recognized to play a crucial role in the *Plasmodium*'s life-cycle stages and red blood cell invasion. The inhibition of this enzyme's function is believed to be a novel mechanism for treating malaria.

Antiplasmodium imidazopyridazine compounds **24** and **25** have previously been shown to target PI4K and PKG independently [33]. Imidazo[1,2-b]pyridazine was first synthesized in the early 1960s by Yoneda and colleagues [46]. It is an essential class of imidazoazine family, which is made up of imidazole ring and pyridazine moiety fused together [47]. The Drug Discovery and Development Center (H3D) and Medicine for Malaria Venture (MMV) have designed a novel antimalarial drug lead MMV652103 **22** based on the imidazopyridazine scaffold, which showed good *in vitro* activity against sensitive (NF54) and multidrug resistance (K1) strains of *P. falciparum*. Additionally, MMV652103 **22** displayed 98 percent activity in a 4-day *in vivo Plasmodium berghei* mouse model [48].

1.5. PYRAZOLOPYRIMIDINE

Pyrazolopyrimidine is a very interesting heterocyclic motif because of its synthesis and pharmacological properties. Allopurinol, anagliptin, dinaciclib, dorsomorphin, indiplon, lorediplon, ocinaplon, pyrazophos, sildenafil, tisopurine and zaleplon are some of the drugs that contain the pyrazolopyrimidine nucleus. Pyrazolopyrimidines are cyclin-dependent kinase (CDK) inhibitors, anti-bacterial, anti-fungal, anti-leishmania, anti-

proliferative and anti-viral agents. Furthermore, pyrazolopyrimidines act as central nervous system depressants, antitrypanosomal and sedative, COX-1 and COX-2 selective inhibitors, serotonin 5-HT6 receptor antagonists, tuberculostatic and corticotrophin releasing factor (CRF) 1 receptor antagonists [49].

It is well known that heterocyclic compounds having a pyrazolopyrimidine nucleus as a pharmacophore are incredibly versatile and effective at unfolding lead molecules with pharmacological activity [50]. There are several pyrazolopyrimidine isomers known, the most important of which are 1H-pyrazolo[3,4-d]pyrimidine, 1H-pyrazolo[4,3-d]pyrimidine, and pyrazolo[1,5-a]pyrimidine. Most importantly, there is a similarity between the pyrazolopyrimidine moiety and the deoxyribonucleic acid's adenine moiety, which inspires scientists to develop diverse synthetic methodologies and assess their biological activities. All the isomers associated with pyrazolopyrimidine are biologically active in nature and are marketed as pharmaceutical agents [51].

1.6. LIPOPHILICITY

Lipophilicity is a fundamental drug phenomenon that is widely used in drug discovery to estimate pharmacokinetics and pharmacodynamics, and it is related to the solubility of the molecule and its passive passage through biological membranes [52]. The role of lipophilicity in drug action has been extensively studied, beginning with pioneering work by Overton and Meyer at the end of the nineteenth century and progressing through the work of Fieser and later Hansch [53]. The logarithm of the partition coefficient between n-octanol and water (LogP) is used to determine the Lipophilicity of the compound [52]. Lipinski's rule of five states that compounds are more likely to have poor absorption when the number of hydrogen bond donors (HBD) is greater than five, the number of hydrogen bond acceptors (HBA) is greater than ten, molecular weight is greater than 500 g/mol and the calculated n-octanol/water partition coefficient (CLogP) is greater than five [54]. High lipophilicity, on the other hand, frequently results in the formation of a compound with rapid metabolic turnover, low solubility, and poor absorption. It can also cause side effects and toxicity by promoting binding to unwanted hydrophobic protein targets [55].

1.7. AIM AND OBJECTIVES

1.7.1. Aim

The aim of the study is to synthesize new imidazopyridazine and pyrazolopyrimidine derivatives that will be tested for their antimalarial activity through the inhibition of *Pv*PI4K and *Pf*PKG.

1.7.2. Objectives

i. To synthesize a new library of imidazopyridazine derivatives, with substituents at 3- and 6-positions.

ii. To synthesize a new library of pyrazolopyrimidine derivatives, with substituents at 3- and 5-positions.

iii. To evaluate the activity of the synthesized compounds against *Plasmodium falciparum.*

iv. To investigate the inhibition of *Pv*PI4K and *Pf*PKG kinases with the synthesized compounds.

1.8. REFERENCES

[1] Kandepedu, N., Gonzàlez Cabrera, D., Eedubilli, S., Taylor, D., Brunschwig, C., Gibhard, L., Njoroge, M., Lawrence, N., Paquet, T., Eyermann, C.J., Spangenberg, T., Basarab, G.S., Street, L.J. and Chibale, K, "Identification, characterization, and optimization of 2, 8-disubstituted-1, 5-naphthyridines as novel Plasmodium falciparum phosphatidylinositol-4-kinase inhibitors with in vivo efficacy in a humanized mouse model of malaria.," *Journal of Medicinal Chemistry,* vol. 61, no. 13, pp. 5692-5703, 2018.

[2] Le Manach, C., Gonzàlez Cabrera, D., Douelle, F., Nchinda, A.T., Younis, Y., Taylor, D., Wiesner, L., White, K.L., Ryan, E., March, C., Duffy, S., Avery, V.L., Waterson, D., Witty, M.J., Wittlin, S., Charman, S.A., Street, L.J. and Chibale, K, "Medicinal chemistry optimization of antiplasmodial imidazopyridazine hits from high throughput screening of a SoftFocus kinase library: part 1.," *Journal of Medicinal Chemistry,* vol. 57, no. 6, pp. 2789-2798, 2014.

[3] Le Manach, C., Paquet, T., Gonzàlez Cabrera, D., Younis, Y., Taylor, D., Wiesner, L., Lawrence, N., Schwager, S., Waterson, D., Witty, M.J. and Wittlin, S., Street, L.J. and Chibale, K, "Medicinal chemistry optimization of antiplasmodial imidazopyridazine hits from high throughput screening of a softfocus kinase library: Part 2.," *Journal of Medicinal Chemistry,* vol. 57, no. 21, pp. 8839-8848, 2014.

[4] Nass, J. and Efferth, T, "Development of artemisinin resistance in malaria therapy," *Pharmacological Research,* vol. 146, p. 104275, 2019.

[5] Ibezim, A., Madukaife, M.S., Osigwe, S.C., Engel, N., Karuppasamy, R. and Ntie-Kang, F, "Fragment-based virtual screening discovers potential new Plasmodium PI4KIIIβ ligands," *BMC Chemistry,* vol. 16, no. 1, pp. 1-9, 2022.

[6] Gomes, A.R.Q., Cunha, N., Varela, E.L.P., Brígido, H.P.C., Vale, V.V., Dolabela, M.F., De Carvalho, E.P. and Percário, S, "Oxidative Stress in Malaria: Potential

Benefits of Antioxidant Therapy," *International Journal of Molecular Sciences,* vol. 23, no. 11, p. 5949, 2022.

[7] Paquet, T., Le Manach, C., Cabrera, D.G., Younis, Y., Henrich, P.P., Abraham, T.S., Lee, M.C., Basak, R., Ghidelli-Disse, S., Lafuente-Monasterio, M.J. and Bantscheff, M., Fidock, D.A., Waterson, D., Street, L.J. and Chibale, K, "Antimalarial efficacy of MMV390048, an inhibitor of Plasmodium phosphatidylinositol 4-kinase," *Science Translational Medicine,* vol. 9, no. 387, p. 9735, 2017.

[8] Penzo, M., de Las Heras-Dueña, L., Mata-Cantero, L., Diaz-Hernandez, B., Vazquez-Muñiz, M.J., Ghidelli-Disse, S., Drewes, G., Fernandez-Alvaro, E. and Baker, D.A, "High-throughput screening of the Plasmodium falciparum cGMP-dependent protein kinase identified a thiazole scaffold which kills erythrocytic and sexual stage parasites.," *Scientific Reports,* vol. 9, no. 1, pp. 1-13, 2019.

[9] Arendse, L.B., Wyllie, S., Chibale, K. and Gilbert, I.H, "Plasmodium kinases as potential drug targets for malaria: challenges and opportunities," *ACS Infectious Diseases,* vol. 7, no. 3, pp. 518-534, 2021.

[10] Kalkman, L.C., Hänscheid, T., Krishna, S. and Grobusch, M.P, "Fluid therapy for severe malaria," *The Lancet Infectious Diseases,* vol. 22, no. 6, pp. 160-170, 2022.

[11] CS Pinheiro, L., M. Feitosa, L., O. Gandi, M., F. Silveira, F. and Boechat, N, "The development of novel compounds against malaria: quinolines, triazolpyridines, pyrazolopyridines and pyrazolopyrimidines.," *Molecules,* vol. 24, no. 22, p. 4095, 2019.

[12] Baker, D.A., Matralis, A.N., Osborne, S.A., Large, J.M. and Penzo, M, "Targeting the malaria parasite cGMP-dependent protein kinase to develop new drugs," *Frontiers in Microbiology,* vol. 11, p. 602803, 2020.

[13] Júnior, J.C.M., Krüger, A., Palmisano, G. and Wrenger, C, "Transporter-Mediated Solutes Uptake as Drug Target in Plasmodium falciparum," *Frontiers in Pharmacology,* p. 13, 2022.

[14] Bennink, S. and Pradel, G, "Vesicle dynamics during the egress of malaria gametocytes from the red blood cell," *Molecular and Biochemical Parasitology,* vol. 243, p. 111372, 2021.

[15] [Online]. Available: https://www.cdc.gov/malaria/diagnosis_treatment/artesunate.html.

[16] Mace, K.E., Lucchi, N.W. and Tan, K.R, "Malaria Surveillance—United States,2017," *MMWR Surveillance Summaries,* vol. 70, no. 2, p. 1, 2021.

[17] Arya, A., Foko, L.P.K., Chaudhry, S., Sharma, A. and Singh, V, "Artemisinin-based combination therapy (ACT) and drug resistance molecular markers: a systematic review of clinical studies from two malaria endemic regions–India and sub-Saharan Africa," *International Journal for Parasitology: Drugs and Drug Resistance,* vol. 15, pp. 43-56, 2021.

[18] Alven, S. and Aderibigbe, B.,, "Combination therapy strategies for the treatment of malaria," *Molecules,* vol. 24, no. 19, p. 3601, 2019.

[19] Maldonado, J.H. and Grundmann, "Drug-drug Interactions of Artemisinin-based Combination Therapies in Malaria Treatment: A narrative review of the literature," *The Journal of Clinical Pharmacology,* 2022.

[20] Ouji, M., Augereau, J.M., Paloque, L. and Benoit-Vical, F, "Plasmodium falciparum resistance to artemisinin-based combination therapies: A sword of Damocles in the path toward malaria elimination," *Parasite,* vol. 25, 2018.

[21] Wu, T., Feng, H., He, M., Yue, R. and Wu, S, "Efficacy of artemisinin and its derivatives in animal models of type 2 diabetes mellitus: a systematic review and meta-analysis," *Pharmacological Research,* vol. 175, p. 105994, 2022.

[22] van der Pluijm, R.W., Amaratunga, C., Dhorda, M. and Dondorp, A.M, "Triple artemisinin-based combination therapies for malaria–a new paradigm?," *Trends in Parasitology,* vol. 37, no. 1, pp. 15-24, 2021.

[23] Peto, T.J., Tripura, R., Callery, J.J., Lek, D., Nghia, H.D.T., Nguon, C., Thuong, N.T.H., van der Pluijm, R.W., Dung, N.T.P., Sokha, M., Van Luong, V., White, N.J. and Dondorp, A.M , "Triple therapy with artemether–lumefantrine plus amodiaquine versus artemether–lumefantrine alone for artemisinin-resistant, uncomplicated falciparum malaria: an open-label, randomised, multicentre tria," *The Lancet Infectious Diseases,* 2022.

[24] Shibeshi, W., Alemkere, G., Mulu, A. and Engidawork, E, "Efficacy and safety of artemisinin-based combination therapies for the treatment of uncomplicated malaria in pediatrics: a systematic review and meta-analysis," *BMC Infectious Diseases,* vol. 21, no. 1, pp. 1-12, 2021.

[25] Nsanzabana, C, "Resistance to artemisinin combination therapies (ACTs): do not forget the partner drug!," *Tropical Medicine and Infectious Disease,* vol. 4, no. 1, p. 26, 2019.

[26] R. Clark, "Safety of Treating Malaria with Artemisinin-Based Combination Therapy in the First Trimester of Pregnancy," *Reproductive Toxicology,* 2022.

[27] van der Pluijm, R.W., Amaratunga, C., Dhorda, M. and Dondorp, A.M, "Triple artemisinin-based combination therapies for malaria–a new paradigm?," *Trends in Parasitology,* vol. 37, no. 1, pp. 15-24, 2021.

[28] van der Pluijm, R.W., Peto, T.J., Hamaluba, M., Callery, J.J., Tripura, R., White, N.J. and Dondorp, A.M, "Is triple artemisinin-based combination therapy necessary for uncomplicated malaria?," *The Lancet Infectious Diseases,* vol. 22, no. 6, pp. 765-766, 2022.

[29] de Haan, F., Boon, W.P., Amaratunga, C. and Dondorp, A.M, "Expert perspectives on the introduction of Triple Artemisinin-based Combination Therapies (TACTs) in Southeast Asia: a Delphi study," *BMC Public Health,* vol. 22, no. 1, pp. 1-14, 2022.

[30] van der Pluijm, R.W., Tripura, R., Hoglund, R.M., Phyo, A.P., Lek, D., Ul Islam, A., Anvikar, A.R., Satpathi, P., Satpathi, S., Behera, P.K., Tripura, A., White, N.J. and

Dondorp, A.M, "Triple artemisinin-based combination therapies versus artemisinin-based combination therapies for uncomplicated Plasmodium falciparum malaria: a multicentre, open-label, randomised clinical trial," *The Lancet,* vol. 395, no. 10233, pp. 1345-1360, 2020.

[31] Tindana, P., de Haan, F., Amaratunga, C., Dhorda, M., van der Pluijm, R.W., Dondorp, A.M. and Cheah, P.Y, "Deploying triple artemisinin-based combination therapy (TACT) for malaria treatment in Africa: ethical and practical considerations," *Malaria Journal,* vol. 20, no. 1, pp. 1-7, 2021.

[32] Patrick, G.L. and Turner, H, "Kinases and kinase inhibitors," in *Antimalarial agents*, Elsevier, 2020, pp. 459-494.

[33] Cheuka, P.M., Centani, L., Arendse, L.B., Fienberg, S., Wambua, L., Renga, S.S., Dziwornu, G.A., Kumar, M., Lawrence, N., Taylor, D., Wittlin, S., Coertzen, D., Reader, J., Van Der Watt, M., Birkholt, L.M. and Chibale, K , "New amidated 3, 6-diphenylated imidazopyridazines with potent antiplasmodium activity are dual inhibitors of Plasmodium phosphatidylinositol-4-kinase and cGMP-dependent protein kinase," *ACS Infectious Diseases,* vol. 7, no. 1, pp. 34-46, 2020.

[34] Eck, T., Laureano de Souza, M., Delvillar, M., Ashraf, K., Yadav Bheemanaboina, R.R., Chakrasali, R., Kreiss, T., Siekierka, J.J., Rotella, D.P., Bhanot, P. and Goodey, N.M, "Characterization of Competitive Inhibitors of Plasmodium falciparum cGMP-Dependent Protein Kinase," *ChemBioChem,* vol. 23, no. 7, p. e202100704, 2022.

[35] Baker, D.A., Stewart, L.B., Large, J.M., Bowyer, P.W., Ansell, K.H., Jiménez-Díaz, M.B., El Bakkouri, M., Birchall, K., Dechering, K.J., Bouloc, N.S., Coombs, P.J., Kettleborough, C.A. and Osborne, S.A, "A potent series targeting the malarial cGMP-dependent protein kinase clears infection and blocks transmission," *Nature Communications,* vol. 8, no. 1, pp. 1-9, 2017.

[36] Large, J.M., Birchall, K., Bouloc, N.S., Merritt, A.T., Smiljanic-Hurley, E., Tsagris, D.J., Wheldon, M.C., Ansell, K.H., Coombs, P.J., Kettleborough, C.A., Whalley, D., Steward, L.B., Bowyer, P.W., Baker, D.A. and Osborne, S.A, "Potent inhibitors of malarial P. Falciparum protein kinase G: Improving the cell activity of a series of imidazopyridines," *Bioorganic & Medicinal Chemistry Letters,* vol. 29, no. 3, pp. 509-514, 2019.

[37] Vanaerschot, M., Murithi, J.M., Pasaje, C.F.A., Ghidelli-Disse, S., Dwomoh, L., Bird, M., Spottiswoode, N., Mittal, N., Arendse, L.B., Owen, E.S. and Wicht, K.J., Niles, J.C. and Fidock, D.A, "Inhibition of resistance-refractory P. falciparum kinase PKG delivers prophylactic, blood stage, and transmission-blocking antiplasmodial activity," *Cell Chemical Biology,* vol. 27, no. 7, pp. 806-816, 2020.

[38] Green, J.L., Moon, R.W., Whalley, D., Bowyer, P.W., Wallace, C., Rochani, A., Nageshan, R.K., Howell, S.A., Grainger, M., Jones, H.M. and Ansell, K.H., Chapman, T,M., Taylor, D.L., Osborne, S.A., Baker, D.A., Tatu, U. and Holder, A.A, "Imidazopyridazine inhibitors of Plasmodium falciparum calcium-dependent protein kinase 1 also target cyclic GMP-dependent protein kinase and heat shock protein 90 to kill the parasite at different stages of intracellular development," *Antimicrobial Agents and Chemotherapy,* vol. 60, no. 3, pp. 1464-1475, 2015.

[39] Hassett, M.R. and Roepe, P.D, "PIK-ing new malaria chemotherapy," *Trends in Parasitology,* vol. 34, no. 11, pp. 925-927, 2018.

[40] Cabrera, D.G., Horatscheck, A., Wilson, C.R., Basarab, G., Eyermann, C.J. and Chibale, K, "Plasmodial kinase inhibitors: license to cure?," *Journal of Medicinal Chemistry,* vol. 61, no. 18, pp. 8061-8077, 2018.

[41] McNamara, C.W., Lee, M., Lim, C.S., Lim, S.H., Roland, J., Nagle, A., Simon, O., Yeung, B.K., Chatterjee, A.K., McCormack, S.L. and Manary, M.J, "Targeting Plasmodium PI (4) K to eliminate malaria," *Nature,* vol. 504, no. 7479, pp. 248-253, 2013.

[42] Le Manach, C., Paquet, T., Brunschwig, C., Njoroge, M., Han, Z., Gonzàlez Cabrera, D., Bashyam, S., Dhinakaran, R., Taylor, D., Reader, J., Botha, M., Ferrer, S., Angulo-Barturen, I., Street, L.J. and Chibale, K, "A novel pyrazolopyridine with in vivo activity in Plasmodium berghei-and Plasmodium falciparum-infected mouse models from structure–activity relationship studies around the core of recently identified antimalarial imidazopyridazines," *Journal of Medicinal Chemistry,* vol. 58, no. 21, pp. 8713-8722, 2015.

[43] Malik, M.S., Alsantali, R.A., Alzahrani, A.Y., Jamal, Q.M.S., Hussein, E.M., Alfaidi, K.A., Al-Rooqi, M.M., Obaid, R.J., Alsharif, M.A., Adil, S.F. and Jassas, R.S, "Multicomponent synthesis, cytotoxicity, and computational studies of novel imidazopyridazine-based N-phenylbenzamides," *Journal of Saudi Chemical Society,* vol. 26, no. 3, p. 101449, 2022.

[44] Bu, H., Yuan, X., Wu, H., Zhou, J. and Zhang, H, "Design, synthesis and biological evaluation of imidazopyridazine derivatives containing isoquinoline group as potent MNK1/2 inhibitors," *Bioorganic & Medicinal Chemistry,* vol. 40, p. 116186, 2021.

[45] Peterson, E.A., Boezio, A.A., Andrews, P.S., Boezio, C.M., Bush, T.L., Cheng, A.C., Choquette, D., Coats, J.R., Colletti, A.E., Copeland, K.W., DuPont, M., Teffera, Y., Yi, S., Cai, T. and La, D.S, "Discovery and optimization of potent and selective imidazopyridine and imidazopyridazine mTOR inhibitors," *Bioorganic & Medicinal Chemistry Letters,* vol. 22, no. 15, pp. 4967-4974, 2012.

[46] Garrido, A., Vera, G., Delaye, P.O. and Enguehard-Gueiffier, C, "Imidazo [1, 2-b] pyridazine as privileged scaffold in medicinal chemistry: An extensive review," *European Journal of Medicinal Chemistry,* vol. 226, p. 113867, 2021.

[47] El Akkaoui, A., Koubachi, J., Guillaumet, G. and El Kazzouli, S, "Synthesis and Functionalization of Imidazo [1, 2-b] Pyridazine by Means of Metal-Catalyzed Cross-Coupling Reactions," *ChemistrySelect,* vol. 6, no. 34, pp. 8985-9011, 2021.

[48] Noonan, T.J., Chibale, K., Cheuka, P.M., Kumar, M., Bourne, S.A. and Caira, M.R, "Five solid forms of a potent imidazopyridazine antimalarial drug lead: a preformulation study," *Crystal Growth & Design,* vol. 19, no. 8, pp. 4683-4697, 2019.

[49] Asati, V., Anant, A., Patel, P., Kaur, K. and Gupta, G.D, "Pyrazolopyrimidines as anticancer agents: A review on structural and target-based approaches," *European Journal of Medicinal Chemistry,* vol. 225, p. 113781, 2021.

[50] Philoppes, J.N., Khedr, M.A., Hassan, M.H., Kamel, G. and Lamie, P.F, "New pyrazolopyrimidine derivatives with anticancer activity: Design, synthesis, PIM-1 inhibition, molecular docking study and molecular dynamics," *Bioorganic Chemistry,* vol. 100, p. 103944, 2020.

[51] Rao, R.N. and Chanda, K, "An assessment study of known pyrazolopyrimidines: chemical methodology and cellular activity," *Bioorganic Chemistry,* vol. 99, p. 103801, 2020.

[52] N. Hosny, "Insights into the lipophilicity of four commonly prescribed antidiabetic drugs and their simultaneous analysis using a simple TLC-spectrodensitometric method: Application to fixed-dose combination tablets and human plasma," *Journal of Chromatography B,* vol. 1206, p. 123341, 2022.

[53] Perry, M.W., Börjesson, U., Nikitidis, A. and Tyrchan, C, "Surprising lipophilicity observations identify unexpected conformational effects," *Bioorganic & Medicinal Chemistry Letters,* vol. 69, p. 128786, 2022.

[54] Chagas, C.M., Moss, S. and Alisaraie, "Drug metabolites and their effects on the development of adverse reactions: Revisiting Lipinski's Rule of Five," *International Journal of Pharmaceutics,* vol. 549, no. 1-2, pp. 133-149, 2018.

[55] Šegan, S., Jevtić, I., Tosti, T., Penjišević, J., Šukalović, V., Kostić-Rajačić, S. and Milojković-Opsenica, D, "Determination of lipophilicity and ionization of fentanyl and its 3-substituted analogs by reversed-phase thin-layer chromatography," *Journal of Chromatography B,* vol. 1211, p. 123481, 2022.

CHAPTER 2: DESIGN, SYNTHESIS, AND CHARACTERIZATION OF IMIDAZOPYRIDAZINE AND PYRAZOLOPYRIMIDINE DERIVATIVES.

2.1. INTRODUCTION

Chapter 2 will discuss the design, synthesis, and characterization of imidazopyridazine and pyrazolopyrimidine derivatives which addresses the following objectives:

i. To synthesize a new library of imidazopyridazine derivatives, with substituents at 3- and 6-positions.
ii. To synthesize a new library of pyrazolopyrimidine derivatives, with substituents at 3- and 5-positions.
iii. To evaluate the activity of synthesized compounds against *Plasmodium falciparum.*
iv. To investigate the inhibition of *Pv*PI4K and *Pf*PKG kinases by the synthesized compounds.

The first-generation series refers to the imidazopyridazine scaffold and the second generation refers to the pyrazolopyrimidine scaffold.

2.2. DISCUSSION OF THE FIRST-GENERATION SERIES

Imidazopyridazine scaffold has been reported to be potent against the sensitive strain (NF54) and the multidrug resistant strain (K1) of the *Plasmodium falciparum* as per prior work [1], [2]. We were interested in exploring this scaffold even further by fixing 4-(methylsulfonyl) phenyl substituent on the right-hand side (3-position) and make a series of derivatives by making changes on the left-hand side (6-position). Based on the previous research [1], [2], the best substituent to have on the 3-position was 4-(methylsulfonyl) phenyl, which prompted us to expand the scope and test for activity against the *Plasmodium* kinases.

2.2.1. The synthesis of 6-chloroimidazo[1,2-b]pyridazine (29) and 6-chloro-3-iodoimidazo[1,2-b]pyridazine (30).

We initiated our investigation with the synthesis of 6-chloroimidazo[1,2-b]pyridazine **29** using the method reported by Le Manach *et.al* [1]. A commercially available 6-chloropyridazin-3-amine **27** and bromoacetaldehyde diethylacetal **28** were used to

synthesize compound **29**. Ethanol (EtOH) and water (H_2O) were combined to be used as a solvent system and hydrobromic acid (HBr) was introduced as shown on reaction **Scheme 2.1**. The reaction was left to reflux for 18 hours (hrs). Compound **29** was obtained in 70% yield in the first attempt. In the second attempt, the pH of the reaction mixture was adjusted to pH 7 and the yield improved to 96%. The compound was characterized using Proton Nuclear Magnetic Resonance (^{1}H NMR). **Figure 2.1** shows the ^{1}H NMR for compound **29 (spectrum A)**. **Spectrum A** shows that the proton peaks were observed between δ 7.10 ppm and δ 8.01 ppm and this correlates with what was expected and reported from literature [1]**.** This data confirms that the correct compound was synthesized.

Compound **29** was further iodinated on the 3-position to afford compound **30**. The resonance effect makes this position more favorable for substitution. The reaction was done using *N*-Iodosuccinimide (NIS) in *N,N*-Dimethylformamide (DMF) solvent at room temperature (25 ℃) for four days (**Scheme 2.1**). Compound **30** was obtained in 74% yield and characterized with ^{1}H NMR. Compound **30 (spectrum B)** in **Figure 2.1** shows a total of three hydrogens which comprises of two doublets (d) and one singlet (s). The two doublets resonate at δ 7.21 - δ 7.24 ppm and δ 8.05 - δ 8.08 ppm respectively, and the singlet resonates at δ 7.89 ppm. **Spectrum B** shows the disappearance of the signal peak at δ 7.95 ppm due to the iodine incorporation. It is also evident that there are fewer hydrogens in **spectrum B** as compared to **spectrum A**. There is also a shifting of chemical shifts, and the splitting pattern has changed from doublet in **spectrum A** to a singlet in **spectrum B** due to the incorporation of iodine. The data confirm the successful synthesis of compound **29** and compound **30**, and it correlates with what was expected and reported [2]**.**

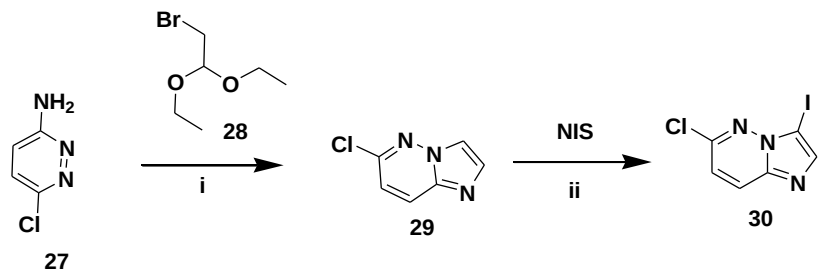

Scheme 2.1: i: **28**, EtOH, H_2O, HBr (2 eq), 18 hrs, reflux. ii: NIS (1.1 eq), DMF, 25 ℃, 4 days.

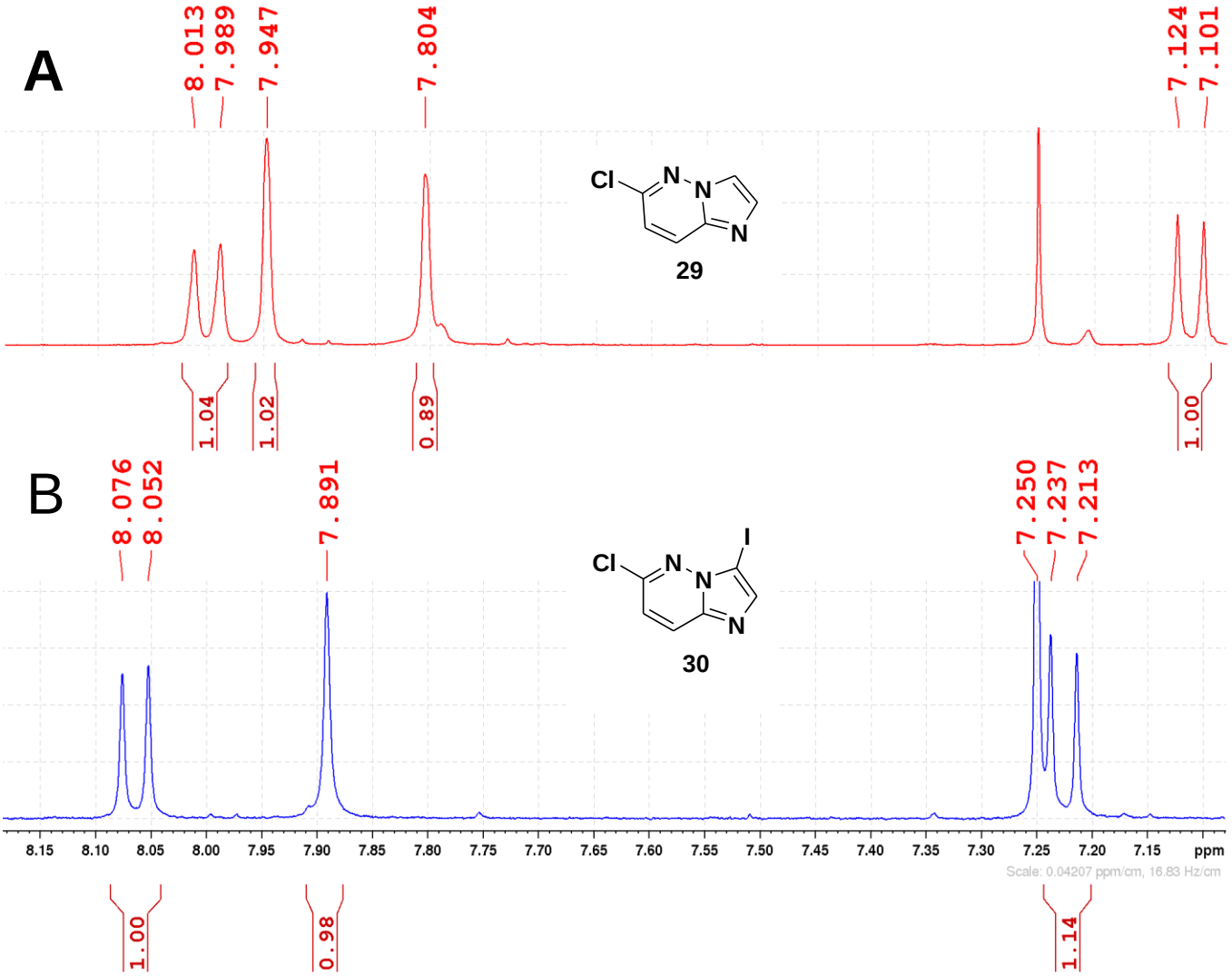

Figure 2.1: ^{1}H NMR for compound **29** and compound **30**.

2.2.2. The synthesis of 6-chloro-3-(4-(methylsulfonyl)phenyl)imidazo[1,2-b]pyridazine (32).

A Suzuki cross coupling reaction was performed on compound **30** to afford compound **32**. The 4-(methylsulfonyl) phenyl boronic acid **31** was coupled on the right-hand side (3-position). The reaction was done in 1,4-dioxane solvent at 90 ℃ for 18 hrs using bis(triphenyphosphine)palladium(II) dichloride ($Pd(PPh_3)_2Cl_2$) as a catalyst and potassium carbonate (K_2CO_3) as a base (**Scheme 2.2**). ^{1}H NMR and Carbon-13 Nuclear Magnetic Resonance (^{13}C NMR) were both used to characterize compound **32** and it was obtained in a yield ranging from 60% to 75%.

Figure 2.2 shows the ^{1}H NMR for compound **32 (spectrum B)** and its starting material **30 (spectrum A)**. **Spectrum B** shows the appearance of the methyl sulfonyl signal peak at δ 3.10 ppm and the two doublets (d) between δ 8.06 ppm and δ 8.30 ppm with each integrating for two hydrogens, indicating the incorporation of 4-(methylsulfonyl) phenyl substituent. There is a shifting of chemical shifts and an increased number of hydrogens from the phenyl ring in **spectrum B** as compared to **spectrum A**. **Spectrum B** also shows a total of ten hydrogens compared to three hydrogens of compound **30** in **spectrum A**. The ^{13}C NMR in **Figure 2.3** shows the incorporation of the methyl sulfonyl carbon peak at δ 44.6 ppm and the carbon peaks between δ 128.0 ppm and δ 140.0 ppm, indicating that the *para* substituted phenyl carbon peaks were incorporated. The data from both ^{1}H NMR and ^{13}C NMR conclude that the correct compound was successfully synthesized and this correlates with what was expected and previously reported [1].

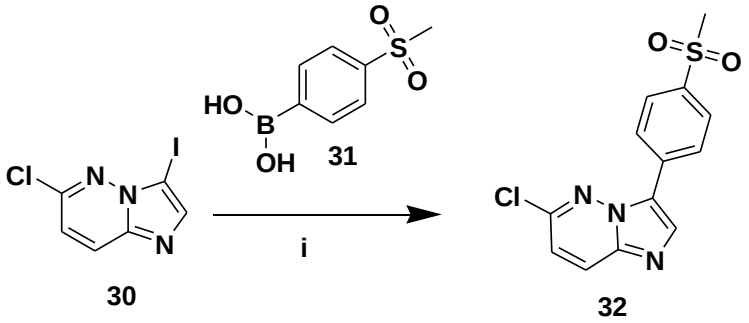

Scheme 2.2: Suzuki coupling on the 3-position: **31** (1.1 eq), i: 1,4-Dioxane, K_2CO_3 (1.5 eq), 90 ℃, 18 hrs.

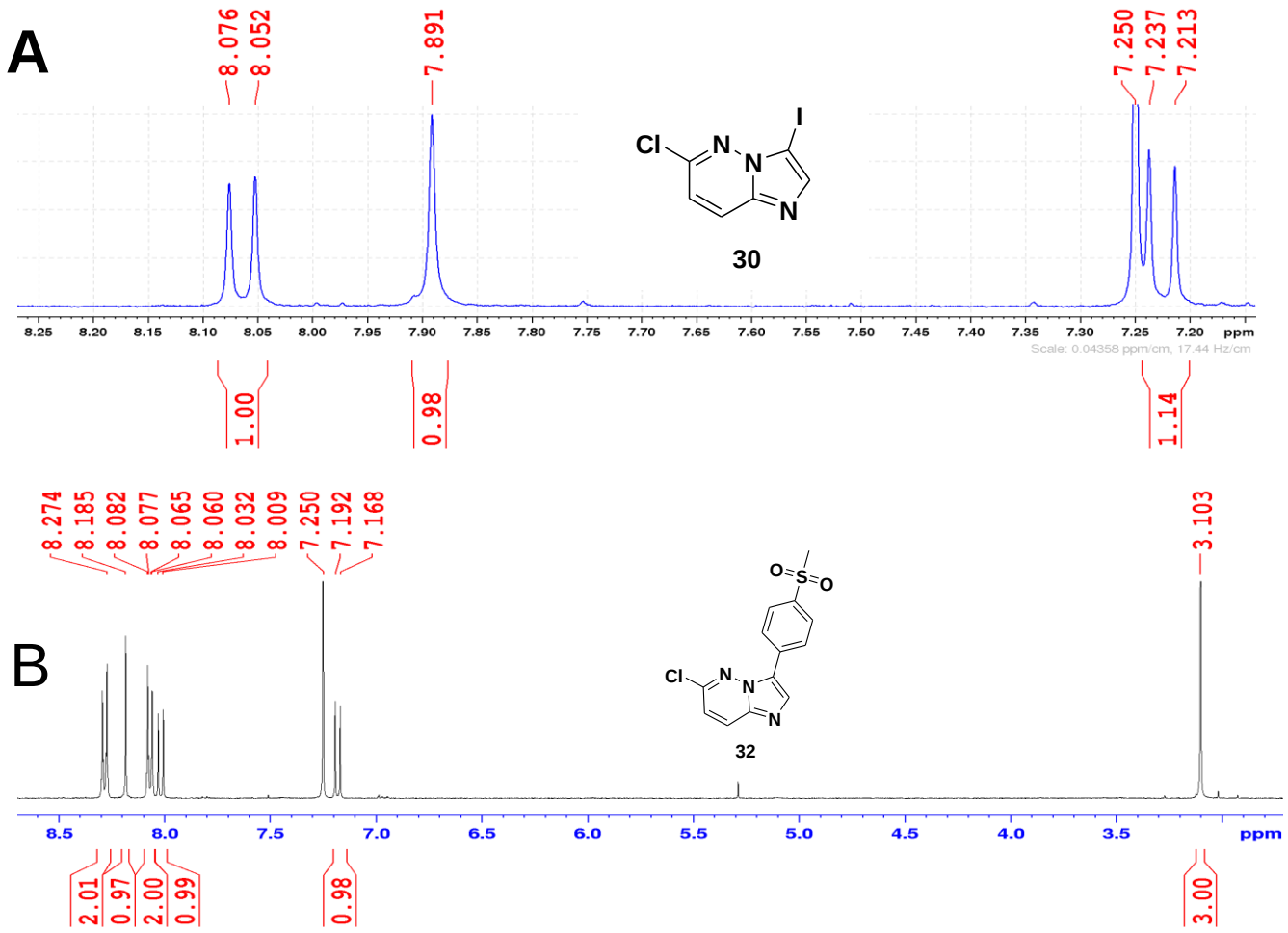

Figure 2.2: [1]H NMR for compound **30** and compound **32**.

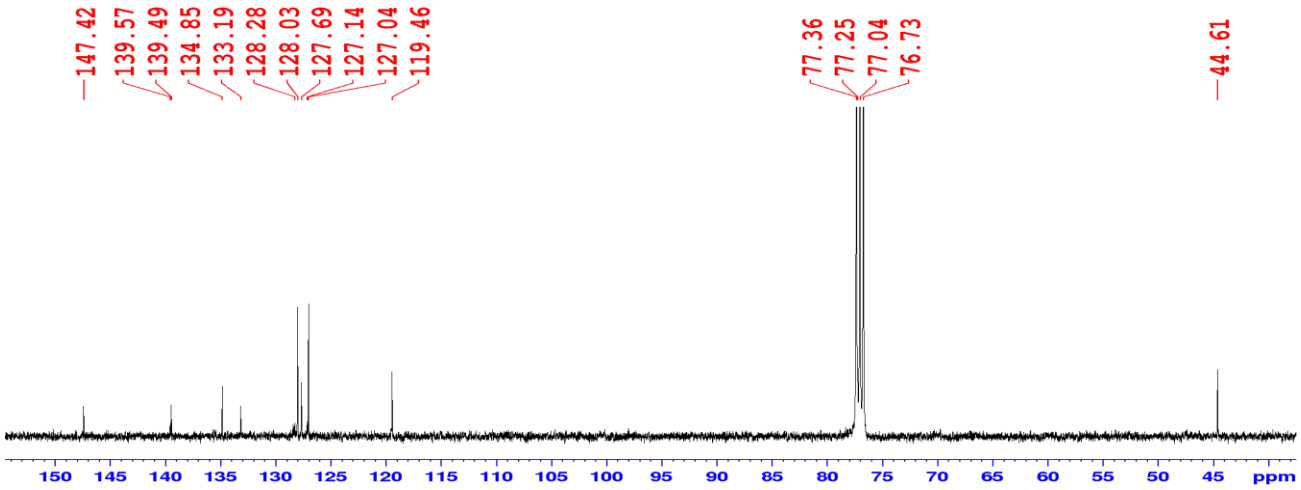

Figure 2.3. [13]C NMR for compound **32**.

2.2.3. The synthesis of first-generation compounds 20A to 20O

A series of imidazopyridazine derivatives were synthesized based on the starting material **32** to produce target compounds **20A** to **20O** as shown in **Table 1**. Different groups of varying sizes and polarities were incorporated as R^1 substituents to check the influence of the molecular weight (MW) and the calculated n-octanol/water partition coefficient (CLogP). Lipinski and co-workers have stated that compounds are most likely to have a very good absorption when their MW is less than 500 g/mol and the CLogP value is less than five [3]. Thus, a Suzuki cross-coupling reaction was performed on compound **32** to afford target compounds **20A** to **20O** which represent a library of novel derivatives. A boronic acid of interest **33** was coupled on the left hand-side (6-position) of the intermediate compound **32**. The reaction was left to reflux under nitrogen gas in 1,4-dioxane solvent at 110 ℃ for 18 hrs using $Pd(PPh_3)_2Cl_2$ as a catalyst and K_2CO_3 as a base (**Scheme 2.4**). The target compounds **20A** to **20O** were obtained and characterized using NMR and High-Resolution Mass Spectrometry (HRMS). Their percentage yields (%), Molecular weights (MW) and the calculated n-octanol/water partition coefficient (CLogP) are shown on **Table 1**.

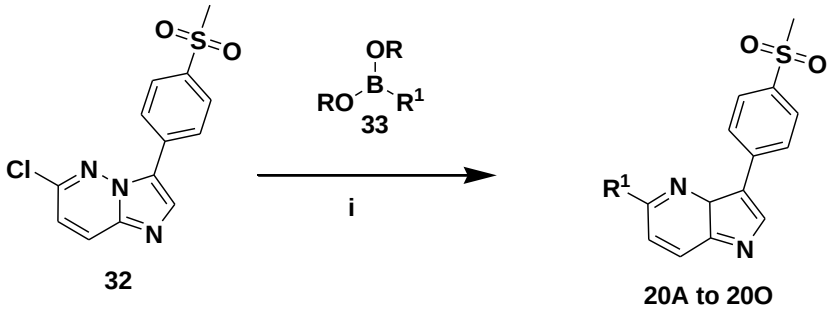

Scheme 2.4: Suzuki coupling on the 6-position: **33** (1.5 eq), i: 1,4-Dioxane, $Pd(PPh_3)_2Cl_2$ (0.05 eq), K_2CO_3 (1.5 eq), 110 ℃, 18 hrs, reflux under nitrogen.

Methoxy functionalities at the *ortho*, *meta* and *para* position of the phenyl ring at the 6-position of the core scaffold were introduced to synthesize target compounds **20A - D**. The yields ranged from 38% to 62%, MW was ranging from 379 g/mol to 406 g/mol and CLogP values ranging from 2.4 to 3.7. The *para* substituted methoxy had better percentage yields. The MW and CLogP values obeyed Lipinski's rules. Compounds **20E**

- G were synthesized to check the influence of the carbonyl functionality. The percentage yields were ranging from 43% to 70%, MW ranged from 421 g/mol to 576 g/mol and CLogP values ranging from 2.5 to 3.7. The molecular weights of compounds **20E** and **20G** are less than 500 g/mol, whereas compound **20F** has MW of greater than 500 g/mol. The CLogP values of these compounds are within the acceptable limit.

The fluorine atoms on the phenyl ring were introduced to synthesize target compounds **20H - J**. Their percentage yields were ranging from 47% to 60%, MW ranged from 367 g/mol to 434 g/mol and CLogP values ranging from 3.2 to 4.2. These values are within the acceptable limit according to Lipinski's rules. Target compounds **20K - N** were synthesized to check the influence of the heteroatom such as sulfur and nitrogen on the ring. The percentage yields were ranging from 32% to 70%, MW ranging from 350 g/mol to 443 g/mol and CLogP values ranging from 1.6 to 3.7. Both the MW and the ClogP values of these compounds are within the permitted range according to Lipinski's rules. The *meta* tolyl **20O** has a percentage yield 69% and it obeyed the Lipinski's rules.

2.2.3.1. 6-(4-Methoxyphenyl)-3-(4-(methylsulfonyl)phenyl)imidazo[1,2-b]pyridazine 20C.

Compound **32**, 4-methoxyphenylboronic acid and $Pd(PPh_3)_2Cl_2$ were dissolved in 1,4-dioxane and aqueous solution of K_2CO_3 was then introduced. The reaction was left to reflux under nitrogen gas for 18 hrs (**Scheme 2.5**). NMR and HRMS were used to characterize compound **20C** which was obtained in 58% yield. Similarly, all compounds listed in **Table 1** were synthesized and characterized following this procedure.

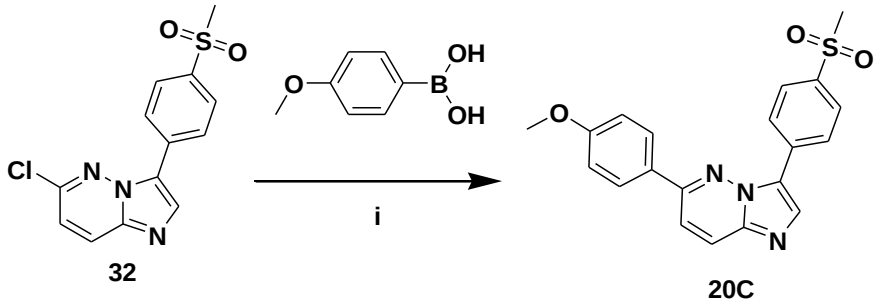

Scheme 2.5: Suzuki coupling on the 6-position: 4-methoxyphenylboronic acid (1.5 eq), i: 1,4-Dioxane, $Pd(PPh_3)_2Cl_2$ (0.05 eq), K_2CO_3 (1.5 eq), 110 ℃, 18 hrs, reflux under nitrogen.

Figure 2.4 shows the ^{1}H NMR for compound **20C (spectrum B)** and its starting material **32 (spectrum A)**. **Spectrum B** shows a total of eleven hydrogens in the aromatic region, three hydrogens from the methyl sulfonyl and another three hydrogens from the methoxy group, whereas the **spectrum A** which was used as the starting material shows a total of seven hydrogens in the aromatic region and three hydrogens from the methyl sulfonyl group. The shifting of chemical shifts, the change in splitting patterns and the increased number of hydrogens show that the 4-methoxyphenyl substituent has coupled to compound **32** to afford compound **20C**. Both the methyl sulfonyl and methoxy peaks in **spectrum B** appear as singlets at δ 3.12 ppm and δ 3.9 ppm, respectively. The two doublets (d) that each integrates for two hydrogens at δ 7.05 - δ 7.08 ppm and δ 7.95 - δ 7.97 ppm show the incorporation of the *para* substituted phenyl ring. The ^{13}C NMR spectrum in **Figure 2.5** shows the incorporation of the methoxy carbon peak at δ 55.5 ppm, the carbon peak at δ 158.7 ppm comes from the carbon that is directly attached to the methoxy. HRMS in **Figure 2.6** gives the $[M+H]^+$ peak of m/z 380.1071 which correlates with the calculated $[M+H]^+ = C_{20}H_{18}N_3O_3S^+ = 380.1063$ m/z. The M + 1 peak which has an intensity of 22% relative to the M peak is equal to 381.1112 m/z. The data confirms that compound **20C** was successfully synthesized.

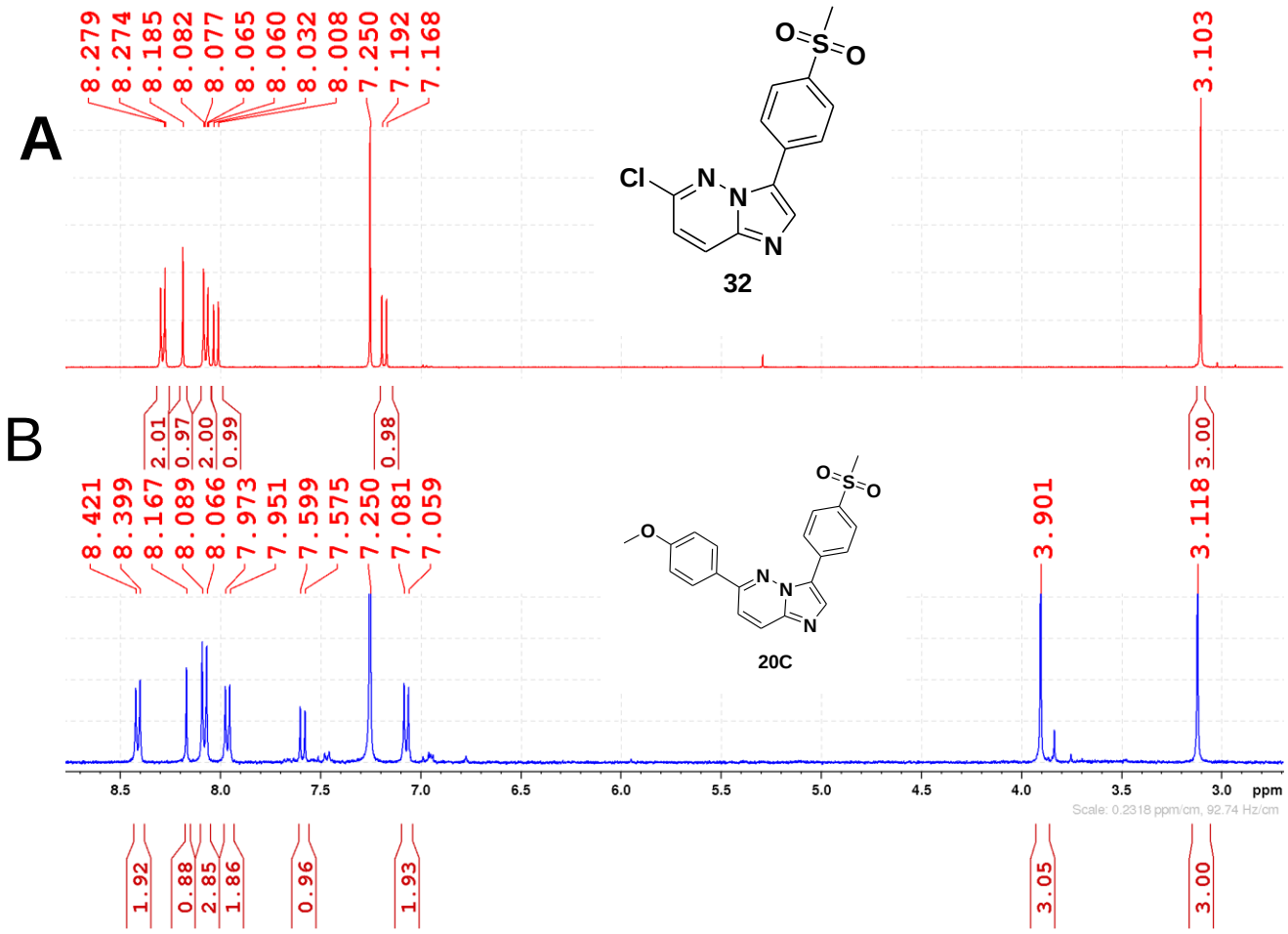

Figure 2.4: ^{1}H NMR for compound **32** and compound **20C**.

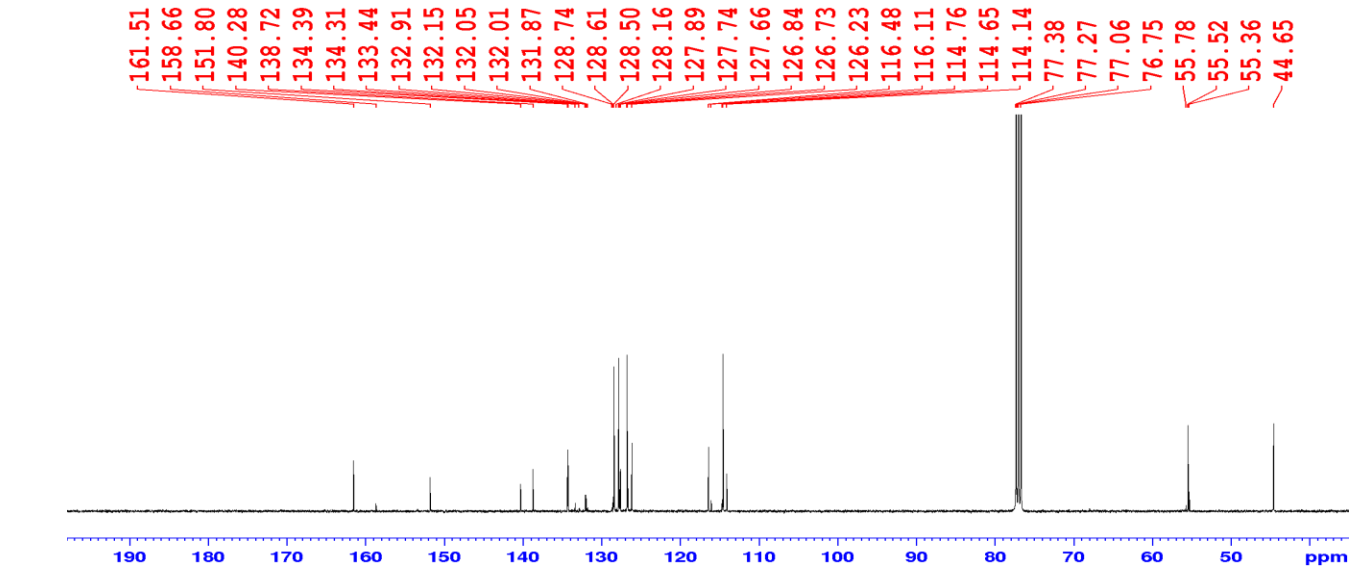

Figure 2.5:^{13}C NMR for compound **20C**.

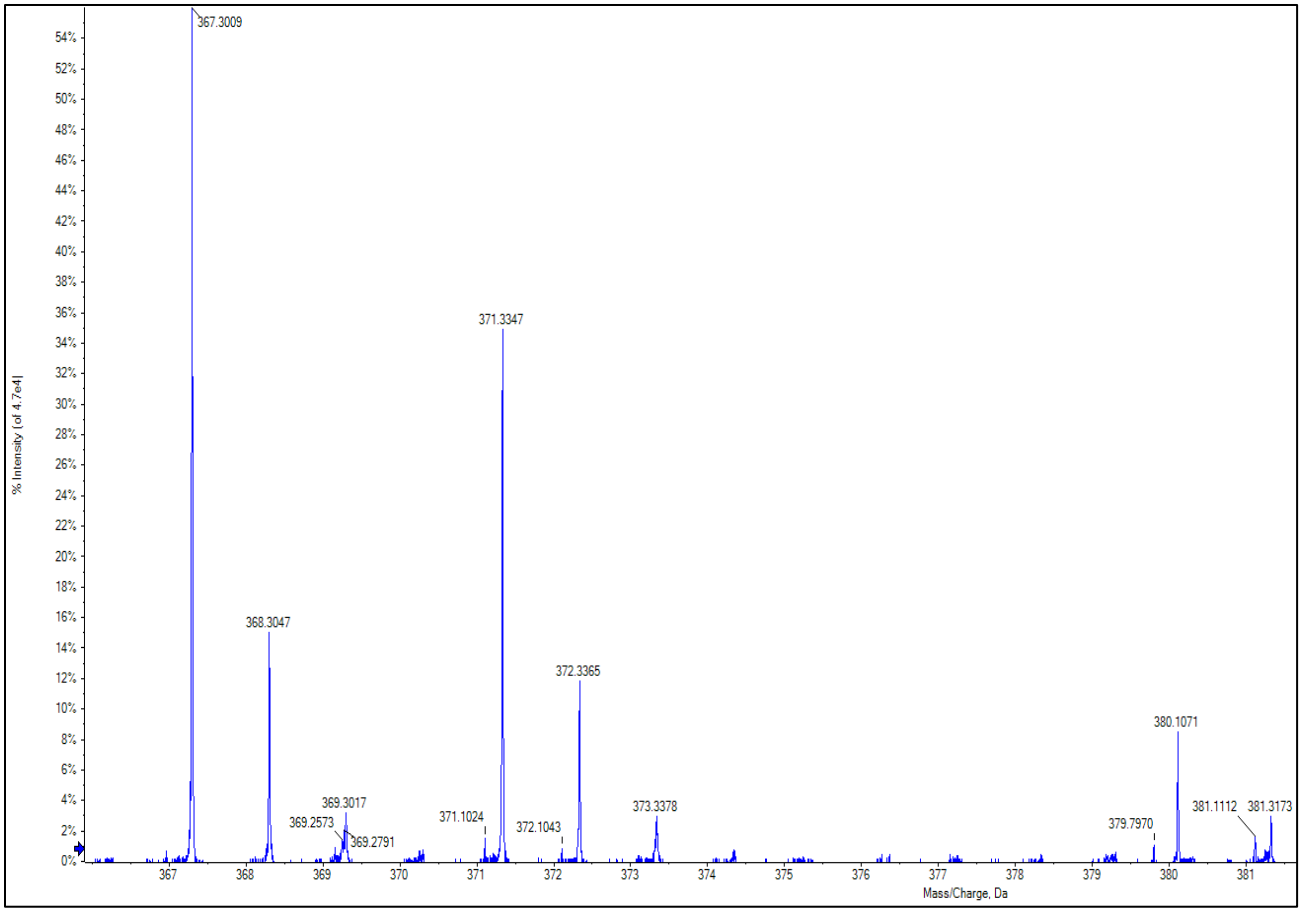

Figure 2.6: HRMS for compound **20C**.

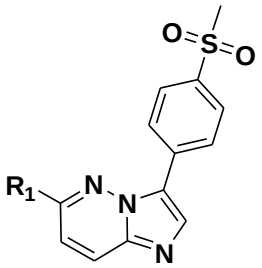

20A to 20O

Table 1: Compounds with their corresponding yields (%), MW and CLogP values.

R_1	Percentage yield (%)	MW (g/mol)	CLogP
20A 	38	379.4323	2.47983
20B 	33	379.4323	3.03983
20C 	58	379.4323	3.03983
20D 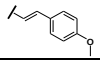	62	405.4696	3.6328
20E 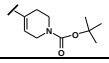	70	454.5419	3.0518
20F 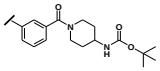	53	575.6785	2.53449
20G 	43	421.4690	3.61831
20H 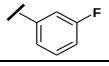	49	367.3968	3.26308
20I 	60	433.4037	3.58883
20J 	48	433.4037	4.14883
20K 	49	355.4340	2.97615

Table 1 continue…….

20L 	45	355.4340	2.76615
20M 	45	350.3944	1.62455
20N 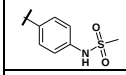	33	442.5113	1.93014
R20O 	69	363.4329	3.6188

2.3. DISCUSSION OF THE SECOND-GENERATION SERIES

The other scaffold that was shown to be active against sensitive strain (NF54) and the multidrug resistant strain (K1) of the *Plasmodium falciparum* as per prior work was pyrazolopyrimidine [4]. We were interested in exploring this scaffold even further by fixing either 3-(methylsulfonyl) phenyl substituent or 4-(methylsulfonyl) phenyl substituent on the left-hand side (5-position) and make a series of derivatives by making changes on the right-hand side (3-position). Based on previous research [4], the best substituent to have on the 5-position was 3-(methylsulfonyl)phenyl. We wanted to see what would happen if we expanded on that scope and fixed 4-(methylsulfonyl)phenyl substituent on the 5-position and test for inhibitory activity against the *Plasmodium* kinases.

2.3.1. The synthesis of 5-(4-(methylsulfonyl) phenyl) pyrazolo[1,5-a] pyrimidine 36 and 5-(3-(methylsulfonyl) phenyl) pyrazolo[1,5-a] pyrimidine (37)

We initiated our investigation with the synthesis of either 5-(4-(methylsulfonyl) phenyl) pyrazolo[1,5-a] pyrimidine **36** or 5-(3-(methylsulfonyl) phenyl) pyrazolo[1,5-a] pyrimidine **37** from the commercially available 5-chloropyrazolo[1,5-a] pyrimidine **34**. A Suzuki cross-coupling reaction was performed on compound **34** to afford either compounds **36** or compound **37.** Either boronic acid **31** or **35** was coupled on the left-hand side (5-position) of compound **34**. The reaction was left to reflux under nitrogen gas in 1,4-dioxane solvent at 110 ℃ for 18 hrs using $Pd(PPh_3)_2Cl_2$ catalyst and K_2CO_3 base (**Scheme 2.6**). NMR was used to characterize compounds **36** and **37** which were obtained in yields of 75% and 82% repectively. **Figure 2.7** shows the ^1H NMR for compound **36 (spectrum B)** and its

starting material **34 (spectrum A)**. The ^{1}H NMR in **spectrum B** shows the appearance of the methyl sulfonyl signal peak at δ 3.11 ppm and the two doublets between δ 8.05 and δ 8.28 which are due to the 4-(methylsulfonyl)phenyl boronic acid incorporation. There is a shifting of chemical shifts and an increased number of hydrogens from the phenyl ring in **spectrum B** as compared to **spectrum A**. The **spectrum B** also shows a total of eleven hydrogens compared to four hydrogens of compound **34** in **spectrum A**. The ^{13}C NMR in **Figure 2.8** shows the incorporation of the methyl sulfonyl carbon peak at δ 44.5 ppm, the carbon peaks between δ 128.0 ppm and δ 140.0 ppm show that the *para* substituted phenyl carbon peaks were incorporated. The data from both ^{1}H NMR and ^{13}C NMR conclude that the correct compound was successfully synthesized. Similarly, compound **37** was synthesized and characterized using this procedure.

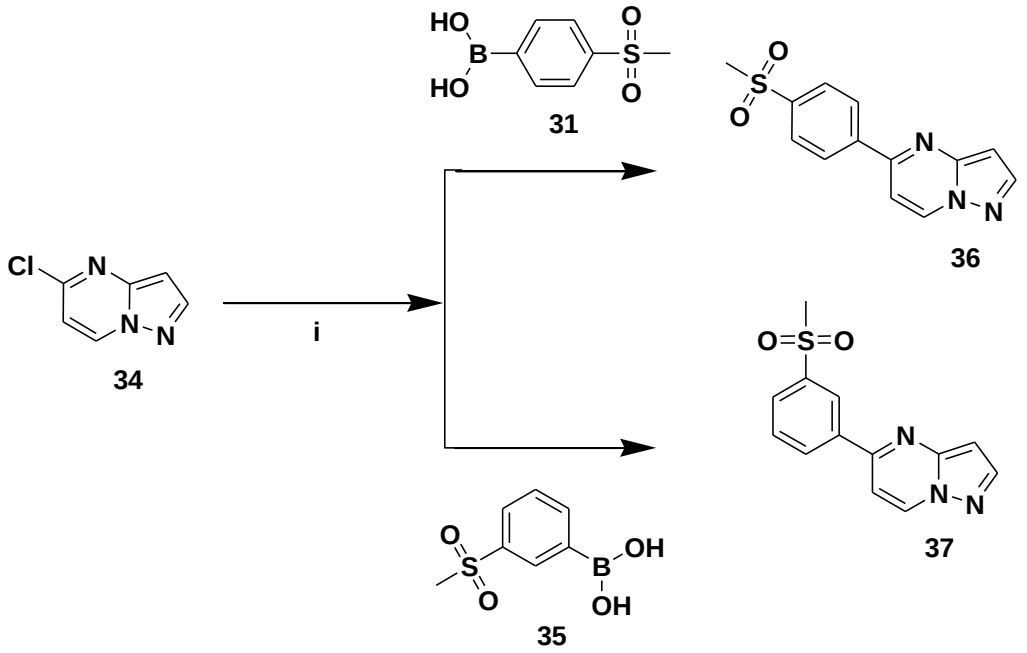

Scheme 2.6: Suzuki coupling on the 5-position: **31** or **35** (1.5 eq), i: 1,4-Dioxane, $Pd(PPh_3)_2Cl_2$ (0.05 eq), K_2CO_3 (1.5 eq), 110 ℃, 18 hrs, reflux under nitrogen.

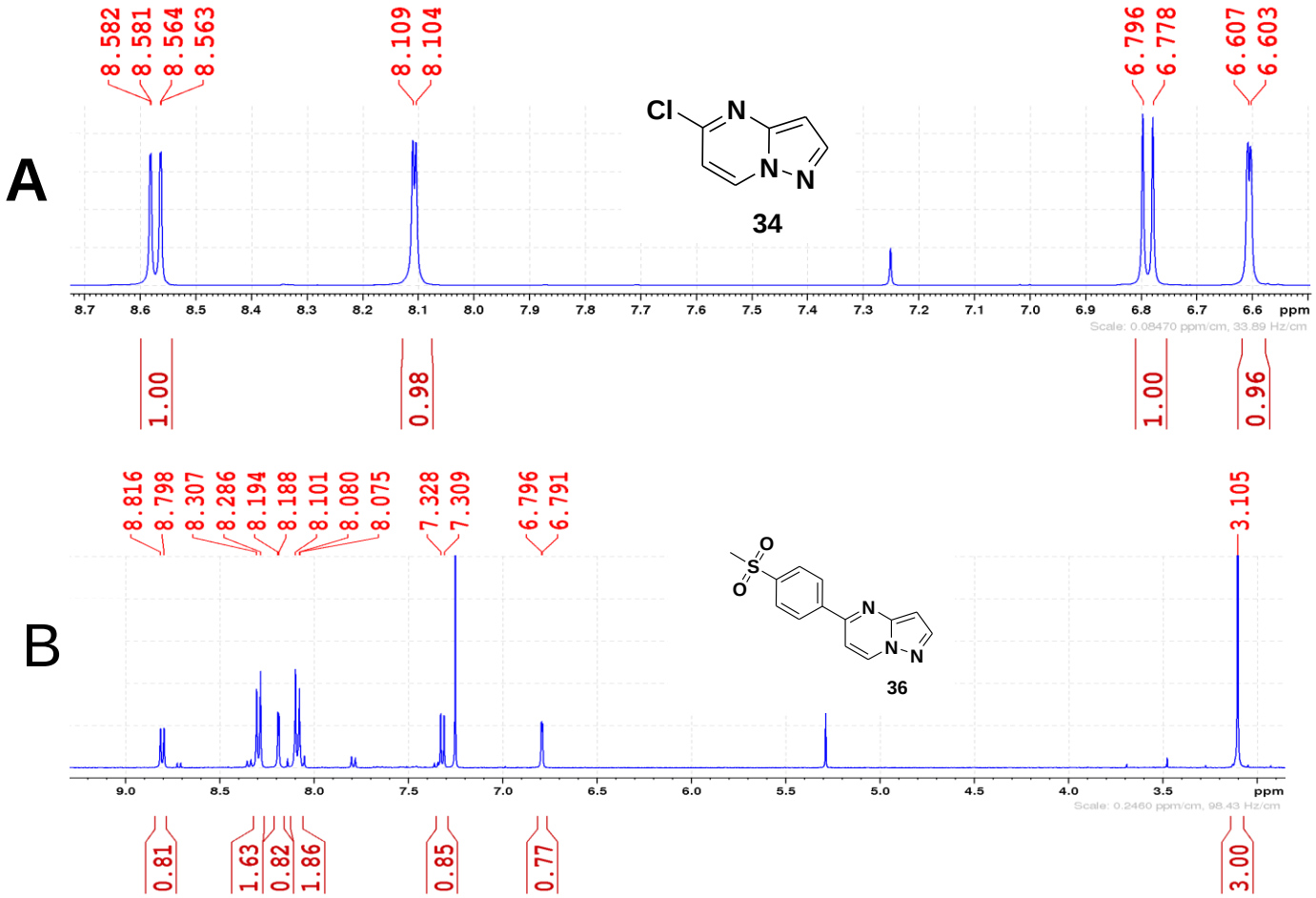

Figure 2.7: ^{1}H NMR for compound **34** and compound **36**

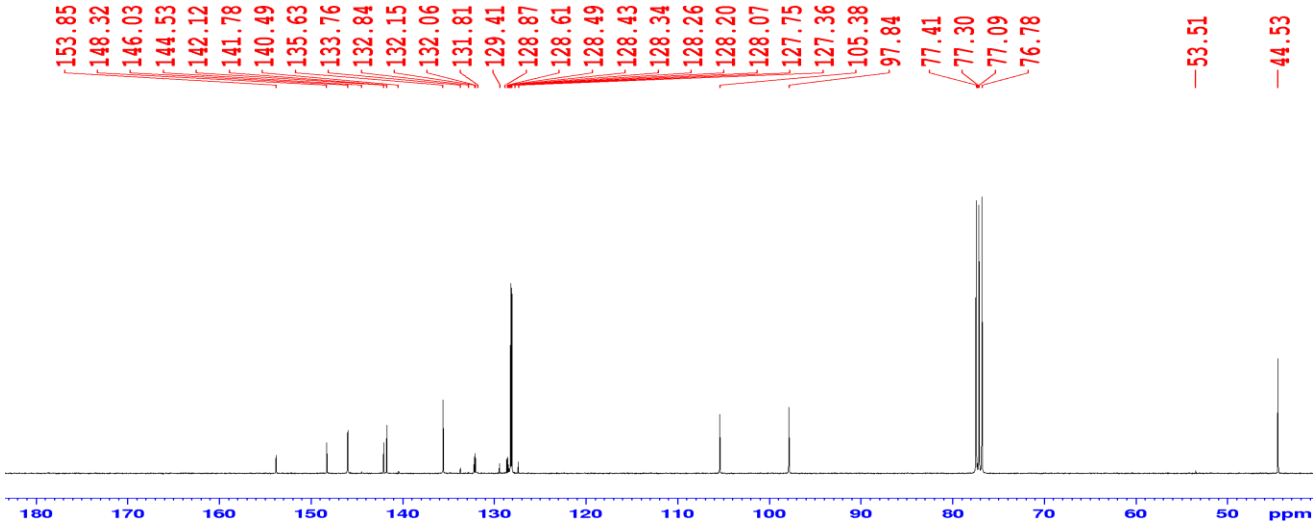

Figure 2.8. ^{13}C NMR for compound **36**.

2.3.2. The synthesis of compound 38 and compound 39

Compounds **36** and **37** were further brominated on the right-hand side (3-position) to afford compounds **38** and **39** respectively. The bromination was done using N-Bromosuccinimide (NBS) in acetonitrile for 18 hrs at temperatures ranging from 0 ℃ to 25 ℃ as shown on **Scheme 2.7**. Compounds **38** and **39** were obtained in percentage yields of 92% and 78% respectively and characterized using NMR.

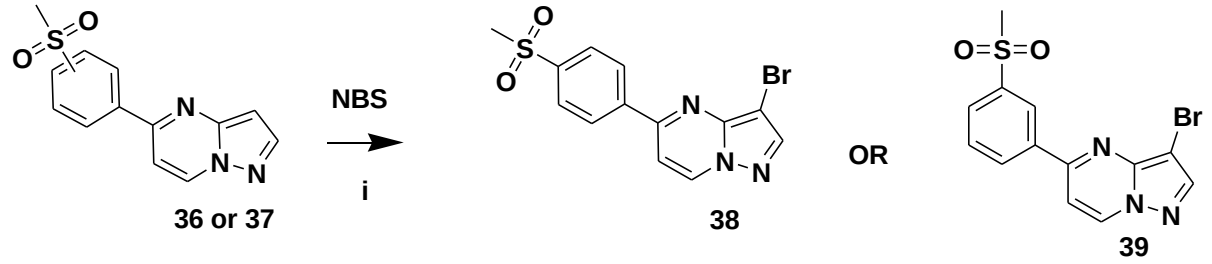

Scheme 2.7: Bromination: NBS (1.1 eq), i: Acetonitrile,18 h, 0 ℃ to 25 ℃.

2.3.3. The synthesis of second-generation compounds

A series of pyrazolopyrimidine derivatives were synthesized based on either compound **38** or compound **39** to produce target compounds **38A** to **38F** and **39A** to **39E** respectively as shown on **Table 2**. Different groups of varying sizes and polarities were incorporated on the R^1 substituent to check the influence of the molecular weight (MW) and the calculated n-octanol/water partition coefficient (CLogP). The reaction was done as shown on **Scheme 2.8**. The target compounds **38A** to **38F** and **39A** to **39E** were obtained and characterized using NMR and HRMS. Their percentage yields (%), molecular weights (MW) and the calculated n-octanol/water partition coefficient (CLogP) were calculated. All the compounds listed in **Table 2** have the MW of less than 500 g/mol and CLogP values of less than 5, therefore, they obeyed Lipinski's rules.

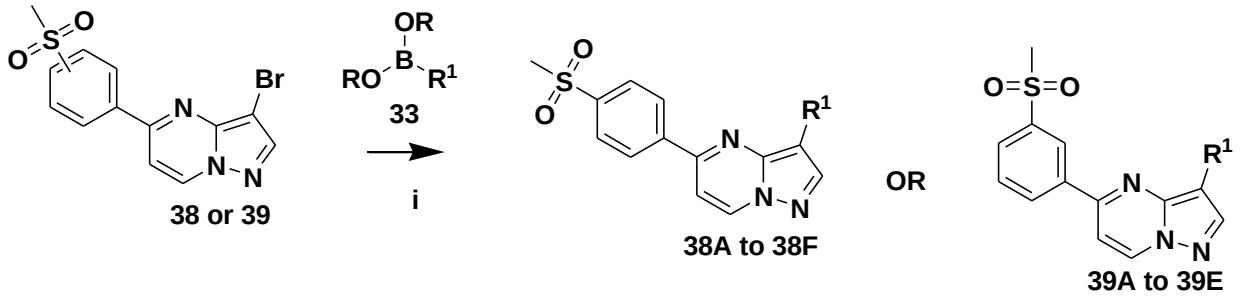

Scheme 2.8: Suzuki coupling on the 3-position: **33** (1.5 eq), i: 1,4-Dioxane, $Pd(PPh_3)_2Cl_2$ (0.05 eq), K_2CO_3 (1.5 eq), 110 ℃, 18 hrs reflux under nitrogen.

The methylsulfonyl functionality on the right-hand side of the core scaffold was introduced to synthesize target compounds **38A** and **38B**. The yields were ranging from 51% to 57%. Compound **38B** had a better percentage yield and CLogP value as compared to compound **38A.** Compounds **38C** and **38D** contained pyridine and dimethylbenzenamine functionalities, respectively. The two compounds were compared based on the nitrogen atoms they contain. Their yields were ranging from 52% to 61%. Compound **38C** had a better percentage yield and CLogP value as compared to compound **38D**. Compounds **38E** and **38F** contain the methoxy functionality and their percentage yields were ranging from 53% to 56%. The target compounds **39A - E** were synthesized to check the influence of the para substitution on the right-hand side (3-position) of the 3-(methylsulfonyl)phenyl substituent scaffold.

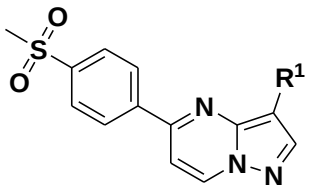

38A to 38F

AND

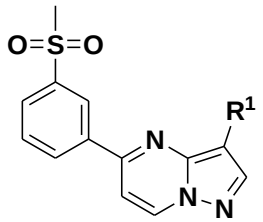

39A to 39E

Table 2: Target compounds based on 4-(methylsulfonyl)phenyl boronic acid and 3-(methylsulfonyl)phenyl boronic acid.

R^1	Percentage yield (%)	MW (g/mol)	CLogP
38A 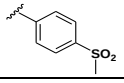	52	427.4967	1.27105
38B 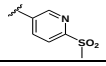	56	428.4847	1.18951
38C 	61	350.3944	1.41565
38D 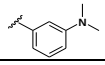	53	392.4741	3.07592
38E 	54	379.4323	2.26983
38F 	56	379.4323	2.82983
39A 	75	350.3944	1.41565
39B 	66	379.4323	2.82983
39C 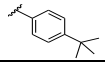	49	405.5126	4.7358
39D 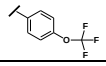	60	433.4037	3.79329
39E 	67	427.4847	1.18951

2.3.4. The synthesis of reduced pyrazolopyrimidine derivatives.

A library of derivatives based on the reduced pyrazolopyrimidine scaffold were synthesized to yield compounds **40A - C**. The reactions were done in a combination of dichloromethane (DCM) and ethanol (ethanol) solvent for 18 hrs at a temperature of 25 ℃, using sodium borohydride ($NaBH_4$) as a reducing agent and $Pd(PPh_3)_2Cl_2$ as a catalyst (**Scheme 2.9)**. The target compounds **40A** to **40C** were synthesized to check the influence of the *para* substitution on the right-hand side (3-position) of 3-(methylsulfonyl)phenyl substituent. Target compounds were obtained in percentage yields ranging from 40% to 65% and characterized using NMR and HRMS.

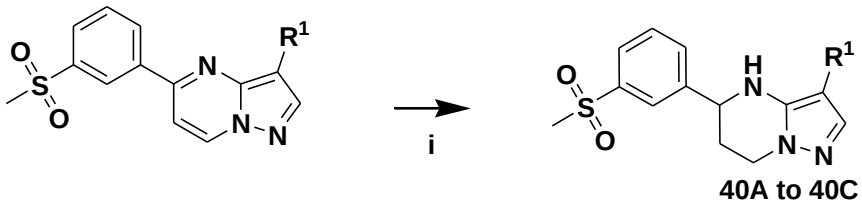

Scheme 2.9: Reduction: i: $NaBH_4$ (10 eq), $Pd(PPh_3)_2Cl_2$ (0.02 eq), DCM:EtOH (3:2), 25 ℃, 2 hrs.

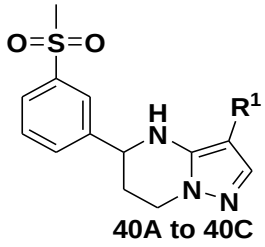

Table 3: Target compounds based reduced pyrazolopyrimidine.

R^1	Percentage yield (%)	MW (g/mol)	CLogP
40A 	41	354.4261	0.565461
40B 	47	383.4640	1.89422
40C 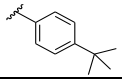	62	409.5444	3.78936

2.4. BIOLOGICAL ASSAY RESULTS

A series of imidazopyridazine (15 compounds) and pyrazolopyrimidine (14 compounds) derivatives were evaluated for their *in vitro* antiplasmodial activity against the sensitive (NF54) strain of the human malaria parasite *Plasmodium falciparum*. The imidazopyridazine compounds were also tested for their inhibitory activity against *Plasmodium falciparum* cGMP-dependent protein kinase (*Pf*PKG) and *Plasmodium vivax* phosphatidylinositoil 4-kinase type III beta (*Pv*PI4Kβ). Selected compounds that demonstrated an activity of less than 0.5 μM against NF54 strain were evaluated for cytotoxicity assays. The assays were performed at the Holistic Drug Discovery and Development (H3D) Center.

The whole cell screening (*In vitro* Antiplasmodial activity)

Target compounds were tested for activity against the wildtype drug sensitive strain (NF54) of the human malaria parasite *Plasmodium falciparum*. Chloroquine and artesunate were used as control drugs in all experiments. Continuous cultures of asexual erythrocyte stages of *P. falciparum* were maintained using the method described by Trager and Jensen [5] with minor modifications. Quantitative assessment of *in vitro* antiplasmodial activity was determined via the parasite lactate dehydrogenase assay using the method described by Makler *et.al* [6]**,** in which parasite viability is determined colourimetrically using the breakdown of a dye by metabolic enzymes of the glycolytic pathway taking place in living parasites as a marker for survival.

2.4.1. *In vitro* antiplasmodial activity for imidazopyridazine compounds

The *in vitro* antiplasmodial activity results for the imidazopyridazine compounds as indicated by their IC_{50} values are summarized in **Table 4**. Target compounds **20B**, **20D**, **20E**, **20F**, **20M** and **20O** showed the inhibitory activity of below 6 μM, which was used as a cut-off to determine good inhibitory activity versus moderate inhibitory activity. The other target compounds have demonstrated a moderate activity of greater than 6 μM. The *meta* and *para* substituted compounds have demonstrated good inhibitory activity as compared to ortho substitution. From the four compounds that contained nitrogen atom substituent on the 6-position, three of them have demonstrated good inhibitory activity of less than 6 μM as seen with compounds **20E**, **20F** and **20M**, whereas **20N** which also contained a

nitrogen atom demonstrated a moderate activity of more than 6 μM. The methoxy groups demonstrated moderate to good inhibitory activity, compounds **20A** and **20C** have demonstrated moderate activity while compounds **20B** and **20D** demonstrated good activity. Both compounds **20C** and **20D** contain a para methoxy groups on a phenyl ring, but compound **20D** contains a double bond between the phenyl ring and the core scaffold. The double bond has positively influenced the activity of compound **20D** as compared to compound **20C** which does not have the double bond between the phenyl ring and the core scaffold. The *meta* tolyl group **20M** also demonstrated good inhibition against *Pf*NF54.

2.4.2. *In vitro* inhibitory activity against *Pf*PKG and *Pv*PI4Kβ for imidazopyridazine compounds.

The imidazopyridazine compounds were evaluated for their inhibitory activity against *Plasmodium falciparum* cGMP-dependent protein kinase (*Pf*PKG) and *Plasmodium vivax* phosphatidylinositoil 4-kinase (*Pv*PI4Kβ). The inhibitory activity data against *Pf*PKG and *Pv*PI4Kβ as indicated by their IC_{50} values in micro molar scale are summarized in **Table 4**. From the table, the compounds were able to inhibit both *Pf*PKG and *Pv*PI4Kβ with different IC_{50} values. However, there was more inhibition of *Pv*PI4Kβ over *Pf*PKG. Four compounds out of the fifteen tested compounds against *Pf*PKG have demonstrated inhibitory activity of less than 10 μM, which was used as a cutoff to determine good inhibitory activity versus moderate inhibitory activity.

The four compounds which demonstrated good inhibitory activity against *Pf*PKG are **20H** which contained a fluorine atom meta substituted to a phenyl ring on the 6-position of the core scaffold, **20L** & **20K** which contained *ortho* and *meta* substituted thiophene at the 6-position of the core scaffold and **20N** which contain a methylsulfonyl and nitrogen attached to a phenyl ring. These four compounds (**20H**, **20K**, **20L and 20N**) have demonstrated good activity against both *Pf*PKG and *Pv*PI4Kβ with IC_{50} values ranging from 0.96 μM to 5.04 μM and 0.006 μM to 0.071 μM respectively. All the remaining compounds listed in **Table 4** have demonstrated moderate activity against *Pf*PKG with IC_{50} values greater than 10 μM. They have shown good inhibitory activity against *Pv*PI4Kβ with IC_{50} values ranging from 0.006 μM to 0.643 μM.

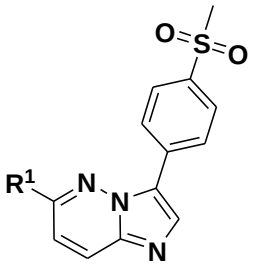

20A to 20O

Table 4: *In vitro* antiplasmodial activity and *Pf*PKG and *Pv*PI4Kβ inhibitory activity for imidazopyridazine compounds.

Compound ID	NF54 IC_{50} (μM)	*Pf*PKG (IC_{50} (μM))	*Pv*PI4Kβ (IC_{50} (μM))
20A 	> 6	>10	0.339
20B 	1.24	>10	0.074
20C 	> 6	>10	0.062
20D 	1.52	>10	0.113
20E 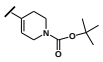	5.91	>10	0.643
20F 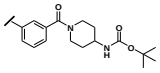	0.372	>10	0.006
20G 	> 6	>10	0.053
20H 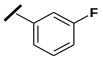	> 6	3.1	0.006
20I 	> 6	>10	0.048

Table 4 continue……

20J 	> 6	>10	0.041
20K 	> 6	2.13	0.071
20L 	> 6	5.04	0.047
20M 	0.82	>10	0.074
20N 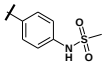	> 6	0.96	0.028
20O 	2.72	>10	0.054
Chloroquine	0.007	-	-
Artesunate	0.004	-	-

2.4.3. *In vitro* antiplasmodial activity for pyrazolopyrimidine compounds

The *in vitro* antiplasmodial activitiy for pyrazolopyrimidine compounds as indicated by their IC_{50} values in micro molar scale are summarized in **Table 5**. All compounds listed in **Table 5** except compound **38E** are demonstrating very good antiplasmodial activities ranging from 0.009 μM to 3.844 μM. Compound **38A** contained a 4-(methylsulfonyl) phenyl substituent on both the Left-hand side (5-position) and the right-hand side (3-position) of the pyrazolopyrimidine scaffold, it had an activity of 0.402 μM. Whereas compound **38B** contained a 6-(methylsulfonyl) pyridin-3-yl substituent on the 3-position and 4-(methylsulfonyl) phenyl substituent on the 5-position, it had an activity of 1.249 μM. These values indicated that the activity had decreased when 4-(methylsufonyl) phenyl substituent was substituted with 6-(methylsulfonyl) pyridin-3-yl and when 4-(methylsulfonyl) phenyl substituent was kept on the 5-position**.**

Compounds **38B** and **39E** both contained 6-(methylsulfonyl) pyridin-3-yl substituent on the 3-position and 4-(methylsulfonyl) phenyl & 3-(methylsulfonyl) phenyl substituents respectively, on the 5-position**.** Compound **39E** reported an activity of 0.009 μM which was very good comparable to compound **38B**, chloroquine (0.007 μM) and artesunate (0.004 μM) which were used as control drugs. Compounds **38C** and **39A** both contained pyridin-4-yl substituent on the 3-position and 4-(methylsulfonyl) phenyl & 3-(methylsulfonyl) phenyl substituents respectively, on the 5-position**.** Compound **39A** demonstrated an activity of 0.013 μM, which was more active than compound **38C** (1.285 μM). Compound **40A** is a reduced derivative from compound **39A** and had an activity of 0.197 μM. The reduction of compound **39A** has resulted with a decreased antiplasmodial activity. Compound **38D** contained a *meta N,N*-dimethylbenzylamine substituent on the 3-position and 4-(methylsulfonyl) phenyl substituent on the 5-position. It had demonstrated an activity of 2.060 μM.

Compound **38E** and **38F** both contained 4-(methylsulfonyl) phenyl substituent on the 5-position and 2-methoxyphenyl & 4-methoxyphenyl substituents respectively on the 3-position. Compound **38E** reported a moderate activity of greater than 6 μM, whereas compound **38F** demonstrated a better activity of 3.844 μM. From these two values we can conclude that para-substitution gives better activity than the ortho-substitution. Compounds **38F** and **39B** contained 4-methoxyphenyl substituent on the 3-position and 4-(methylsulfonyl) phenyl & 3-(methylsulfonyl) phenyl substituents respectively, on the 5-position**.** Compound **39B** demonstrated an activity of 0.190 μM, which was more active than compound **38F** (3.844 μM). Compound **40B** is a reduced derivative from compound **39B** and had an activity of 1.056 μM. The reduction of compound **39B** has resulted with a decreased activity. Compound **39C** contained 4-*tert*-butylphenyl substituent on the 3-position and 3-(methylsulfonyl) phenyl substituent on the 5-position. It had demonstrated an activity of 1.504 μM. Compound **40C** is a reduced derivative from compound **39C** and had an activity of 2.113 μM. The reduction of compound **39C** has also resulted with a decreased activity. Compound **39D** contained a 4-(trifluoromethoxy) phenyl substituent on the 3-position and 3-(methylsulfonyl) phenyl substituent on the 5-position with an activity of 0.390 μM. The data in the discussion and **Table 5** demonstrated that 3-

(methylsulfonyl) phenyl was a better substituent to have on the left-hand side of the pyrazolopyrimidine core scaffold than 4-(methylsulfonyl) phenyl substituent.

2.4.4. Cytotoxicity

When we design a drug, we look for a drug that will target the disease of interest over the normal human cells to avoid severe side effects. In the laboratory, if a compound is active against a pathogen of interest (e.g., *Plasmodium* parasite), before progressing it further it has to be tested against normal mammalian cells Chinese Hamster Ovary (CHO) or Human hepatoma (HepG2), to see if it does or does not have similar affinity for these cells compared to the parasite of interest and then we check what is known as selectivity index (SI). This will then give an idea of whether the compound is cytotoxic or not. For example, if you have *Pf*NF54 IC_{50} = 0.02 μM, CHO IC_{50} = 0.05 μM; the SI will be CHO IC_{50} /*Pf*NF54 IC_{50} = 2.5, based on the requirement of SI you cannot progress this compound. But if you have *Pf*NF54 IC_{50} = 0.02 μM, CHO IC_{50} = 5.00 μM; SI = 250, therefore it meets the chosen SI of >100, meaning it has more affinity for your parasite than the normal cells and gives some hope to be progressed further.

Selected compounds demonstrating an activity with IC_{50} of less than 0.5 μM against *Pf*NF54 strain were evaluated for cytotoxicity assays. For a compound to be progressed further, it must have SI of more than 100. Compounds **38A**, **39B**, **39D** and **39E** listed in **Table 5** met the requirements, therefore they will be progressed further for solubility (to check if a compound is soluble in aqueous media because for a drug to be absorbed, it must be soluble enough. It must also have good properties of lipophilicity to be able to pass through lipid membranes), chemical stability (to check the stability of a chemical in a certain environment or conditions), microsomal stability (m,r,h) (this is subjecting the compound to mouse (m) liver microsomes, rat (r) liver microsomes and human (h) liver microsomes to study the rate at which the compound is metabolized by the drug metabolizing enzymes found in these liver microsomes.) and *in vitro* PfK1, Dd2 (these are tests done in the laboratory using chloroquine resistant strains of *Plasmodium falciparum* (*Pf*) known as K1 and Dd2. Chloroquine is known to be inactive against K1 or Dd2 strains, that is why they are called chloroquine resistant strains. They are normally used to check what is known as cross resistance, to see if the potential drug/molecule

designed is also inactive (suffering resistant) against these strains just like chloroquine) assays.

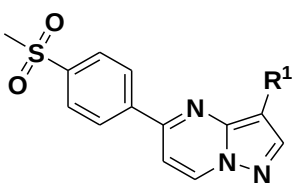

38A to 38F

,

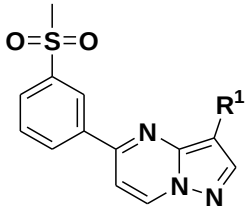

39A to 39E

AND

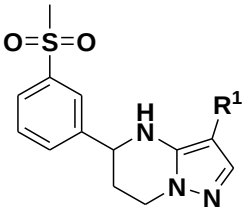

40A to 40C

Table 5: *In vitro* antiplasmodial activity, cytotoxicity, and selectivity index for pyrazolopyrimidine compounds.

Compound ID	NF54 IC_{50} (μM)	Cytotoxicity (CHO) IC_{50} (μM)	Selectivity Index
38A 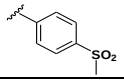	0.402	> 50	124
38B 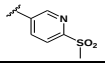	1.249	-	-
38C 	1.285	-	-
38D 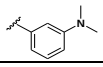	2.060	-	-
38E 	> 6	-	-
38F 	3.844	-	-
39A 	0.013	8.018	685
39B 	0.190	> 50	357
39C 	1.504	-	-
39D 	0.390	> 50	202
39E 	0.009	19.743	2632

Table 5 continue…..

40A 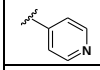	0.197	-	-
40B 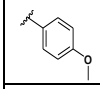	1.056	-	-
40C 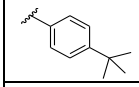	2.113	-	-
Chloroquine	0.007	-	-
Artesunate	0.004	-	-

2.4.5. Imidazopyridaze compared with pyrazolopyrimidine.

Pyrazolopyrimidine compounds demonstrated very good *in vitro* antiplasmodial activity against the sensitive (NF54) strain as compared to the imidazopyridazine compounds.

2.5. REFERENCES

[1] Le Manach, C., Gonzàlez Cabrera, D., Douelle, F., Nchinda, A.T., Younis, Y., Taylor, D., Wiesner, L., White, K.L., Ryan, E., March, C. and Duffy, S., Avery V.M., Waterson D., Witty M.J., Wittlin S., Charman S.A., Street L.J. and Chibale K, "Medicinal chemistry optimization of antiplasmodial imidazopyridazine hits from high throughput screening of a SoftFocus kinase library: part 1," *Journal of Medicinal Chemistry,* vol. 57, no. 6, pp. 2789-2798, 2014.

[2] Le Manach, C., Paquet, T., Gonzàlez Cabrera, D., Younis, Y., Taylor, D., Wiesner, L., Lawrence, N., Schwager, S., Waterson, D., Witty, M.J. and Wittlin, S., Street L.J. and Chibale K, "Medicinal chemistry optimization of antiplasmodial imidazopyridazine hits from high throughput screening of a softfocus kinase library: Part 2," *Journal of Medicinal Chemistry,* vol. 57, no. 21, pp. 8839-8848, 2014.

[3] Chagas, C.M., Moss, S. and Alisaraie, L, "Drug metabolites and their effects on the development of adverse reactions: Revisiting Lipinski's Rule of Five," *International Journal of Pharmaceutics,* vol. 549, no. 1-2, pp. 133-149, 2022.

[4] Le Manach, C., Paquet, T., Brunschwig, C., Njoroge, M., Han, Z., Gonzàlez Cabrera, D., Bashyam, S., Dhinakaran, R., Taylor, D., Reader, J. and Botha, M., Churchyard A., Lauterbach S., Coetzer T.L., Birkholtz L., Meister S., Street L.J. and Chibale K, "A novel pyrazolopyridine with in vivo activity in Plasmodium berghei-and Plasmodium falciparum-infected mouse models from structure–activity relationship studies around the core of recently identified antimalarial imidazopyridazines," *Journal of Medicinal Chemistry,* vol. 58, no. 21, pp. 8713-8722, 2015.

[5] Trager, William, and James B. Jensen, "Human malaria parasites in continuous culture," *Science,* vol. 193, no. 4254, pp. 673-675, 1976.

[6] Makler, M.T., Ries, J.M., Williams, J.A., Bancroft, J.E., Piper, R.C., Gibbins, B.L. and Hinrichs, D.J, "Parasite lactate dehydrogenase as an assay for Plasmodium

falciparum drug sensitivity," *The American Journal of Tropical Medicine and Hygiene,* vol. 48, no. 6, pp. 739-741, 1993.

CHAPTER 3: OVERALL CONCLUSION

3.1. CONCLUSION

This study highlighted the need to develop and synthesis novel compounds with new mechanism of action against malaria, because resistance to previously effective anti-malarial drugs and ACTs has emerged. This study reported the synthesis of imidazopyridazine and pyrazolopyrimidine derivatives, which were then tested against the sensitive (NF54) strain of the human malaria parasite *Plasmodium falciparum* and the *Plasmodium falciparum* cGMP-dependent protein kinase (*Pf*PKG) and *Plasmodium vivax* phosphatidylinositoil 4-kinase type III β (*Pv*PI4Kβ). Classical optimization techniques were employed to achieve the overall objectives of investigating the structure activity relationship (SAR). The target compounds under the imidazopyridazine were obtained by fixing 4-(methylsulfonyl) phenyl substituent on the right-hand side (3-position) and varying substituents on the left-hand side (6-position). The final compounds under the pyrazolopyrimidine were obtained by fixing either 4-(methylsulfonyl) phenyl or 3-(methylsulfonyl) phenyl substituent on the left-hand side (5-position) and varying substituents on the right-hand side (3-position).

In this study we focused on synthesizing a new library of imidazopyridazine and pyrazolopyrimidine derivatives, with substituents at 3- & 6- positions and 3- & 5- positions respectively. The compounds were successfully synthesized and characterized by NMR and HRMS. The imidazopyridazine derivatives percentage yields ranged from 38% to 70%, whereas the percentage yields for the pyrazolopyrimidine derivatives ranged from 41% to 75%. All the imidazopyridazine compounds were evaluated for their *in vitro* antiplasmodial activities against NF54 strain and inhibitory activity against *Pf*PKG and *Pv*PI4Kβ. The pyrazolopyrimidine compounds were only evaluated for their *in vitro* antiplasmodial activity against the NF54 strain.

The *in vitro* antiplasmodial activities of Imidazopyridazine compounds as indicated by their IC_{50} values in micro molar scale are summarized in **Table 4**. The inhibitory activity data against *Pf*PKG and *Pv*PI4K as indicated by their IC_{50} values in micro molar scale are summarized in **Table 4**. Compounds **20B**, **20D**, **20E**, **20F**, **20M** and **20O** demonstrated *in vitro* antiplasmodial activity of below 6 μM against NF54 strain, which was used as a cut-

off to determine good activity versus moderate activity. Compounds **20A**, **20C**, **20G**, **20H**, **20I**, **20J**, **20K**, **20L** and **20N** demonstrated a moderate activity of greater than 6 μM against NF54 strain. Compounds **20H**, **20K**, **20L and 20N** demonstrated good activity against both *Pf*PKG and *Pv*PI4Kβ with IC_{50} values ranging from 0.96 μM to 5.04 μM and 0.006 μM to 0.071 μM, respectively. Compounds **20A**, **20B**, **20C**, **20D**, **20E**, **20F**, **20G**, **20I**, **20J**, **20M** and **20O** demonstrated moderate activity of greater than 10 μM against *Pf*PKG and good activity against *Pv*PI4Kβ with IC_{50} values ranging from 0.006 μM to 0.643 μM.

The *in vitro* antiplasmodial activitiy for pyrazolopyrimidine compounds as indicated by their IC_{50} values in micro molar scale are summarized in **Table 5**. All compounds listed in **Table 5** except compound **38E** demonstrated very good antiplasmodial activities ranging from 0.009 μM to 3.844 μM. Compounds **39A** (0.013 μM) and **39E** (0.009 μM) demonstrated the highest activities against the NF54 strain. The reduction of the pyrazolopyrimidine scaffold did not improve the potency, as it was seen with compounds **39A** (0.013 μM) reduced to **40A** (0.197 μM), compound **39B** (0.190 μM) reduced to **40B** (1.056 μM) and compound **39C** (1.504 μM) reduced to **40C** (2.113 μM). The data in the discussion and **Table 5** demonstrated that 3-(methylsulfonyl) phenyl was a better substituent to have on the left-hand side of the pyrazolopyrimidine core scaffold than 4-(methylsulfonyl) phenyl substituent.

From the pyrazolopyrimidine scaffold, compounds **38A**, **38A**, **39B**, **39D** and **39E** have the selectivity index of more than 100. Therefore, they will be progressed further for solubility (to check if a compound is soluble in aqueous media because for a drug to be absorbed, it must be soluble enough. It must also have good properties of lipophilicity to be able to pass through lipid membranes), chemical stability (to check the stability of a chemical in a certain environment or conditions), microsomal stability (m,r,h) (this is subjecting the compound to mouse (m) liver microsomes, rat (r) liver microsomes and human (h) liver microsomes to study the rate at which the compound is metabolized by the drug metabolizing enzymes found in these liver microsomes.) and *in vitro* PfK1, Dd2 (these are tests done in the laboratory using chloroquine resistant strains of *Plasmodium falciparum* (*Pf*) known as K1 and Dd2. Chloroquine is known to be inactive against K1 or

Dd2 strains, that is why they are called chloroquine resistant strains. They are normally used to check what is known as cross resistance, to see if the potential drug/molecule designed is also inactive (suffering resistant) against these strains just like chloroquine) assays.

Pyrazolopyrimidine compounds demonstrated very good *in vitro* antiplasmodial activity against the sensitive (NF54) strain as compared to the imidazopyridazine compounds. Therefore, pyrazolopyrimidine is a better scaffold to explore to eradicate malaria.

3.2. Future work

Future work will include the following:

- Evaluation of pyrazolopyrimidine series for biological activity against *Pf*PKG and *Pv*PI4Kβ.
- Compounds demonstrating selectivity index of 100 and above will be evaluated for solubility, chemical stability, microsomal stability (m,r,h) and *in vitro* PfK1, Dd2.

CHAPTER 4: EXPERIMENTAL SECTION

4.1. GENERAL INFORMATION

Commercially available reagents and solvents were purchased from Sigma Aldrich and Merck (South Africa) and used without further purification. All reactions involving moisture-sensitive reagents were carried out in an oven-dried glassware under a nitrogen (N2) atmosphere. Reactions that needed hot or cold temperatures were carried out at the appropriate temperatures in an oil bath and an ice bath, respectively. All the measurements were carried out in room temperature with fluctuations ranging from 20 ℃ to 27 ℃. Glassware was thoroughly washed with distilled water, followed by rinsing with acetone and oven dried at 80 °C the day before use. Thin layer chromatography (TLC) on aluminum-baked Merck silica 60 F254 was visualized under Ultra-Violent light with wavelength of 254 nm to monitor the reaction progress. Lasec Cole-Parmer Stuart SMP30 was used to record the melting point. Biological assays were performed at the Holistic Drug Discovery and Development (H3D) Centre at the University of Cape Town, South Africa.

4.2. ANALYSIS AND CHARACTERIZATION TECHNIQUES

The ^{1}H NMR and ^{13}C NMR spectra were obtained from Nuclear Magnetic Resonance (NMR) (Bruker Ascend 400 MHz Topspin 3.2). The NMR spectra were referenced internally using solvent signals. For ^{1}H NMR, the signals were 7.25 ppm for $CDCl_3$, 2.50 ppm for DMSO-d_6, 3.31 ppm for MeOD, and for ^{13}C NMR, the signals were 77.0 ppm for $CDCl_3$, 39.9 ppm for DMSO-d_6, 49.1 ppm for MeOD respectively at room temperature. The ^{1}H NMR spectra were presented as follows: (I) chemical shift (δ) in ppm, (II) Multiplicity (s = singlet, d = doublet, dd = doublet of doublets, t = triplet, m = multiplet), (III) Coupling constant (J) in Hz. The structural properties of the compounds were recorded and confirmed by using High-Resolution Mass Spectrometry (HRMS).

4.3. BIOLOGICAL ASSAYS

4.3.1. Evaluation of the antiplasmodial activity

4.3.1.1. Introduction

The test samples were tested in triplicate over 72 hours on two separate occasions against the wild-type drug sensitive strain (NF54) of the human malaria parasite *Plasmodium falciparum*. Continuous cultures of asexual erythrocyte stages of *P. falciparum* were maintained using the method described by Trager and Jensen [1] with minor modifications. Quantitative assessment of antiplasmodial activity in vitro was determined via the parasite lactate dehydrogenase assay using the method described by Makler *et.al* [2], in which parasite viability is determined colourimetrically using the breakdown of a dye by metabolic enzymes of the glycolytic pathway taking place in living parasites as a marker for survival.

4.3.1.2. Method

The test samples were prepared to a 10 mmol/L stock solution in 100% dimethyl sulfoxide (DMSO). Samples were tested as a suspension if not completely dissolved. Further dilutions to the desired starting concentration were freshly prepared in growth media on each occasion of the experiment. The standard antimalarial drugs chloroquine (CQ) and artesunate (Arts) were used as the reference drug in all experiments. A full dose-response was performed for all compounds in a 96-well plate to determine the concentration inhibiting 50% of parasite growth (IC_{50}–value). Test samples were tested at a starting concentration of 6 mmol/L, which was then serially diluted 2-fold in growth medium to generate the tested concentration range. The same dilution technique was used for all samples. CQ and Arts were tested from a starting concentration of 1 µg/mL. The highest concentration of solvent to which the parasites were exposed was < 0.1% and has no measurable effect on the parasite viability. The assay plate was incubated at 37℃ for 72 h in a sealed gas chamber under 3% O_2 and 4% CO_2 with the balance being N_2. After 72 h, the wells in the assay plate were gently resuspended, and 15 µL from each well was transferred to a duplicate plate containing 100 µL of Malstat reagent and 25 µL of nitroblue tetrazolium solution in each well. Plates were left to develop for 20 minutes in the dark and then absorbance of each well was quantified using a spectrophotometer at 620 nm wavelength.

The remaining population of parasites at each concentration of the test compound was determined by comparing the absorbance of each well to the absorbance of a well containing the drug-free control. Survival was plotted against concentration and the IC-values were obtained using a non-linear dose-response curve fitting analysis via the Dotmatics software platform.

4.3.2. *In vitro Plasmodium* kinase inhibition assays

4.3.2.1. Introduction

Target compounds were tested for inhibitory activity in *Plasmodium* kinase assays. Half-maximal inhibitory concentrations (IC_{50} values) were determined against purified recombinant *P. vivax* phosphatidylinositol 4-kinase type III beta (*Pv*PI4Kβ) and *P. falciparum* cGMP-dependent protein kinase (*Pf*PKG) using an in vitro ADP Glo kinase assay.

4.3.2.2. Method for *in vitro Pf*PKG inhibition assays

Full length *Pf*PKG (*PF*3D7_1436600) was expressed in *E.coli* Rosetta 2 (Novagen, EMD_BIO-71402) as previously described [3]**.** Briefly, the N-terminal His-tagged recombinant *Pf*PKG protein was purified using a HisTrap HP column (GE Healthcare), followed by anion exchange and size exclusion chromatography (HiLoad 16/600 Superdex 200 pg column, GE Healthcare). Final buffer composition of purified protein was 50 mM Tris-HCl pH 8.0, 150 mM NaCl, 10 mM β-mercaptoethanol, 10% glycerol.

*Pf*PKG IC_{50} assays were preformed based on previously described methods using the ADP-Glo Kinase Assay (Promega) to measure ADP formation [4], [5]. Briefly, a 3-fold serial dilution of each inhibitor was carried out in DMSO and inhibitors were subsequently diluted into assay buffer (25 mM HEPES pH 7.4, 0.1 mg/mL BSA, 0.01% (v/v) Triton-X 100, 20 mM MgCl2, 2 mM DTT, 10 µM cGMP) to 1.5 × the final required concentration. 2 µL of each inhibitor dilution was transferred into a white 384-shallow well plate (Nunc #264706). A MANTIS* Liquid Handler (Formulatrix) was used to dispense the remaining assay components. 0.5 µL *Pf*PKG protein, followed by 0.5 µL substrate buffer (ATP and peptide substrate GRTGRRNSI-NH2), was added to each well. The final 3 µL kinase reaction contained ~1 nM *Pf*PKG protein, 10 µM ATP, 20 µM GRTGRRNSI-NH2, 1% (v/v)

DMSO and inhibitor in assay buffer. Reactions were incubated for 45 minutes at 22°C (resulting in < 10% ATP conversion).

ADP formation was measured using the ADP-Glo Kinase Kit (Promega). Briefly, 2 µL ADP-Glo reagent was added to each well and incubated for 40 minutes at 22°C to deplete the remaining ATP. 2 µL of Kinase Detection Reagent was then added and the reaction was incubated for a further 30 minutes at 22°C. The plate was sealed with an adhesive foil seal for all incubation steps. Luminescent signal was measured using the EnSpire Multimode Plate Reader (PerkinElmer). The data was normalized based on the 100% activity controls (1% DMSO only) and the 100% inhibition controls (10 µM ML10 (N-[5-[3-[2-(cyclopropylmethylamino) pyrimidin-4-yl]-7- [(dimethylamino) methyl]-6-methylimidazo [1,2-a]pyridin-2-yl]-2-fluorophenyl] methanesulfonamide), LifeArc). Mean IC_{50} values were calculated from N ≥ 2 independent experiments, each with technical duplicates (log(inhibitor) vs. normalized response - Variable slope). IC_{50} values within 3-fold from independent experiments are considered reproducible.

4.3.2.3. Method for *in vitro Pv*PI4K*β* inhibition assays

Full-length *Pv*PI4Kβ (PVX_098050) recombinant protein was expressed in a baculovirus-insect cell expression system and purified as previously described [5]**,** [67]**.** Briefly, N-terminal His-tagged recombinant *Pv*PI4Kβ protein was purified using a HisTrap HP column (GE Healthcare), followed by size exclusion chromatography (HiLoad 16/600 Superdex 200 pg column, GE Healthcare). Final buffer composition of purified protein was 20 mM HEPES pH 7.5, 500 mM NaCl, 5% (v/v) glycerol, 10 mM β-mercaptoethanol. *Pv*PI4Kβ kinase inhibition assays were performed using the ADP-Glo kinase assay kit (Promega) to measure ADP formation.

L-alpha-phosphatidylinositol (PI; Avanti Polar Lipid, cat. 840042P) dissolved in 3% n-Octylglucoside to a stock concentration of 20 mg/mL was used as the lipid substrate. Briefly, a 3- fold serial dilution of each inhibitor was carried out in DMSO, and inhibitors were subsequently diluted into assay buffer (25 mM HEPES pH 7.4, 100 mM NaCl, 3 mM MgCl2, 1 mM DTT, 0.025 mg/ml BSA, 0.2% (v/v) Triton-X-100) to 1.5 × the final required concentration. 2 µL of each inhibitor dilution was transferred into a white 384-shallow well

plate (Nunc #264706). A MANTIS* Liquid Handler (Formulatrix) was used to dispense the remaining assay components.

0.5 µL *Pv*PI4Kβ protein followed by 0.5 µL substrate buffer (ATP and PI), was added to each well. The final 3 µL kinase reaction contains ~8 nM *Pv*PI4Kβ protein, 10 µM ATP, 0.1 mg/ml PI, 1% (v/v) DMSO and inhibitor in assay buffer. Reactions were incubated for 45 minutes at 22°C (resulting in < 10% ATP conversion). ADP formation was measured using the ADP-Glo Kinase Kit (Promega) as described for *Pf*PKG, the only difference being that 10 mM $MgCl_2$ was added to the ADP-Glo reagent prior to use. *Pv*PI4Kβ inhibitor MMV390048 at 10 µM was used as the control (100% inhibition) and data were analyzed as described for *Pf*PKG.

4.4. SYNTHESIS

4.4.1. Synthesis of 6-chloroimidazo[1,2-b]pyridazine (29)

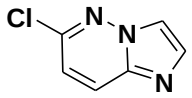

29

Bromoacetaldehyde diethylacetal (4.6 mL, 30.8 mmol, 2 eq) and 3-amino-6-chloropyridazine **27** (2.0 g, 15.4 mmol, 1 eq) were dissolved in ethanol (20 mL) and water (30 mL). Hydrobromic acid (1.76 mL) was then added. The reaction mixture was heated under reflux for 18 hrs at 103 ℃. After completion (monitored by TLC, 50% ethyl acetate/ hexane), the reaction mixture was allowed to cool to room temperature (25 ℃). Ethanol was removed under reduced pressure. The pH of the remaining solution was adjusted to pH 7 using 15% sodium hydroxide (NaOH) solution. The aqueous work-up was done using ethyl acetate. The organic phases were combined and rinsed with brine, followed by drying over anhydrous sodium sulphate ($NaSO_4$). Ethyl acetate was removed in vacuo to afford the compound **29** (2.3 g, 96%). The crude product was purified by Combi flash chromatography using 50% ethyl acetate/ hexane if unclean [2], [68]. ^{1}H NMR (400 MHz, $CDCl_3$), δ (ppm): 8.00 (d, 1H, J = 9.6 Hz), 7.95 (d, 1H), 7.80 (d, 1H), 7.11 (d, 1H, J = 9.2 Hz).

4.4.2. Synthesis of 6-chloro-3-iodoimidazo[1,2-b]pyridazine (30)

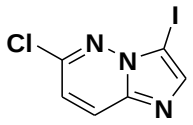

30

N-Iodosuccinimide (NIS) (2.4 g, 10.7 mmol, 1.1 eq) and compound **29** (1.5 g, 9. 8 mmol, 1 eq) were dissolved in *N,N*-Dimethylformamide (DMF) (30 mL). The solution was stirred at room temperature (25 ℃) for 4 days. After completion as monitored by TLC, DMF was removed under reduced pressure. The aqueous work-up was done using dichloromethane (DCM). The organic phases were combined and washed with saturated solution of sodium metabisulfite ($Na_2SO_2O_5$), followed by rinsing with brine and dried over anhydrous $NaSO_4$. DCM was removed in vacuo and the resulting compound was crystallized in diethyl ether (Et_2O) to afford compound **30** (2.0g, 74% yield) [1], [2]. ^1H NMR (400 MHz, $CDCl_3$), δ (ppm): 8.06 (d, 1H, J = 9.6 Hz), 7.89 (s, 1H), 7.23 (d, 1H, J = 9.6 Hz).

4.4.3. Synthesis of 6-chloro-3-(4-(methylsulfonyl)phenyl)imidazo[1,2-b]pyridazine (32)

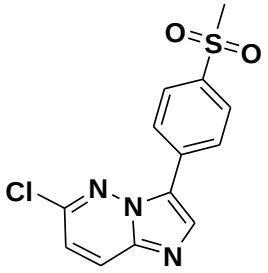

32

Compound **30** (1.8 g, 6.6 mmol, 1 eq), 4-(methylsulfonyl)phenyl boronic acid (1.4 g, 7.2 mmol, 1.1 eq) and bis(triphenyphosphine)palladium (II) dichloride ($Pd(PPh_3)_2Cl_2$) (0.2 g, 0.3 mmol, 0.05 eq) were dissolved in 1.4-Dioxane (50 mL). The resulting mixture was flushed with nitrogen gas for 15 to 20 minutes while stirring. An aqueous solution of potassium carbonate (K_2CO_3) (1.3 g, 9.8 mmol, 1.5 eq) was then added. The reaction mixture was heated under reflux for 18 hrs at 90 ℃. After completion (monitored by TLC, 5% MeOH)/ DCM, the reaction mixture was allowed to cool to room temperature (25 ℃).

1,4-Dioxane was removed under reduced pressure. The resulting mixture was diluted with 10% MeOH/DCM and filtered through celite. The aqueous work-up was done using DCM (3x30 mL). The organic phases were combined and rinsed with brine, followed by drying over anhydrous $NaSO_4$. The solvents were removed in vacuo and the residues were purified by Combi Flash chromatography using 5% MeOH/DCM to afford compound **32** (1.5 g, 75% yield) [2], [68]. ^{1}H NMR (400 MHz, $CDCl_3$), δ (ppm): 8.29 (d, 2H, J = 8.7 Hz), 8.19 (s, 1H), 8.07 (d, 2H, J = 8.7 Hz), 8.02 (d, 1H, J = 9.4 Hz), 7.18 (d, 1H, J = 9.4 Hz), 3.10 (s, 3H). ^{13}C NMR (100 MHz, $CDCl_3$), δ (ppm): 44.6, 119.5, 127,0, 127.1, 127.7, 128.0, 128.3, 133.2, 134.8, 139.5, 139.6, 147.4.

4.4.4. General procedure for the synthesis of compound 20A to 20O

Compound **32** (60.0 mg, 0.2 mmol, 1 eq), 2-methoxyphenylboronic acid (44.5 mg, 0.3 mmol, 1.5 eq) and Bis(triphenyphosphine)palladium (II) dichloride ($Pd(PPh_3)_2Cl_2$) (6.8 mg, 0.0098 mmol, 0.05 eq) were dissolved in 1.4-Dioxane (6 mL). The resulting mixture was flushed with nitrogen gas for 15 to 20 minutes while stirring. An aqueous solution of potassium carbonate (K_2CO_3) (40.4 mg, 0.3 mmol, 1.5 eq) was then added. The reaction mixture was heated under reflux for 18 hrs at 110 ℃. After completion (monitored by TLC, 5% methanol (MeOH)/ DCM), the reaction mixture was allowed to cool to room temperature (25 ℃). 1,4-Dioxane was removed under reduced pressure. The resulting mixture was diluted with 10% MeOH/DCM and dried over celite. The aqueous work-up was done using DCM. The organic phases were combined and rinsed with brine, followed by drying over anhydrous $NaSO_4$. The solvents were removed in vacuo and the residues were purified by Combi Flash chromatography using 5% MeOH/DCM to afford compound **20A** to **20O** [2], [68].

6-(2-methoxyphenyl)-3-(4-(methylsulfonyl)phenyl)imidazo[1,2-b]pyridazine.

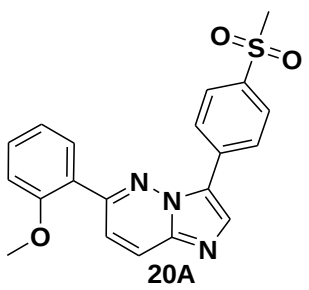

20A

2-methoxyphenylboronic acid 32.9 mg, Obtained mass: 29 mg, Percentage yield 38%. Mp: 204.7 to 207.1 ℃. ^{1}H NMR (400 MHz, $CDCl_3$), δ (ppm): 3.08 (s, 3H), 3.91 (s,3H), 7.10 (m, 2H), 7.50 (m, 1H), 7.65 (d, 1H, *J* = 9.5 Hz), 7.71 (m, 1H), 8.02 (d, 3H, *J* = 8.3 Hz), 8.19 (s, 1H), 8.39 (d, 2H, *J* = 8.2 Hz). ^{13}C NMR (100 MHz, $CDCl_3$), δ (ppm): 44.6, 55.7, 114.0, 119.1, 120.3, 121.3, 124.7, 126.7, 127.9, 128.6, 129.6, 134.1, 134.4, 157.0, 157.4. HRMS $[M+H]^+$, m/z, calculated: $C_{20}H_{18}N_3O_3S^+$= 380.1063, found = 380.1062.

6-(3-methoxyphenyl)-3-(4-(methylsulfonyl)phenyl)imidazo[1,2-b]pyridazine

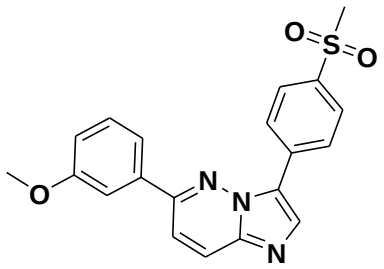

20B

3-methoxyphenylboronic acid 32.9 mg, Obtained mass: 25 mg, Percentage yield: 33%. Mp: 208.4 to 212.1 ℃. ^{1}H NMR (400 MHz, $CDCl_3$), δ (ppm): 3.11 (s, 3H), 3.91 (s, 3H), 7.07 (m, 1H), 7.47 (m, 1H), 7.55 (m, 2H,), 7.61 (d, 1H, *J* = 9.5 Hz), 8.07 (d, 2H, *J* = 8.6 Hz), 8.11 (d, 1H, *J* = 9.5 Hz), 8.20 (s, 1H), 8.42 (d, 2H, *J* = 8.6 Hz).^{13}C NMR (100 MHz, $CDCl_3$), δ (ppm): 44.7, 55.5, 112.2, 112.5, 113.0, 113.6, 115.6, 116.9, 119,5, 128.5, 128.6, 130.4, 132.1, 132.2, 134.2, 134.7, 160.2. HRMS $[M+H]^+$, m/z, calculated: $C_{20}H_{18}N_3O_3S^+$= 380.1063, found = 380.1068.

6-(4-methoxyphenyl)-3-(4-(methylsulfonyl)phenyl)imidazo[1,2-b]pyridazine

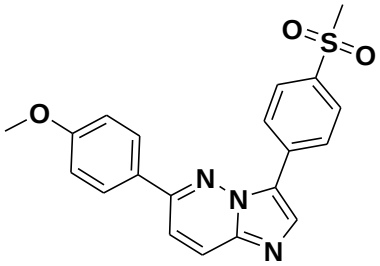

20C

4-methoxyphenylboronic acid 32.9 mg, Obtained mass: 43 mg, Percentage yield: 58%. Mp: 215.9 to 216.4 ℃. ^{1}H NMR (400 MHz, $CDCl_3$), δ (ppm): 3.10 (s, 3H), 3.90 (s, 3H), 7.06 (d, 2H, *J* = 8.9 Hz), 7.57 (d, 1H, *J* = 9.5 Hz), 7.95 (d, 2H, *J* = 8.8 Hz), 8.06 (d, 3H, *J* = 8.9 Hz), 8.15 (s, 1H), 8.40 (d, 2H, *J* = 8.6 Hz).^{13}C NMR (100 MHz, $CDCl_3$), δ (ppm): 44.7, 55.5, 114.8, 126.2, 126.8, 127.6, 127.7, 127.9, 128.5, 134.4,138.7, 140.3, 158.7, 161.5. HRMS $[M+H]^+$, m/z, calculated: $C_{20}H_{18}N_3O_3S^+$= 380.1063, found = 380.1071.

6-(4-methoxystyryl)-3-(4-(methylsulfonyl)phenyl)imidazo[1,2-b]pyridazine.

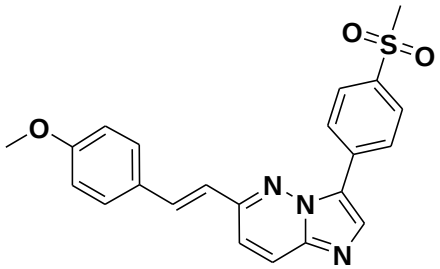

20D

(E)-2-(4-methoxyphenyl)vinylboronic acid 52.0 mg, Obtained mass: 49 mg, Percentage yield: 62%. Mp: 217.3 to 219.4 ℃. ^{1}H NMR (400 MHz, $CDCl_3$), δ (ppm): 3.12 (s, 3H), 3.90 (s, 3H), 7.06 (d, 2H, *J* = 8.9 Hz), 7.57 (d, 1H, *J* = 9.5 Hz), 7.95 (d, 2H, *J* = 8.9 Hz), 8.07 (d, 3H, *J* = 8.9 Hz), 8.16 (s, 1H), 8.40 (d, 2H, *J* = 8.7 Hz). ^{13}C NMR (100 MHz, $CDCl_3$), δ (ppm): 44.7, 55.5, 116.5, 126.2, 126.8, 127.9, 128.5, 132.0, 132.2, 134.3, 134.4, 138.7, 140.3, 151.8, 161.5.

tert-butyl 5,6-dihydro-4-(3-(4-(methylsulfonyl)phenyl)imidazo[1,2-b] pyridazin-6-yl) pyridine-1(2H)-carboxylate

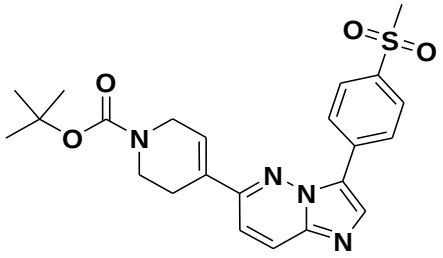

20E

Tert-butyl 5,6-dihydro-4-(4,4,5,5-tetramethyl-1,3,2-dioxaborolan-2-yl) pyridine-1(2H)-carboxylate 90.4 mg, Obtained mass: 62 mg, Percentage yield: 70%. Mp: 215.9 to 216.4 ℃. ^{1}H NMR (400 MHz, $CDCl_3$), δ (ppm): 1.49 (s, 9H), 2.76 (m, 2H), 3.11 (s, 3H), 3.69 (t, 2H, *J* = 5.2 Hz), 4.20 (m, 2H), 6.61 (m, 1H), 7.42 (d, 1H, *J* = 9.6 Hz), 7.99 (d, 1H, *J* = 9.6 Hz), 8.04 (d, 2H, *J* = 8.6 Hz), 8.13 (s, 1H), 8.31 (d, 2H, *J* = 8.6 Hz). ^{13}C NMR (100 MHz, $CDCl_3$), δ (ppm): 28.5, 29.7, 41.2, 43.5, 44.6, 80.2, 125.7, 126.8, 127.9, 128.5, 128.6, 132.1, 132.2, 134.3, 138.8, 140.3, 151.5, 154.7. HRMS [M+H] $^{+}$, m/z, calculated: $C_{23}H_{27}N_4O_4S^{+}$= 455.1748, found = 455.1753.

Compound 20F.

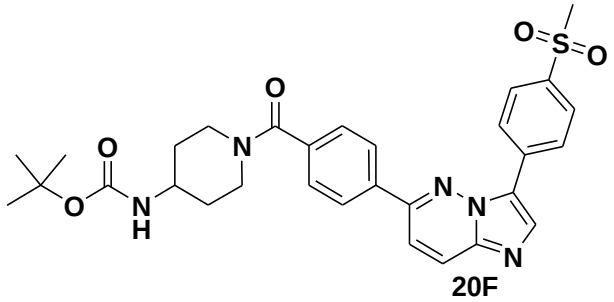

20F

Boronic acid 101.9 mg, Obtained mass: 55 mg, Percentage yield: 53%. Mp: 147.5 to 150.2 ℃. ^{1}H NMR (400 MHz, $CDCl_3$), δ (ppm): 1.41 (s, 9H), 2.02 (m, 2H), 3.12 (s, 3H), 2.98 (m, 2H), 3.73 (m, 3H), 4.70 (m, 2H), 7.50 (d, 1H, *J* = 7.6 Hz), 7.60 (m, 3H), 8.00 (s, 1H), 8.06 (d, 3H, *J* = 8.5 Hz), 8.13 (d, 1H, *J* = 9.5 Hz), 8.19 (s, 1H), 8.36 (d, 2H, *J* = 8.5 Hz). ^{13}C NMR (100 MHz, $CDCl_3$), δ (ppm): 29.7, 31.0, 41.3, 44.6, 47.9, 79.7, 125.7, 126.7,

127.9, 128.3, 128.6, 129.5, 134.0, 134.9, 135.8, 139.0, 151.3, 155.2, 169.7. HRMS [M+H]$^{+}$, m/z, calculated: $C_{30}H_{34}N_5O_5S^+$= 476.2275, found = 476.2255

ethyl 2-(3-(4-(methylsulfonyl)phenyl)imidazo[1,2-b]pyridazin-6-yl)benzoate

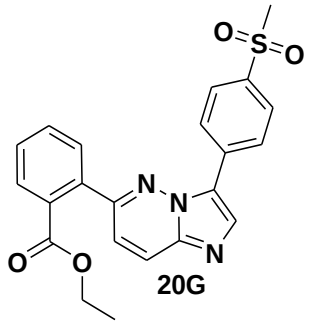

20G

2-(ethoxycarbonyl)phenylboronic acid 56.8 mg, Obtained mass: 35 mg, Percentage yield: 43%. Mp: 185.5 to 187.5 ℃. ^{1}H NMR (400 MHz, $CDCl_3$), δ (ppm): 1.02 (t, 3 H, J = 7.1 Hz), 3.07 (s, 3H), 4.10 (q, 2H, J = 7.1 Hz), 7.29 (d, 1H, J = 9.3 Hz), 7.45 (m, 1H), 7.60 (m, 1H, J = 8.7 Hz), 7.66 (m, 1H), 8.00 (d, 3H, J = 8.4 Hz), 8.08 (d, 1H, J = 9.3 Hz), 8.21 (s, 1H), 8.31 (d, 2H, J = 8.4 Hz). ^{13}C NMR (100 MHz, $CDCl_3$), δ (ppm): 14.2, 44.6, 61.4, 119.6, 125.4, 126.8, 127.9, 128.5, 128.6, 129.7, 130.4, 130.7, 132.0, 132.2, 134.0, 134.5, 137.1, 138.8, 154.0, 167.4. HRMS [M+H] $^{+}$, m/z, calculated: $C_{22}H_{20}N_3O_4S^+$= 422.1169, found = 422.1162

6-(3-fluorophenyl)-3-(4-(methylsulfonyl)phenyl)imidazo[1,2-b]pyridazine.

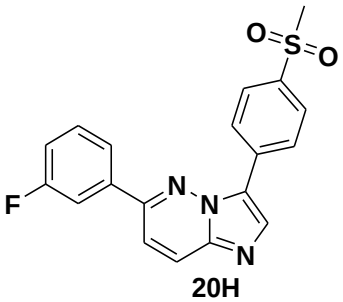

20H

3-fluorophenylboronic acid 40.9 mg, Obtained mass: 35 mg, Percentage yield: 49%. Mp: 230.5 to 232.5 ℃. ^{1}H NMR (400 MHz, $CDCl_3$), δ (ppm): 3.12 (s, 3H), 7.20 (m, 1H), 7.45 (m, 1H), 7.52 (m, 2H), 7.60 (d, 1H, J = 9.5 Hz), 8.08 (d, 2H, J = 8.6 Hz), 8.13 (d, 1H, J = 9.5 Hz), 8.21 (s, 1H), 8.37 (d, 2H, J = 8.5 Hz). ^{13}C NMR (100 MHz, $CDCl_3$), δ (ppm): 44.6, 114.02, 117.3, 122.8, 126.7, 126.9, 128.0, 128.6, 128.7, 130.9, 134.9, 137.5, 139.0,

162.0, 164.5. HRMS [M+H] $^{+}$, m/z, calculated: $C_{19}H_{15}FN_2O_2S^{+}$ = 368.0864, found = 368.0875.

3-(4-(methylsulfonyl)phenyl)-6-(2-(trifluoromethoxy)phenyl)imidazo[1,2-b]pyridazine.

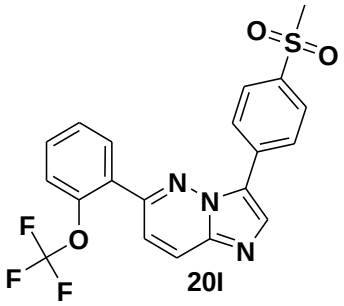

20I

2-(trifluoromethoxy)phenylboronic acid 60.3 mg, Obtained mass: 51 mg, Percentage yield: 60%. Mp: 152.1 to 155.5 ℃. ^{1}H NMR (400 MHz, $CDCl_3$), δ (ppm): 3.09 (s, 3H), 7.45 (m, 1H), 7.50 (d, 1H, *J* = 9.5 Hz), 7.57 (m, 1H), 7.65 (m, 1H), 7.79 (d, 1H, *J* = 9.4 Hz), 8.04 (d, 2H, *J* = 8.7 Hz), 8.12 (d, 1H, *J* = 9.5 Hz), 8.23 (s, 1H), 8.36 (d, 2H, *J* = 8.6 Hz). ^{13}C NMR (100 MHz, $CDCl_3$), δ (ppm): 44.6, 119.1, 121.7, 125.8, 126.9, 127.6, 127.9, 128.5, 128.7, 129.7, 134.8, 138.9, 140.1, 146.8, 150.2. HRMS [M+H] $^{+}$, m/z, calculated: $C_{19}H_{15}FN_2O_2S^{+}$= 434.0781, found = 434.0787.

3-(4-(methylsulfonyl)phenyl)-6-(4-(trifluoromethoxy)phenyl)imidazo[1,2-b]pyridazine.

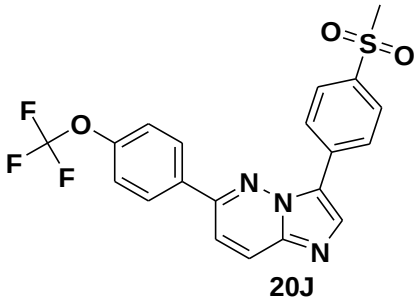

20J

4-(trifluoromethoxy)phenylboronic acid 60.3 mg, Obtained mass: 41 mg, Percentage yield: 48%. Mp: 162.3 to 164.5 ℃. ^{1}H NMR (400 MHz, $CDCl_3$), δ (ppm): 3.12 (s, 3H), 7.41 (d, 2H, *J* = 8.4 Hz), 7.60 (d, 1H, *J* = 9.5 Hz), 8.04 (d, 2H, *J* = 8.8 Hz), 8.09 (d, 2H, *J* = 8.7 Hz), 8.16 (d, 1H, *J* = 9.6 Hz), 8.22 (s, 1H), 8.38 (d, 2H, *J* = 8.6 Hz). ^{13}C NMR (100 MHz,

$CDCl_3$), δ (ppm): 44.6, 116.4, 121.5, 126.7, 127.0, 128.0, 128.5, 128.7, 128.8, 132.0, 132.1, 139.1, 151.0. HRMS $[M+H]^+$, m/z, calculated: $C_{19}H_{15}FN_2O_2S^+$= 434.0781, found = 434.0777.

3-(4-(methylsulfonyl)phenyl)-6-(thiophen-2-yl)imidazo[1,2-b]pyridazine.

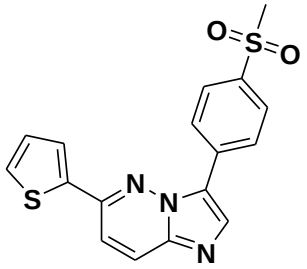

20K

Thiophen-2-yl-2-boronic acid 61.5 mg, Obtained mass: 34 mg, Percentage yield: 49%. Mp: 208.8 to 211.8 ℃. ^{1}H NMR (400 MHz, $CDCl_3$), δ (ppm): 3.12 (s, 3H), 7.18 (m, 1H), 7.45 (m, 1H), 7.54 (m, 1H), 7.65 (m, 1H), 8.06 (m, 3H), 8.17 (s, 1H), 8.42 (d, 2H, *J* = 8.5 Hz). ^{13}C NMR (100 MHz, $CDCl_3$), δ (ppm): 44.7, 126.3, 126.7, 127.4, 127.9, 128.3, 128.5, 128.6, 129.3, 134.5, 138.3, 138.8, 139.5, 147.8. HRMS $[M+H]^+$, m/z, calculated: $C_{17}H_{14}N_3O_2S_2^+$= 356.0522, found = 356.0521.

3-(4-(methylsulfonyl)phenyl)-6-(thiophen-3-yl)imidazo[1,2-b]pyridazine.

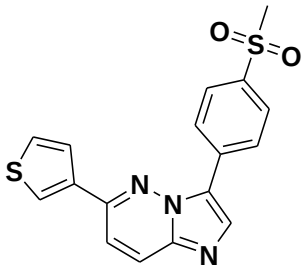

20L

Thiophen-3-yl-3-boronic acid 61.5 mg, Obtained mass: 31 mg, Percentage yield: 45%. Mp: 205.8 to 206.7 ℃. ^{1}H NMR (400 MHz, $CDCl_3$), δ (ppm): 3.11 (s, 3H), 7.19 (d, 1H, *J* = 9.4 Hz), 7.50 (m, 1H), 7.55 (d, 1H, *J* = 9.4 Hz), 7.93 (m, 1H), 8.04 (d, 1H, *J* = 9.4 Hz), 8.19 (s, 1H), 8.29 (d, 2H, *J* = 8.6 Hz), 8.39 (d, 2H, *J* = 8.6 Hz). ^{13}C NMR (100 MHz, $CDCl_3$), δ (ppm): 44.7, 126.3, 119.5, 125.4, 126.0, 126.4, 126.9, 127.0, 127.9, 128.0, 134.8, 137.7,

138.9, 139.5, 147.4. HRMS $[M+H]^+$, m/z, calculated: $C_{17}H_{14}N_3O_2S_2^+$= 356.0522, found = 356.0536.

3-(4-(methylsulfonyl)phenyl)-6-(pyridin-4-yl)imidazo[1,2-b]pyridazine.

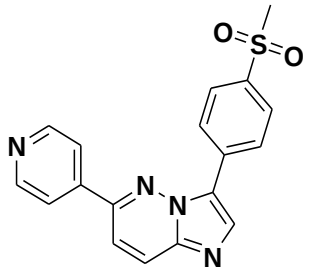

20M

Pyridin-4-yl-4-boronic acid 36.0 mg, Obtained mass: 31 mg, percentage yield: 45%. Mp: 273.1 to 275.2 ℃. ^{1}H NMR (400 MHz, $CDCl_3$), δ (ppm): 3.37 (s, 3H), 8.08 (d, 1H, *J* = 9.5 Hz), 8.11 (d, 2H, *J* = 8.5 Hz), 8.17 (d, 2H, *J* = 5.9 Hz), 8.46 (d, 1H, *J* = 9.5 Hz), 8.55 (d, 3H, *J* = 8.2 Hz), 8.82 (d, 2H, *J* = 5.5 Hz). ^{13}C NMR (100 MHz, $CDCl_3$), δ (ppm): 44.0, 117.1, 121.8, 126.7, 127.1, 127.4, 128.1, 133.5, 136.1, 139.6, 142.6, 149.8, 151.1.

Compound 20N.

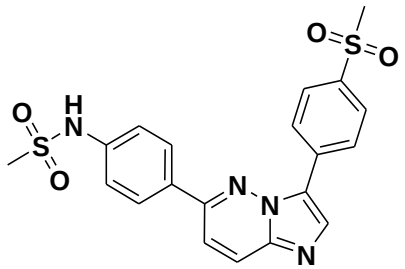

20N

Boronic acid 87.0 mg, Obtained mass: 28 mg, Percentage yield: 33%. Mp: 285.8 to 288.2 ℃. ^{1}H NMR (400 MHz, $CDCl_3$), δ (ppm): 3.11 (s, 3H), 3.29 (s, 3H), 7.41 (d, 2H, *J* = 8.8 Hz), 7.96 (d, 1H, *J* = 9.6 Hz), 8.10 (d, 2H, *J* = 8.7 Hz), 8.18 (d, 2H, *J* = 8.8 Hz), 8.35 (d, 1H, *J* = 9.6 Hz), 8.50 (s, 1H), 8.57 (d, 2H, *J* = 8.7 Hz), 10.21 (s, 1H). ^{13}C NMR (100 MHz, $CDCl_3$), δ (ppm): 44.0, 119.5, 126.8, 127.0, 128.1, 128.8, 130.1, 133.8, 139.4, 141.0, 151.4. HRMS $[M+H]^+$, m/z, calculated: $C_{18}H_{15}N_4O_2S^+$= 443.0842, found = 443.0843.

3-(4-(methylsulfonyl)phenyl)-6-m-tolylimidazo[1,2-b]pyridazine.

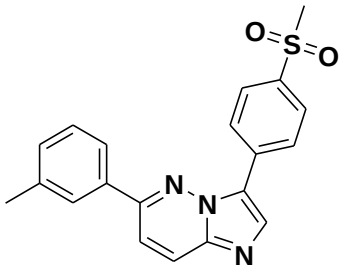

20O

3-methylphenylboronic acid 39.8 mg, Obtained mass: 49 mg, Percentage yield: 69%. Mp: 199.8 to 202.6 ℃. ^{1}H NMR (400 MHz, $CDCl_3$), δ (ppm): 2.49 (s, 3H), 3.12 (s,3H), 7.36 (m, 1H), 7.45 (m, 1H), 7.61 (d, 1H, *J* = 9.5 Hz), 7.79 (d, 2H, *J* = 7.1 Hz), 8.07 (d, 2H, *J* = 8.6 Hz), 8.11 (d, 1H, *J* = 9.5 Hz), 8.20 (s, 1H), 8.42 (d, 2H, *J* = 8.6 Hz). ^{13}C NMR (100 MHz, $CDCl_3$), δ (ppm): 29.7, 44.7, 116.9, 124.4, 126.3, 126.9, 127.8, 127.9, 129.2, 131.2, 134.6. HRMS $[M+H]^+$, m/z, calculated: $C_{20}H_{18}N_3O_2S^+$= 364,1114 found = 364.1110.

4.4.5. General procedure for the bromination

Compound **36** or **37** (317 mg, 1.2 mmol, 1 eq) was dissolved in ice cold acetonitrile (20 mL) and NBS (227 mg, 1.3 mmol, 1.1 eq) was added dropwise. The reaction was allowed to reach room temperature (25℃) while stirring for 2 hrs. After completion (monitored by TLC 50% ethyl acetate/hexane), acetonitrile was removed. The aqueous work-up was done using ethyl acetate (3x15 mL). The organic phases were combined and rinsed with brine, followed by drying over anhydrous $NaSO_4$. The solvents were removed in vacuo and the residues were purified by Combi Flash chromatography using 50% ethyl acetate/hexane to afford compound **38** and **39** [1], [2].

3-bromo-5-(4-(methylsulfonyl)phenyl)pyrazolo[1,5-a]pyrimidine.

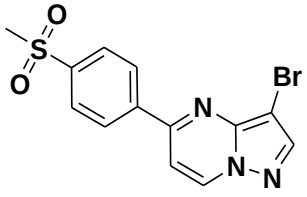

38

Obtained mass: 374 mg. Percentage yield 92%. ^{1}H NMR (400 MHz, $CDCl_3$), δ (ppm): 3.11 (s, 3H), 7.36 (d, 1H, *J* = 7.4 Hz), 8.10 (d, 2H, *J* = 8.2 Hz), 8.17 (s, 1H), 8.35 (d, 2H, *J* = 8.5 Hz), 8.74 (d, 1H, *J* = 7.4 Hz).

3-bromo-5-(3-(methylsulfonyl)phenyl)pyrazolo[1,5-a]pyrimidine.

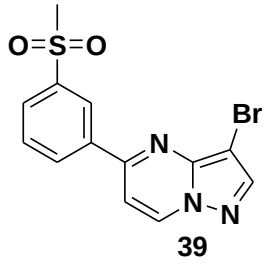

39

Obtained mass: 319 mg. Percentage yield 78%. ^{1}H NMR (400 MHz, $CDCl_3$), δ (ppm): 3.14 (s, 3H), 7.37 (d, 1H, *J* = 7.3 Hz), 7.75 (m, 1H), 8.08 (d, 1H, *J* = 7.8 Hz), 8.16 (s, 1H), 8.50 (d, 1H, *J* = 7.9 Hz), 8.65 (m, 1H), 8.74 (d, 1H, *J* = 7.4 Hz).

4.4.6. General procedure for the synthesis of compound 38A to 38F and 39A to 39E.

Compound **38** or **39** (60.0 mg, 0.2 mmol, 1 eq), 2-methoxyphenylboronic acid (44.5 mg, 0.3 mmol, 1.5 eq) and Bis(triphenyphosphine)palladium (II) dichloride ($Pd(PPh_3)_2Cl_2$) (6.8 mg, 0.0098 mmol, 0.05 eq) were dissolved in 1.4-Dioxane (6 mL). The resulting mixture was flushed with nitrogen gas for 15 to 20 minutes while stirring. An aqueous solution of potassium carbonate (K_2CO_3) (40.4 mg, 0.3 mmol, 1.5 eq) was then added. The reaction mixture was heated under reflux for 18 hrs at 110 ℃. After completion (monitored by TLC, 5% methanol (MeOH)/ DCM), the reaction mixture was allowed to cool to room temperature (25 ℃). 1,4-Dioxane was removed under reduced pressure. The resulting mixture was diluted with 10% MeOH/DCM and dried over celite. The aqueous work-up was done using DCM (3x15 mL). The organic phases were combined and rinsed with brine, followed by drying over anhydrous $NaSO_4$. The solvents were removed in vacuo and the residues were purified by Combi Flash chromatography using 5% MeOH/DCM to afford compound **38A to 38F and 39A to 39E**.

3,5-bis(4-(methylsulfonyl)phenyl)pyrazolo[1,5-a]pyrimidine.

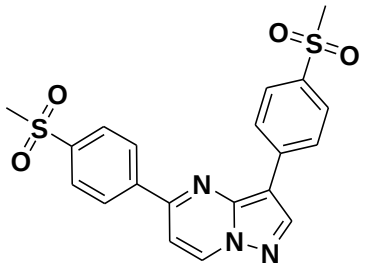

38A

4-(methylsulfonyl)phenylboronic acid 51.1 mg, Obtained mass: 38 mg, Percentage yield: 52%. Mp: 294.3 to 295.6 ℃. ^{1}H NMR (400 MHz, $CDCl_3$), δ (ppm): 3.11 (s, 3H), 3.13 (s, 3H), 7.44 (d, 1H, *J* = 7.3 Hz), 7.79 (d, 1H, *J* = 8.5 Hz), 8.05 (d, 2H, *J* = 8.5 Hz), 8.14 (d, 2H, *J* = 8.5 Hz), 8.36 (m, 3H), 8.58 (s, 1H), 8.84 (d, 1H, *J* = 7.3 Hz). ^{13}C NMR (100 MHz, $CDCl_3$), δ (ppm): 44.5, 96.7, 126.5, 127.0, 127.9, 128.5, 134.7, 137.7, 139.1, 140.2, 157.8. HRMS $[M+H]^+$, m/z, calculated: $C_{20}H_{18}N_3O_4S_2^+$= 428,0733 found = 428.0733.

5-(4-(methylsulfonyl)phenyl)-3-(6-(methylsulfonyl)pyridin-3-yl)pyrazolo[1,5-a]pyrimidine

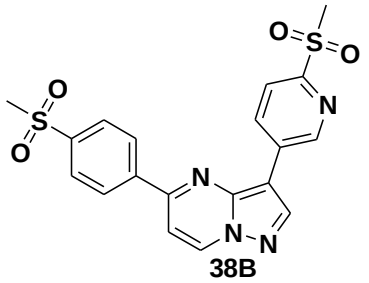

38B

5-(4,4,5,5-tetramethyl-1,3,2-dioxaborolan-2-yl)-2-(methylsulfonyl)pyridine 72.4 mg, Obtained mass: 41 mg, Percentage yield: 56%. Mp: 253.8 to 254.4 ℃. ^{1}H NMR (400 MHz, $CDCl_3$), δ (ppm): 3.14 (s, 3H), 3.27 (s, 3H), 7.49 (d, 1H, *J* = 7.4 Hz), 8.14 (d, 2H, *J* = 8.5 Hz), 8.35 (d, 2H, *J* = 8.5 Hz), 8.63 (m, 2H), 8.87 (d, 1H, *J* = 7.3 Hz), 8.97 (d, 1H, *J* = 1.2 Hz), 9.60 (d, 1H, *J* = 1.6 Hz). ^{13}C NMR (100 MHz, $CDCl_3$), δ (ppm): 40.5, 44.5, 65.9, 106.5, 121.5, 128.3, 128.4, 134.0, 136.5, 137.1, 147.5, 148.5. HRMS $[M+H]^+$, m/z, calculated: $C_{19}H_{17}N_4O_4S_2^+$= 429,0686 found = 428.0696.

5-(4-(methylsulfonyl)phenyl)-3-(pyridin-4-yl)pyrazolo[1,5-a]pyrimidine.

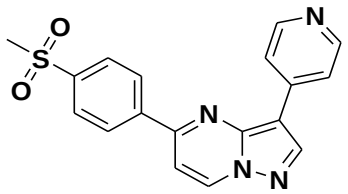

38C

Pyridin-4-yl-4-boronic acid 34.0 mg, Obtained mass: 40 mg, Percentage yield: 61%. Mp: 254.5 to 255.8 ℃. ^{1}H NMR (400 MHz, $CDCl_3$), δ (ppm): 3.15 (s, 3H), 7.64 (d, 1H, 7.4 Hz), 8.21 (d, 2H, 8.2 Hz), 8.37 (d, 2H, 8.4 Hz), 8.63 (m, 4H), 8.74 (s, 1H), 8.96 (d, 1H, 7.3 Hz). ^{13}C NMR (100 MHz, $CDCl_3$), δ (ppm): 44.7, 87.6, 126.5, 127.0, 127.9, 128.5, 128.8 129.0, 139.1, 140.2, 147.8. HRMS $[M+H]^+$, m/z, calculated: $C_{18}H_{15}N_4O_2S^+$= 351,0910 found = 351.0923.

N,N-dimethyl-3-(5-(4-(methylsulfonyl)phenyl)pyrazolo[1,5-a]pyrimidin-3-yl)benzenamine.

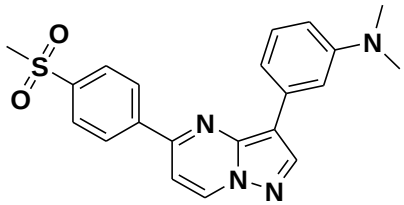

38D

3-(dimethylamino)phenylboronic acid 45.7 mg, Obtained mass: 38 mg, Percentage yield: 53%. Mp: 217.5 to 219.3 ℃. ^{1}H NMR (400 MHz, $CDCl_3$), δ (ppm): 3.09 (s, 6H), 3.12 (s, 3H), 7.35 (d, 1H, J = 7.4 Hz), 7.45 (m, 2H), 7.53 (m, 1H), 7.65 (m, 1H), 8.10 (d, 2H, J = 8.4 Hz), 8.40 (d, 2H, J = 8.3 Hz), 8.51 (s, 1H), 8.78 (d, 1H, J = 7.3 Hz). ^{13}C NMR (100 MHz, $CDCl_3$), δ (ppm): 44.5, 105.1, 128.1, 128.5, 128.6, 129.6, 132.0, 132.1, 132.2, 135.9, 141.8, 142.1, 143.9, 144.5. HRMS $[M+H]^+$, m/z, calculated: $C_{21}H_{21}N_4O_2S^+$= 393,1380 found = 393.1376.

3-(2-methoxyphenyl)-5-(4-(methylsulfonyl)phenyl)pyrazolo[1,5-a]pyrimidine.

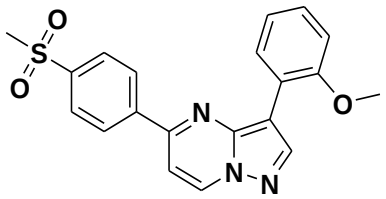

38E

2-methoxyphenylboronic acid 38.8 mg, Obtained mass: 37 mg, Percentage yield: 54%. Mp: 230.5 to 232.5 ℃. ^{1}H NMR (400 MHz, $CDCl_3$), δ (ppm): 3.10 (s, 3H), 3.95 (s, 3H), 7.04 (d, 1H, *J* = 8.2 Hz), 7.14 (m, 1H), 7.32 (m, 2H), 8.09 (d, 2H, *J* = 8.6 Hz), 8.34 (d, 2H, *J* = 8.5 Hz), 8.44 (m, 1H), 8.80 (d, 2H, *J* = 6.4 Hz). ^{13}C NMR (100 MHz, $CDCl_3$), δ (ppm): 43.5, 54.5, 104.0, 119.9, 126.7, 127.0, 127.1, 127.4, 128.6, 134.7, 140.6, 146.0, 152.2, 155.4. HRMS $[M+H]^+$, m/z, calculated: $C_{20}H_{18}N_3O_3S^+$= 380,1063 found = 380.1058.

3-(4-methoxyphenyl)-5-(4-(methylsulfonyl)phenyl)pyrazolo[1,5-a]pyrimidine.

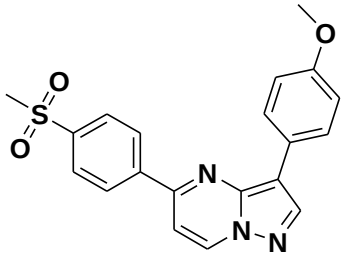

38F

4-methoxyphenylboronic acid 38.8 mg, Obtained mass: 39 mg, Percentage yield: 56%. Mp: 236.5 to 237.9 ℃. ^{1}H NMR (400 MHz, $CDCl_3$), δ (ppm): 3.11 (s, 3H), 3.87 (s, 3H), 7.04 (d, 2H, *J* = 8.9 Hz), 7.30 (d, 1H, *J* = 7.4 Hz), 8.04 (d, 2H, *J* = 8.9 Hz), 8.10 (d, 2H, *J* = 8.6 Hz), 8.34 (d, 2H, *J* = 8.6 Hz), 8.43 (s, 1H), 8.74 (d, 1H, *J* = 7.4 Hz). ^{13}C NMR (100 MHz, $CDCl_3$), δ (ppm): 43.5, 54.5, 96.7, 110.5,113.3, 126.5, 127.0, 127.9, 134.7, 140.7, 141.1, 142.2, 157.4, 157.6. HRMS $[M+H]^+$, m/z, calculated: $C_{20}H_{18}N_3O_3S^+$= 380,1063 found = 380.1063.

5-(3-(methylsulfonyl)phenyl)-3-(pyridin-4-yl)pyrazolo[1,5-a]pyrimidine

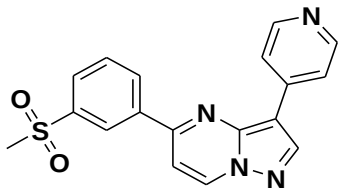

39A

Pyridin-4-yl-4-boronic acid 34.0 mg, Obtained mass: 48 mg, Percentage yield: 75% Mp: 255.7 to 256.2 ℃. ^{1}H NMR (400 MHz, $CDCl_3$), δ (ppm): 3.40 (s, 3H), 7.92 (m, 1H), 8.04 (d, 1H, *J* = 7.4 Hz), 8.15 (d, 1H, *J* = 8.0 Hz), 8.45 (d, 2H, *J* = 5.0 Hz), 8.74 (m, 4H), 9.13 (s, 1H), 9.46 (d, 1H, *J* = 7.4 Hz). ^{13}C NMR (100 MHz, $CDCl_3$), δ (ppm): 44.8, 126.5, 129.8, 130.9, 132.9, 137.7, 138.5, 142.4. HRMS [M+H] $^{+}$, m/z, calculated: $C_{18}H_{15}N_4O_2S^{+}$= 351,0910 found = 351.0915.

3-(4-methoxyphenyl)-5-(3-(methylsulfonyl)phenyl)pyrazolo[1,5-a]pyrimidine.

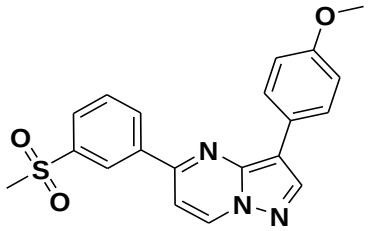

39B

4-methoxyphenylboronic acid 38.8 mg, Obtained mass: 43 mg, Percentage yield: 66%. Mp: 235.7 to 236.2 ℃. ^{1}H NMR (400 MHz, $CDCl_3$), δ (ppm): 3.36 (s, 3H), 3.81 (s, 3H), 7.06 (d, 2H, *J* = 8.9 Hz), 7.83 (d, 1H, *J* = 7.4 Hz), 7.89 (m, 1H), 8.11 (d, 1H, *J* = 8.2 Hz), 8.16 (d, 2H, *J* = 8.8 Hz), 8.64 (d, 1H, *J* = 8.0 Hz), 8.74 (m, 2H), 9.28 (d, 1H, *J* = 7.4 Hz). ^{13}C NMR (100 MHz, $CDCl_3$), δ (ppm): 43.8, 55.6, 106.1, 114.7, 124.8, 126.0, 127.5, 129.2, 130.9, 132.5, 138.2, 142.3, 153.9, 158.2. HRMS [M+H] $^{+}$, m/z, calculated: $C_{20}H_{18}N_3O_3S^{+}$= 380,1063 found = 380.1056.

3-(4-tert-butylphenyl)-5-(3-(methylsulfonyl)phenyl)pyrazolo[1,5-a]pyrimidine.

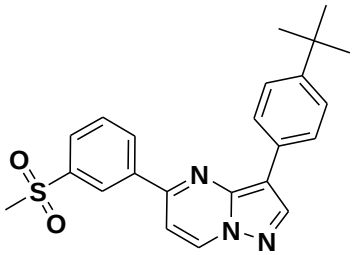

39C

4-tert-butylphenylboronic acid 45.5 mg, Obtained mass: 34 mg, Percentage yield: 49%. Mp: 140.0 to 140.8 ℃. ^{1}H NMR (400 MHz, $CDCl_3$), δ (ppm): 1.37 (s, 9H), 3.14 (s, 3H), 7.34 (d, 1H, J = 7.4 Hz), 7.52 (d, 2H, J = 8.5 Hz), 7.76 (m, 1H), 8.05 (m, 3H), 8.46 (s, 1H), 8.55 (d, 1H, J = 7.9 Hz), 8.63 (m, 1H), 8.75 (d, 1H, J = 7.4 Hz). ^{13}C NMR (100 MHz, $CDCl_3$), δ (ppm): 31.4, 34.7, 44.6, 105.0, 111.5, 125.9, 126.1, 128.8, 130.4, 132.5, 136.2, 138.6, 141.6, 143.6, 144.3, 149.6, 153.4. HRMS $[M+H]^+$, m/z, calculated: $C_{23}H_{24}N_3O_2S^+$= 406,1584 found = 406.1583.

5-(3-(methylsulfonyl)phenyl)-3-(4-(trifluoromethoxy)phenyl)pyrazolo[1,5-a]pyrimidine.

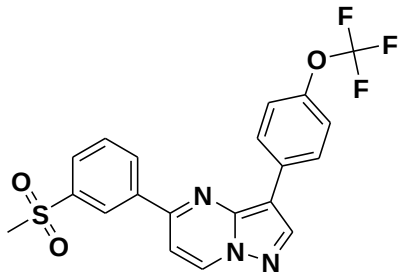

39D

4-(trifluoromethoxy)phenylboronic acid 52.6 mg, Obtained mass: 39 mg, Percentage yield: 53%. Mp: 162.5 to 165.1 ℃. ^{1}H NMR (400 MHz, $CDCl_3$), δ (ppm): 3.14 (s, 3H), 7.33 (d, 2H, J = 8.0 Hz), 7.40 (d, 1H, J = 7.4 Hz), 7.79 (m, 1H), 8.08 (d, 1H, J = 7.8 Hz), 8.15 (d, 2H, J = 8.8 Hz), 8.47 (s, 1H), 8.55 (d, 1H, J = 7.8 Hz), 8.63 (m, 1H), 8.79 (d, 1H, J = 7.3 Hz). ^{13}C NMR (100 MHz, $CDCl_3$), δ (ppm): 44.6, 105.4, 121.5, 126.0, 127.5, 129.2, 130.4, 132.5, 136.1,139.6, 142.4, 144.6, 150.6, 154.5. HRMS $[M+H]^+$, m/z, calculated: $C_{20}H_{15}F_3N_3O_3S^+$= 434,0781 found = 434.0792.

5-(3-(methylsulfonyl)phenyl)-3-(6-(methylsulfonyl)pyridin-3-yl)pyrazolo[1,5-a]pyrimidine.

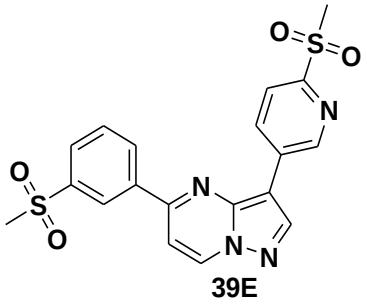

39E

5-(4,4,5,5-tetramethyl-1,3,2-dioxaborolan-2-yl)-2-(methylsulfonyl)pyridine 72.4 mg, Obtained mass: 49 mg, Percentage yield: 67%. Mp: 256.8 to 257.4 ℃. ^{1}H NMR (400 MHz, $CDCl_3$), δ (ppm): 3.16 (s, 3H), 3.27 (s, 3H), 7.52 (d, 1H, J = 7.4 Hz), 7.82 (m, 1H), 8.12 (d, 1H, J = 7.8 Hz), 8.18 (m, 2H), 8.61 (m, 3H), 8.86 (d, 1H, J = 7.3 Hz), 9.58 (d, 1H, J = 1.6 Hz). ^{13}C NMR (100 MHz, $CDCl_3$), δ (ppm): 44.6, 106.3, 121.7, 126.1, 128.9, 129.7, 130.6, 131.9, 132.3, 132.7,134.1, 137.1, 138.3, 141.7, 143.4, 154.6, 155.5. HRMS $[M+H]^+$, m/z, calculated: $C_{19}H_{17}N_4O_4S_2^+$= 429,0686 found = 429.0648.

4.3.7. General synthesis of 40A, 40B and 40C

Compound **39A** or **39B** or **39C** (24 mg, 0.059 mmol, 1 eq) and $Pd(PPh_3)_2Cl_2$ (0.83 mg, 0.0012 mmol, 0.02 eq) were dissolved in a mixture of DCM and EtOH in 3:2 ratio. Sodium borohydride ($NaBH_4$) (22 mg, 0.59 mmol, 10 eq) was then added. The reaction was allowed to stir at room temperature (25℃) for 18 hrs. After completion (monitored by TLC DCM/MeOH (98:2)), ethanol was removed. The aqueous work-up was done using DCM (3x15 mL). The organic phases were combined and rinsed with brine, followed by drying over anhydrous $NaSO_4$. The solvents were removed in vacuo and the residues were purified by Combi Flash chromatography using DCM/MeOH (98:2) to afford compound **40A**, **40B** and **40C** [42].

4,5,6,7-tetrahydro-5-(3-(methylsulfonyl)phenyl)-3-(pyridin-4-yl)pyrazolo[1,5-a]pyrimidine.

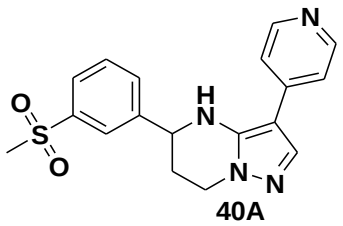

40A

Obtained mass: 10 mg, Percentage yield: 41%. Mp: 220.5 to 222.5 ℃. ^{1}H NMR (400 MHz, $CDCl_3$), δ (ppm): 2.35 (m, 2H), 3.07 (s, 3H), 4.20 (m, 2H), 4.65 (t, 1H, *J* = 6.3 Hz), 4.85 (s, 1H), 7.24 (m, 3H), 7.63 (m, 2H), 7.76 (d, 1H, *J* = 7.8 Hz), 7.92 (d, 1H, *J* = 8.0 Hz), 8.00 (m, 1H), 8.48 (m, 1H).). ^{13}C NMR (100 MHz, $CDCl_3$), δ (ppm): 38.4, 43.3, 44.5, 57.3, 44.8, 126.6, 129.9, 131.0, 133.0, 137.8, 138.6, 142.5.

4,5,6,7-tetrahydro-3-(4-methoxyphenyl)-5-(3-(methylsulfonyl)phenyl)pyrazolo[1,5-a]pyrimidine.

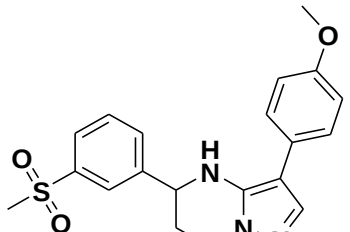

40B

Obtained mass: 11 mg, Percentage yield: 47%. Mp: 184.0 to 185.7 ℃. ^{1}H NMR (400 MHz, $CDCl_3$), δ (ppm): 2.28 (m, 2H), 3.01 (s, 3H), 3.73 (s, 3H), 4.20 (m, 2H), 4.55 (t, 1H, *J* = 6.2 Hz), 4.61 (s, 1H) 6.84 (d, 2H, *J* = 8.8 Hz), 7.23 (d, 2H, *J* = 8.8 Hz), 7.43 (s, 1H), 7.55 (m, 1H), 7.68 (d, 1H, *J* = 7.8 Hz), 7.84 (m, 1H), 7.93 (m, 1H). ^{13}C NMR (100 MHz, $CDCl_3$), δ (ppm): 38.3, 41.3, 43.8, 55.6, 57.4, 106.1, 124.8, 126.0, 127.5, 129.2, 130.9, 132.5, 142.3, 153.9, 158.2. HRMS [M+H] $^{+}$, m/z, calculated: $C_{20}H_{22}N_3O_3S^{+}$= 384,1376 found = 384.1381.

3-(4-tert-butylphenyl)-4,5,6,7-tetrahydro-5-(3-(methylsulfonyl)phenyl)pyrazolo[1,5-a]pyrimidine.

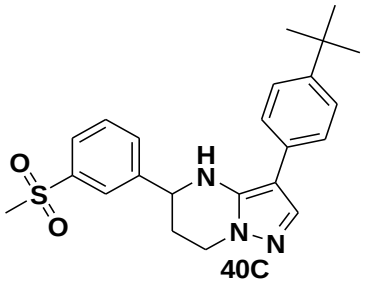

40C

Obtained mass: 15 mg. Percentage yield: 62%. Mp: 219.8 to 220.8 ℃. ^{1}H NMR (400 MHz, $CDCl_3$), δ (ppm): 1.24 (s, 9H), 2.29 (m, 2H), 3.01 (s, 3H), 4.20 (m, 2H), 4.54 (t, 1H, *J* = 6.2 Hz), 4.65 (s, 1H), 7.24 (d, 2H, *J* = 8.5 Hz), 7.33 (d, 2H, *J* = 8.4 Hz), 7.47 (s, 1H), 7.55 (m, 1H), 7.68 (d, 1H, *J* = 7.8 Hz), 7.84 (m, 1H), 7.93 (m, 1H). ^{13}C NMR (100 MHz, $CDCl_3$), δ (ppm): 31.3, 34.5, 34.6, 44.5, 44.7, 58.2, 113.4, 125.7, 126.1, 127.3, 129.8, 130.2, 131.9, 137.1, 141.3, 143.8, 148.7. HRMS [M+H] $^{+}$, m/z, calculated: $C_{23}H_{28}N_3O_2S^{+}$= 410,1897 found = 410.1879.

4.4. REFERENCES

[1] Trager, W. and Jensen, J.B, "Human malaria parasites in continuous culture," *Science,* vol. 193, no. 4254, pp. 673-675, 1976.

[2] Makler, M.T., Ries, J.M., Williams, J.A., Bancroft, J.E., Piper, R.C., Gibbins, B.L. and Hinrichs, D.J, "Parasite lactate dehydrogenase as an assay for Plasmodium falciparum drug sensitivity," *The American Journal of Tropical Medicine and Hygiene,* vol. 48, no. 6, pp. 739-741, 1993.

[3] Baker, D.A., Stewart, L.B., Large, J.M., Bowyer, P.W., Ansell, K.H., Jiménez-Díaz, M.B., El Bakkouri, M., Birchall, K., Dechering, K.J., Bouloc, N.S., Coombs, P.J., Merritt, A.T., Croft, S.L., Gutteridge, W.E., kettleborough, C.A. and Osborne, S.A., "A potent series targeting the malarial cGMP-dependent protein kinase clears infection and blocks transmission," *Nature Communications,* vol. 8, no. 1, pp. 1-9, 2017.

[4] Penzo, M., de Las Heras-Dueña, L., Mata-Cantero, L., Diaz-Hernandez, B., Vazquez-Muñiz, M.J., Ghidelli-Disse, S., Drewes, G., Fernandez-Alvaro, E. and Baker, D.A, "High-throughput screening of the Plasmodium falciparum cGMP-dependent protein kinase identified a thiazole scaffold which kills erythrocytic and sexual stage parasites," *Scientific Reports,* vol. 9, no. 1, pp. 1-13, 2019.

[5] Cheuka, P.M., Centani, L., Arendse, L.B., Fienberg, S., Wambua, L., Renga, S.S., Dziwornu, G.A., Kumar, M., Lawrence, N., Taylor, D., Wittlin, S., Coertzen, D., Van Der Watt, M., Reader, J., Birkholtz M. and Chibale K, "New amidated 3, 6-diphenylated imidazopyridazines with potent antiplasmodium activity are dual inhibitors of Plasmodium phosphatidylinositol-4-kinase and cGMP-dependent protein kinase," *ACS Infectious Diseases,* vol. 7, no. 1, pp. 34-46, 2020.

[6] McNamara, C.W., Lee, M., Lim, C.S., Lim, S.H., Roland, J., Nagle, A., Simon, O., Yeung, B.K., Chatterjee, A.K., McCormack, S.L., Manary, M.J., Tully, D.C., Kocken, H.M., Glynne, R.J., Bodenreider, C., Fidock, D.A., Diagana, T.T. andWinzeler, E.A., "Targeting Plasmodium PI (4) K to eliminate malaria," *Nature,* vol. 504, no. 7479, pp. 248-253, 2013.

[7] Le Manach, C., Gonzàlez Cabrera, D., Douelle, F., Nchinda, A.T., Younis, Y., Taylor, D., Wiesner, L., White, K.L., Ryan, E., March, C., Duffy, S., Avery, V.L., Waterson, D., Witty, M.J., Wittlin, S., Charman, S.A., Street, L.J. and Chibale, K, "Medicinal chemistry optimization of antiplasmodial imidazopyridazine hits from high throughput screening of a SoftFocus kinase library: part 1.," *Journal of Medicinal Chemistry,* vol. 57, no. 6, pp. 2789-2798, 2014.

[8] Le Manach, C., Paquet, T., Gonzàlez Cabrera, D., Younis, Y., Taylor, D., Wiesner, L., Lawrence, N., Schwager, S., Waterson, D., Witty, M.J. and Wittlin, S., Street L.J. and Chibale K, "Medicinal chemistry optimization of antiplasmodial imidazopyridazine hits from high throughput screening of a softfocus kinase library: Part 2," *Journal of Medicinal Chemistry,* vol. 57, no. 21, pp. 8839-8848, 2014.

[9] Le Manach, C., Paquet, T., Brunschwig, C., Njoroge, M., Han, Z., Gonzàlez Cabrera, D., Bashyam, S., Dhinakaran, R., Taylor, D., Reader, J., Botha, M., Ferrer, S., Angulo-Barturen, I., Street, L.J. and Chibale, K, "A novel pyrazolopyridine with in vivo activity in Plasmodium berghei-and Plasmodium falciparum-infected mouse models from structure–activity relationship studies around the core of recently identified antimalarial imidazopyridazines," *Journal of Medicinal Chemistry,* vol. 58, no. 21, pp. 8713-8722, 2015.

CHAPTER 5: APPENDIX

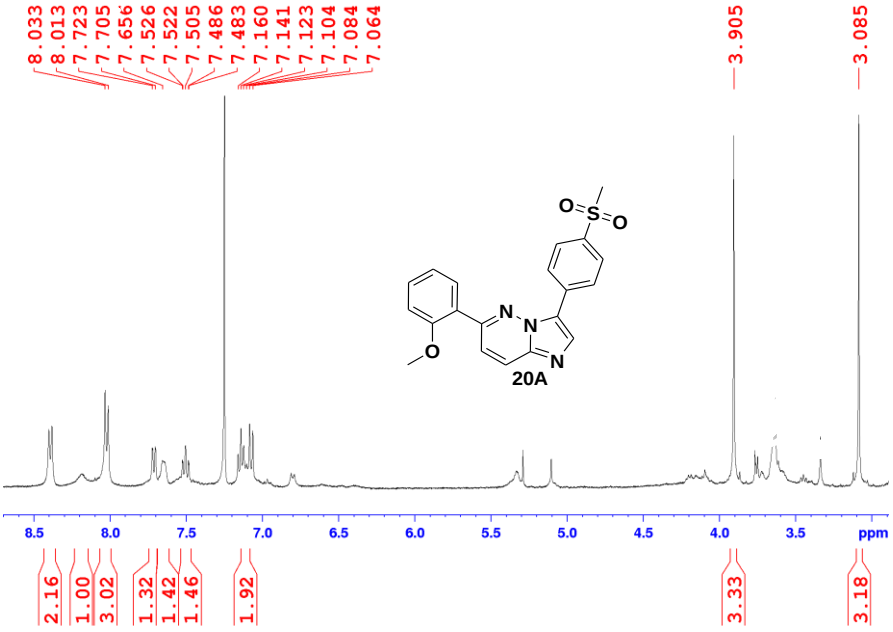

Figure 5.1: ^{1}H NMR of 6-(2-methoxyphenyl)-3-(4-(methylsulfonyl)phenyl)imidazo[1,2-b]pyridazine.

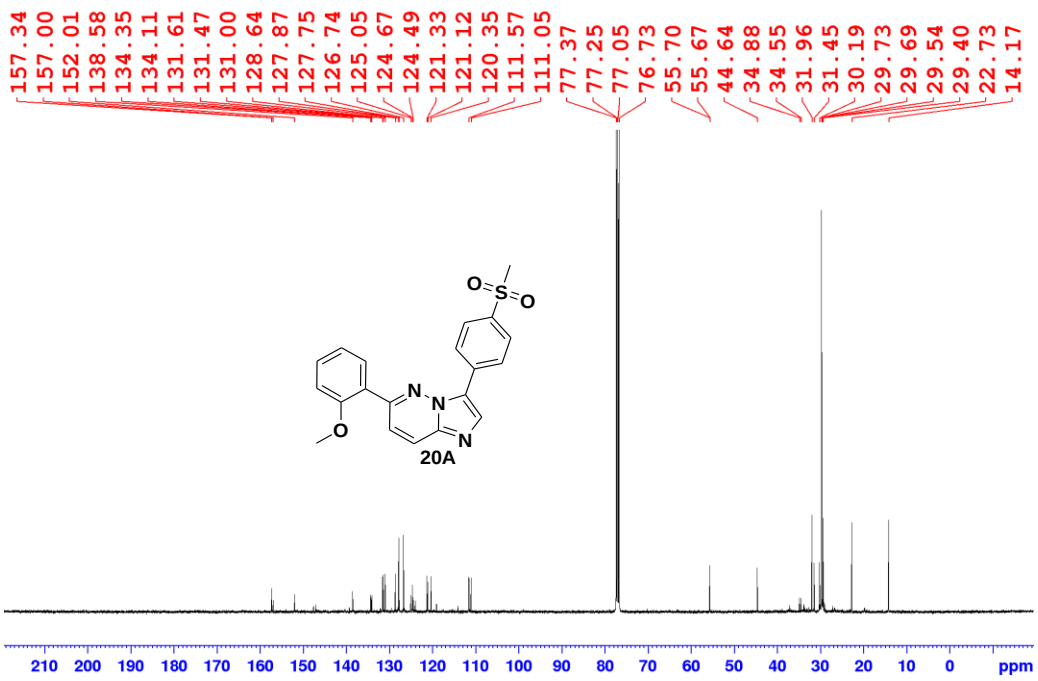

Figure 5.2: ^{13}C NMR of 6-(2-methoxyphenyl)-3-(4-(methylsulfonyl)phenyl)imidazo[1,2-b]pyridazine.

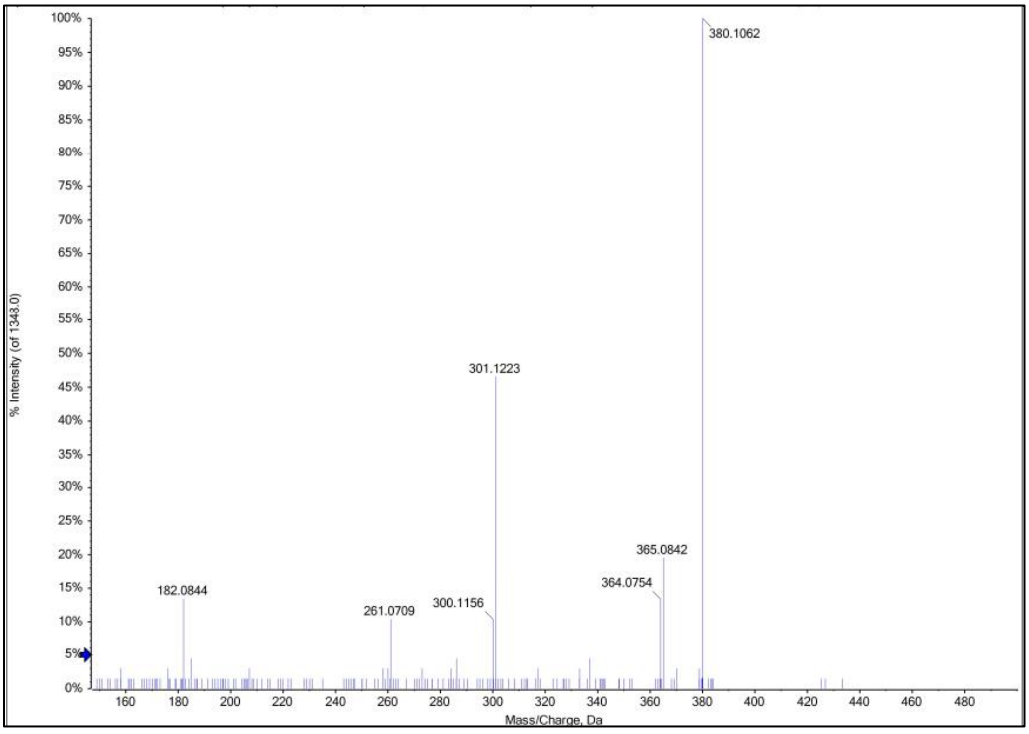

Figure 5.3: MS of 6-(2-methoxyphenyl)-3-(4-(methylsulfonyl)phenyl)imidazo[1,2-b] pyridazine.

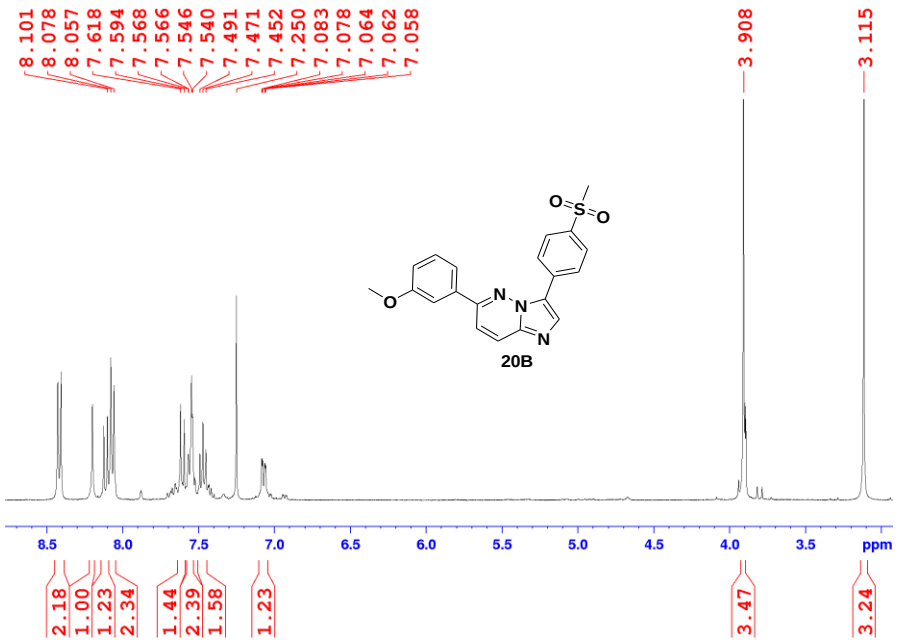

Figure 5.4: ^{1}H NMR of 6-(3-methoxyphenyl)-3-(4-(methylsulfonyl)phenyl)imidazo[1,2-b]pyridazine.

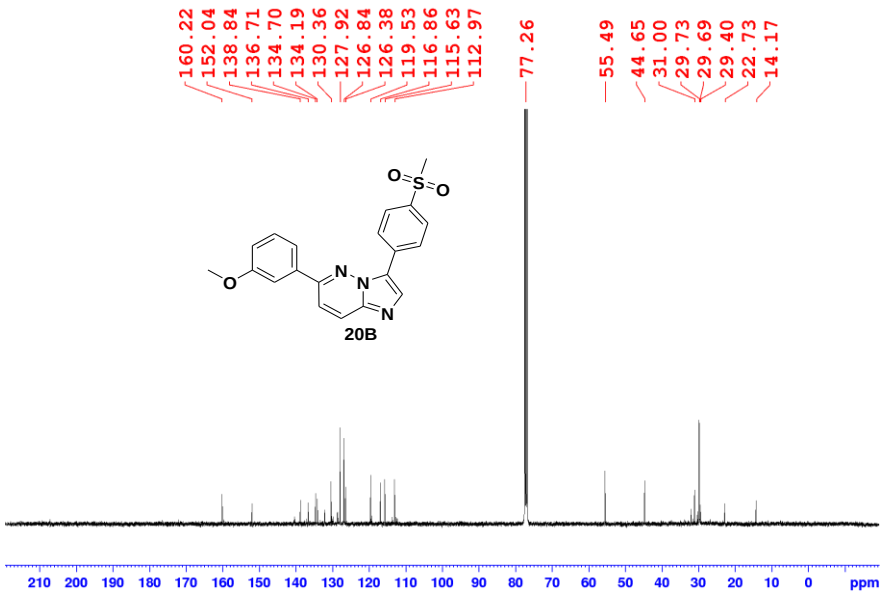

Figure 5.5: ^{13}C NMR of 6-(3-methoxyphenyl)-3-(4-(methylsulfonyl)phenyl)imidazo[1,2-b]pyridazine.

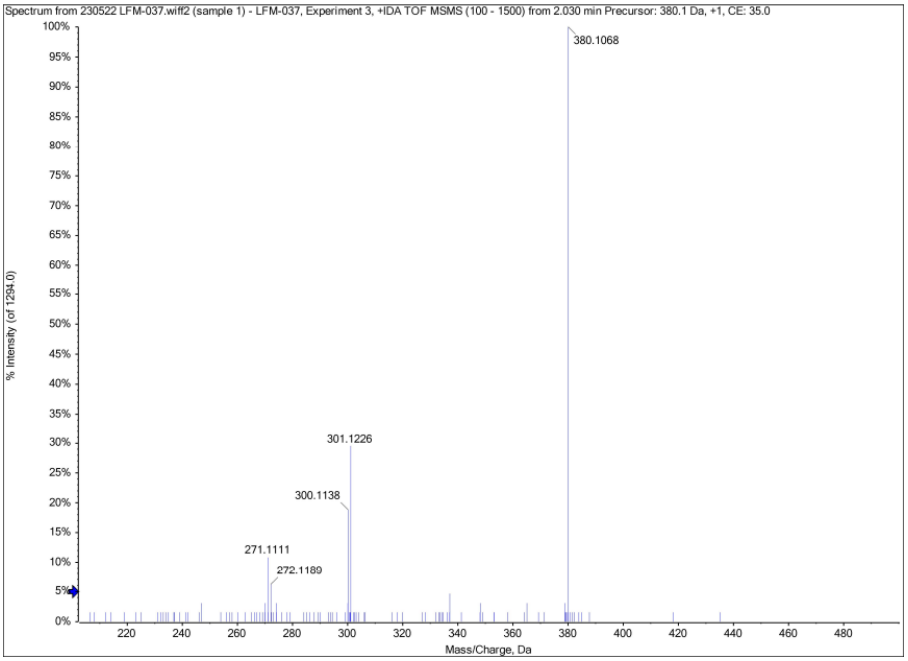

Figure 5.6:MS of 6-(3-methoxyphenyl)-3-(4-(methylsulfonyl)phenyl)imidazo[1,2-b] pyridazine.

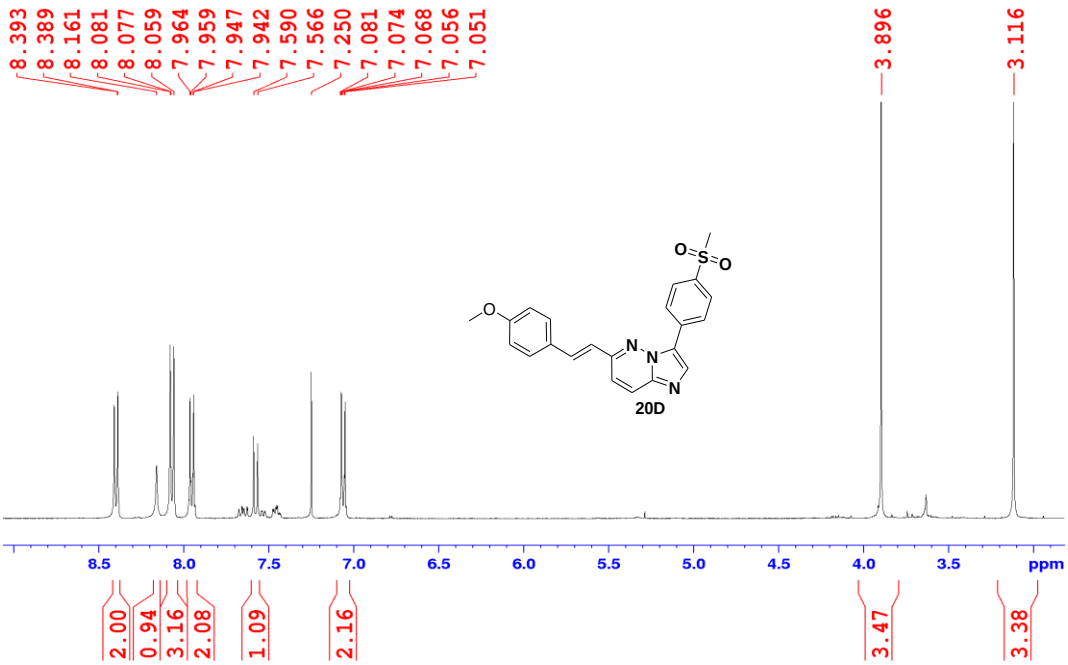

Figure 5.7: ^{1}H NMR of 6-(4-methoxystyryl)-3-(4-(methylsulfonyl)phenyl)imidazo[1,2-b]pyridazine.

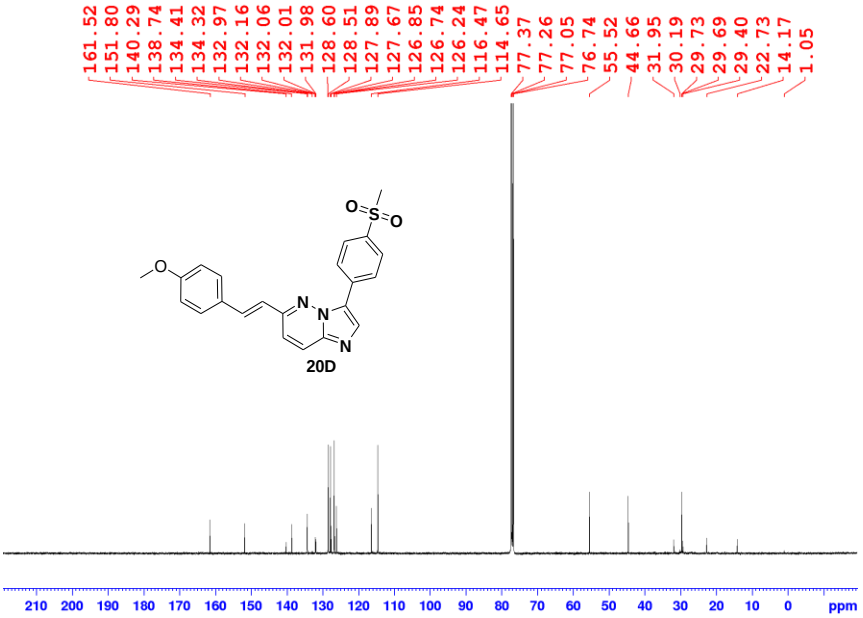

Figure 5.8: ^{13}C NMR of 6-(4-methoxystyryl)-3-(4-(methylsulfonyl)phenyl)imidazo[1,2-b]pyridazine.

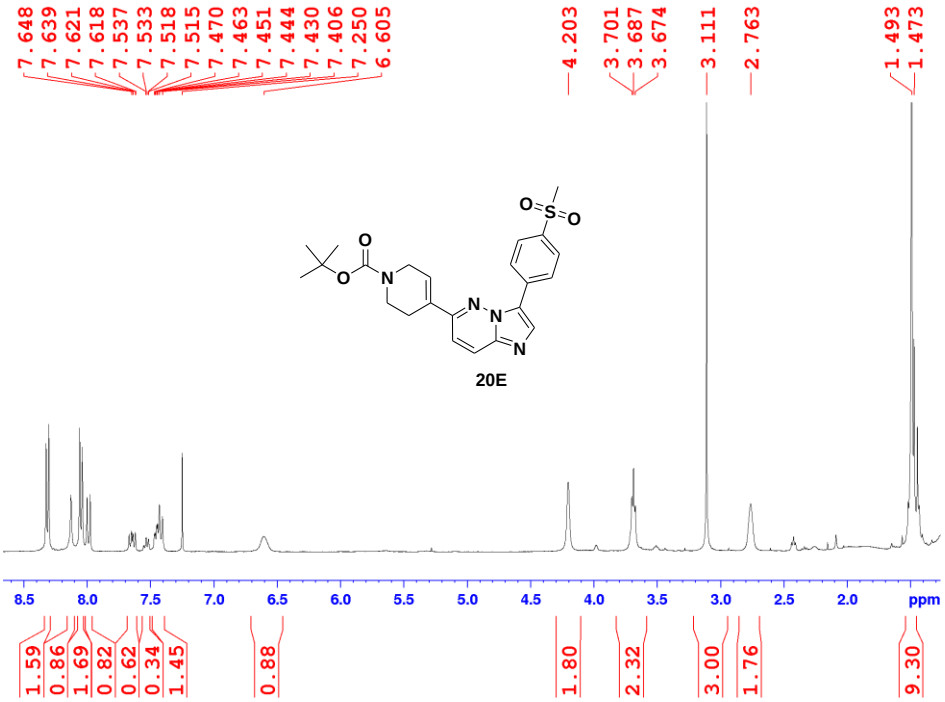

Figure 5.9: ^{1}H NMR of tert-butyl 5,6-dihydro-4-(3-(4-(methylsulfonyl)phenyl)imidazo[1,2-b]pyridazin-6-yl)pyridine-1(2H)-carboxylate.

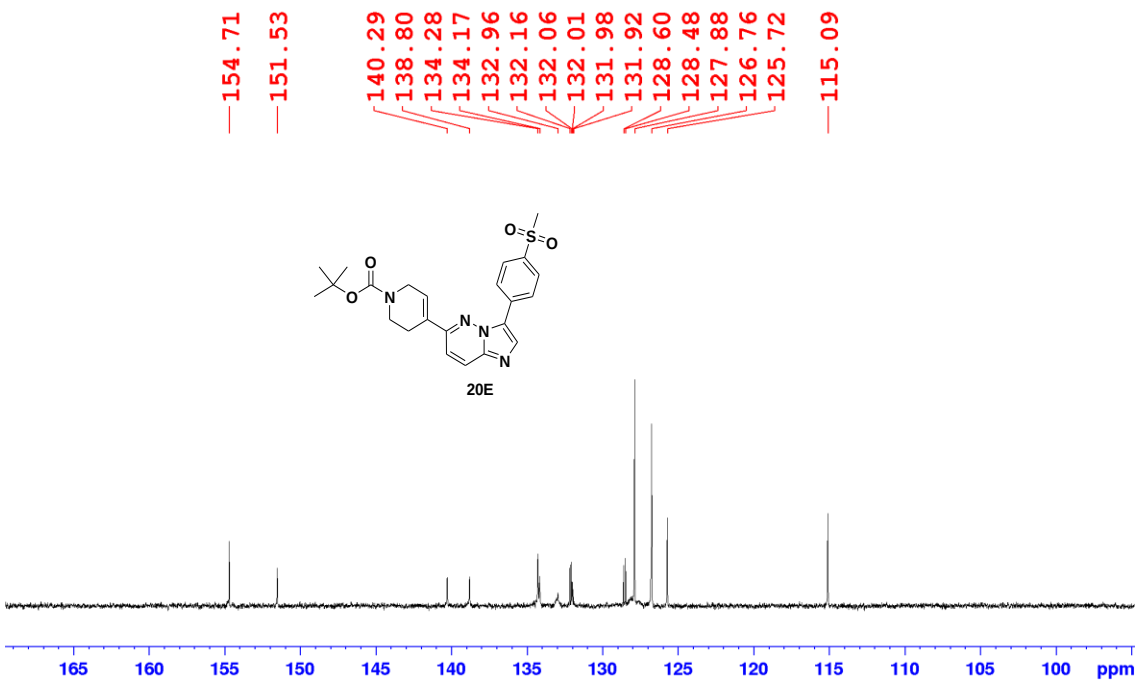

Figure 5.10: ^{13}C NMR tert-butyl 5,6-dihydro-4-(3-(4-(methylsulfonyl)phenyl)imidazo[1,2-b]pyridazin-6-yl)pyridine-1(2H)-carboxylate.

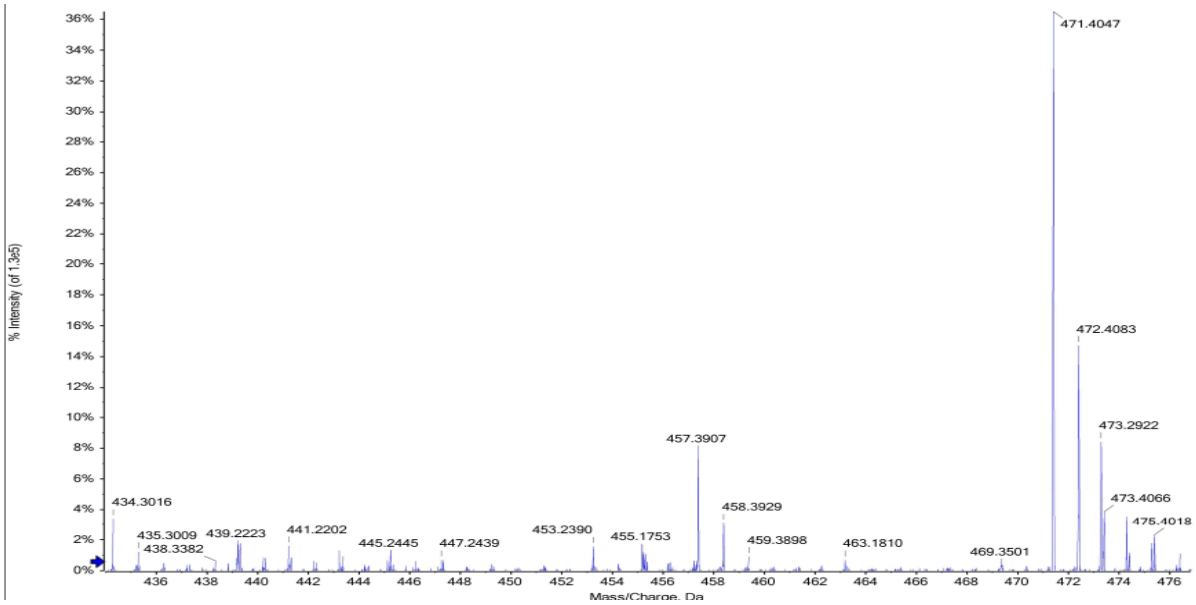

Figure 5.11: MS of tert-butyl 5,6-dihydro-4-(3-(4-(methylsulfonyl)phenyl)imidazo[1,2-b]pyridazin-6-yl)pyridine-1(2H)-carboxylate.

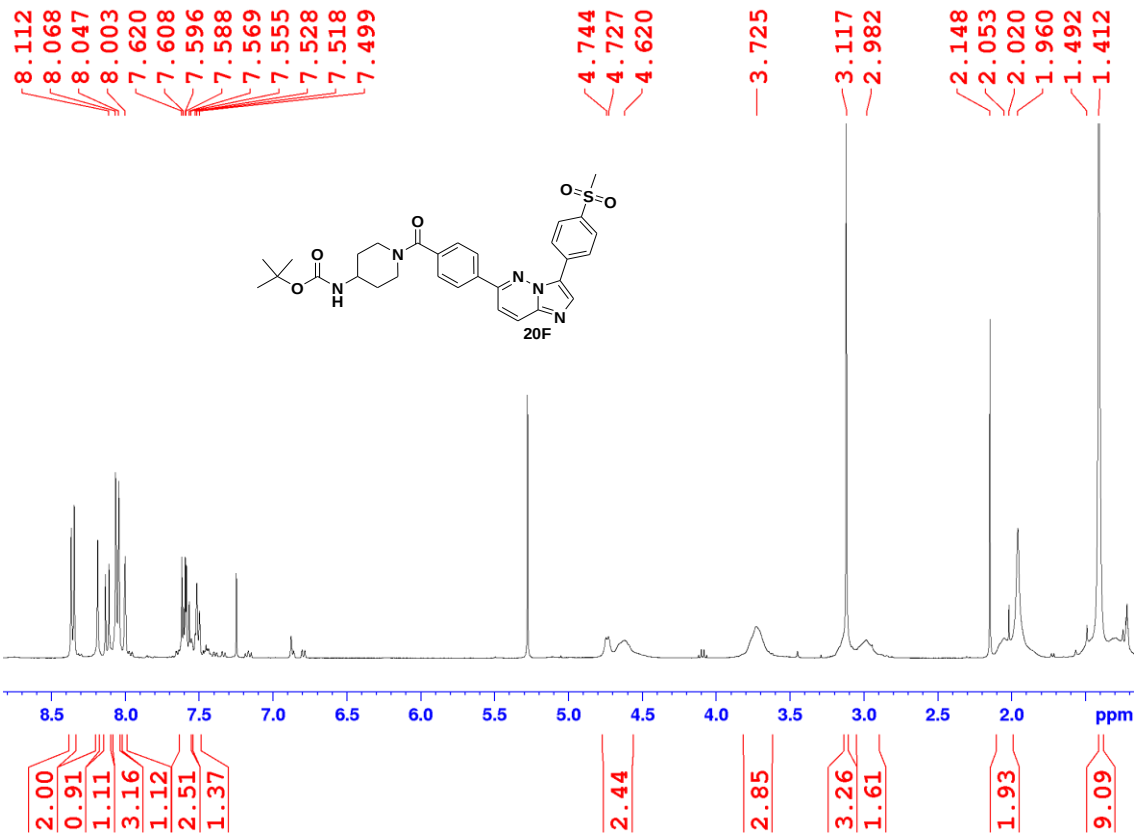

Figure 5.12: ^{1}H NMR of compound 20F.

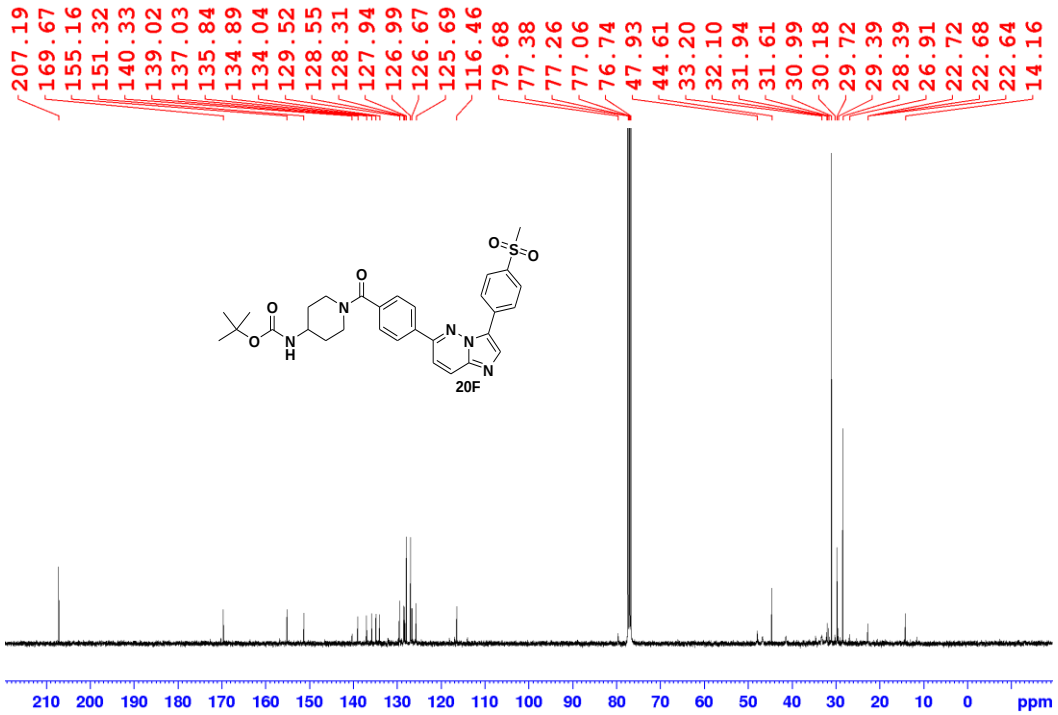

Figure 5.13: ^{13}C NMR of compound 20F.

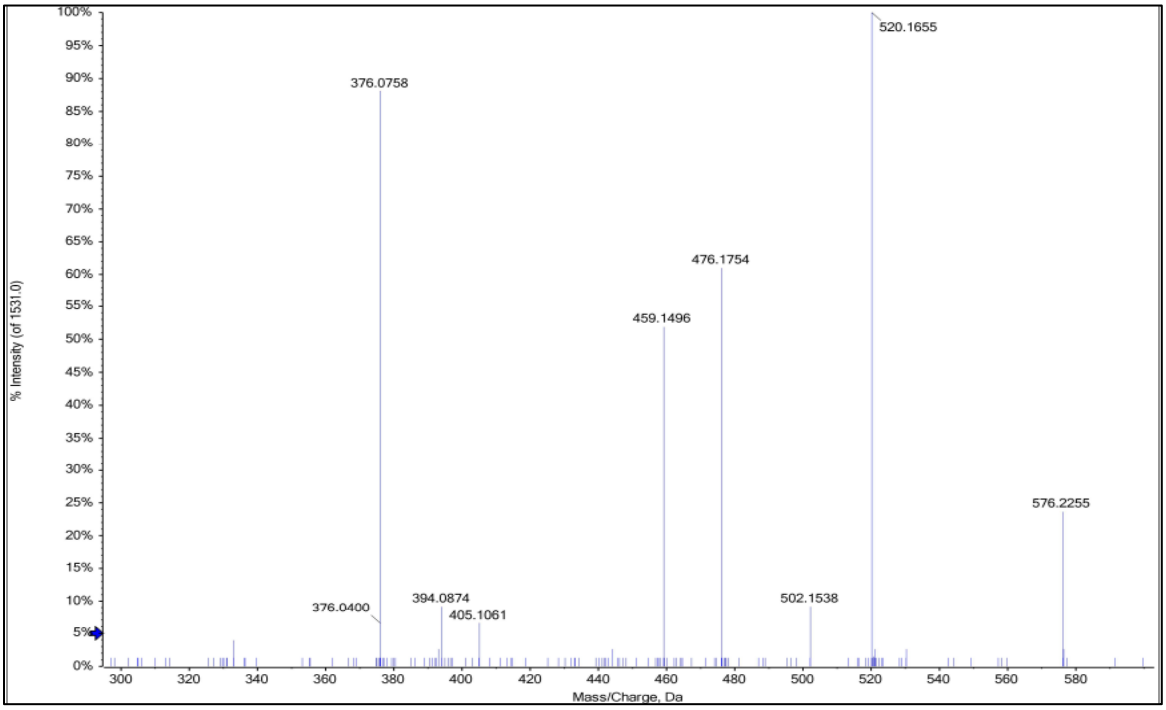

Figure 5.14: MS of compound 20F.

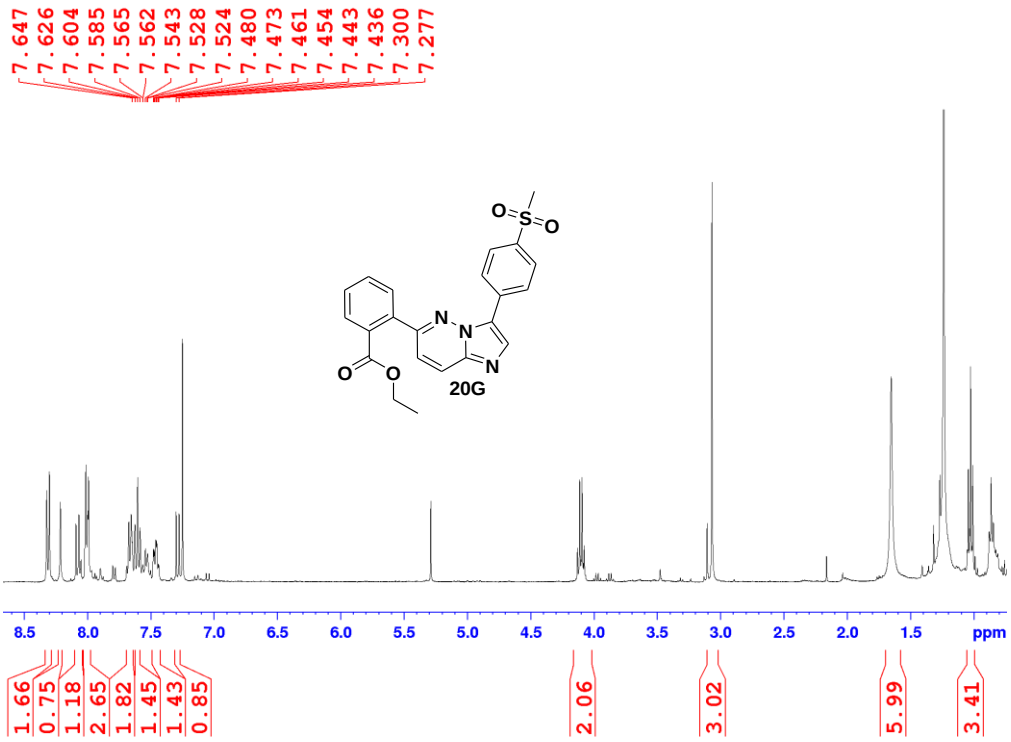

Figure 5.15: ^{1}H NMR of ethyl 2-(3-(4-(methylsulfonyl)phenyl)imidazo[1,2-b]pyridazin-6-yl)benzoate.

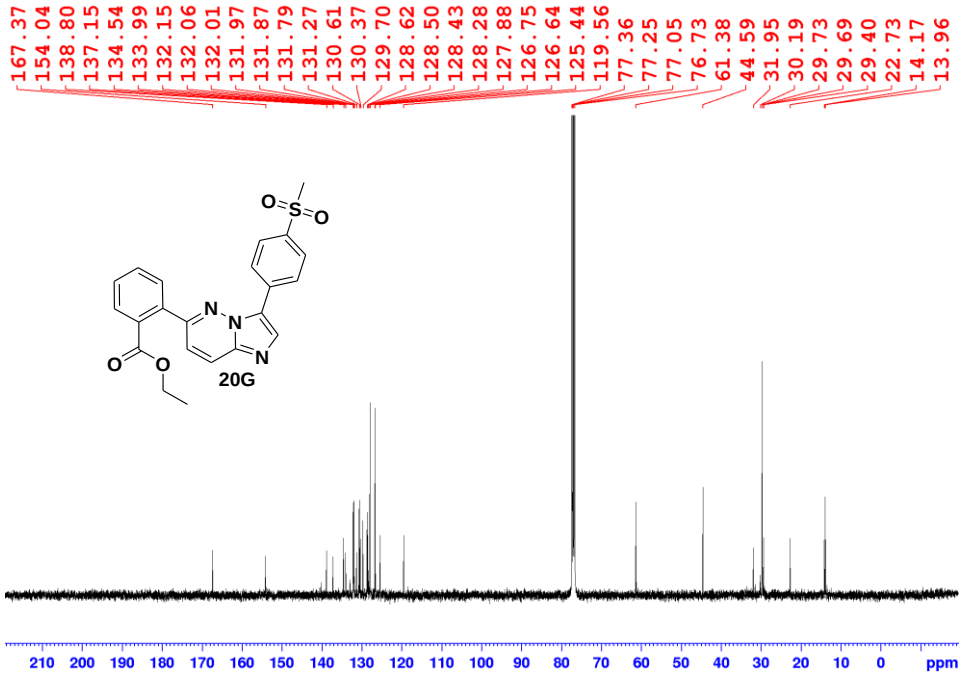

Figure 5.16: ^{13}C NMR of ethyl 2-(3-(4-(methylsulfonyl)phenyl)imidazo[1,2-b]pyridazin-6-yl)benzoate.

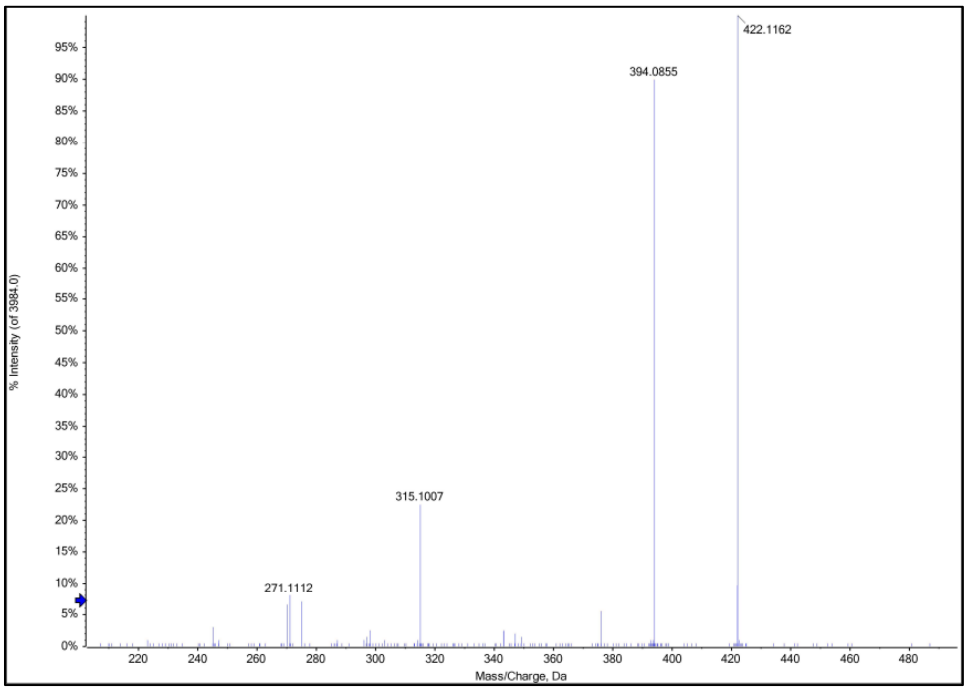

Figure 5.17: MS of ethyl 2-(3-(4-(methylsulfonyl)phenyl)imidazo[1,2-b]pyridazin-6-yl)benzoate.

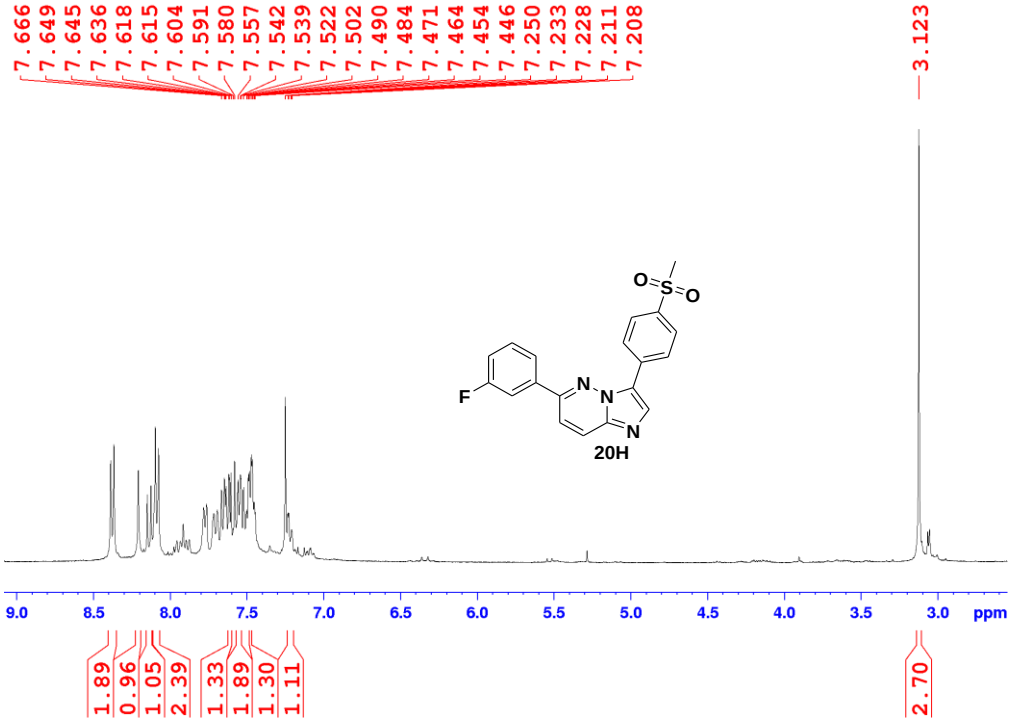

Figure 5.18: ^{1}H NMR of 6-(3-fluorophenyl)-3-(4-(methylsulfonyl)phenyl)imidazo[1,2-b]pyridazine.

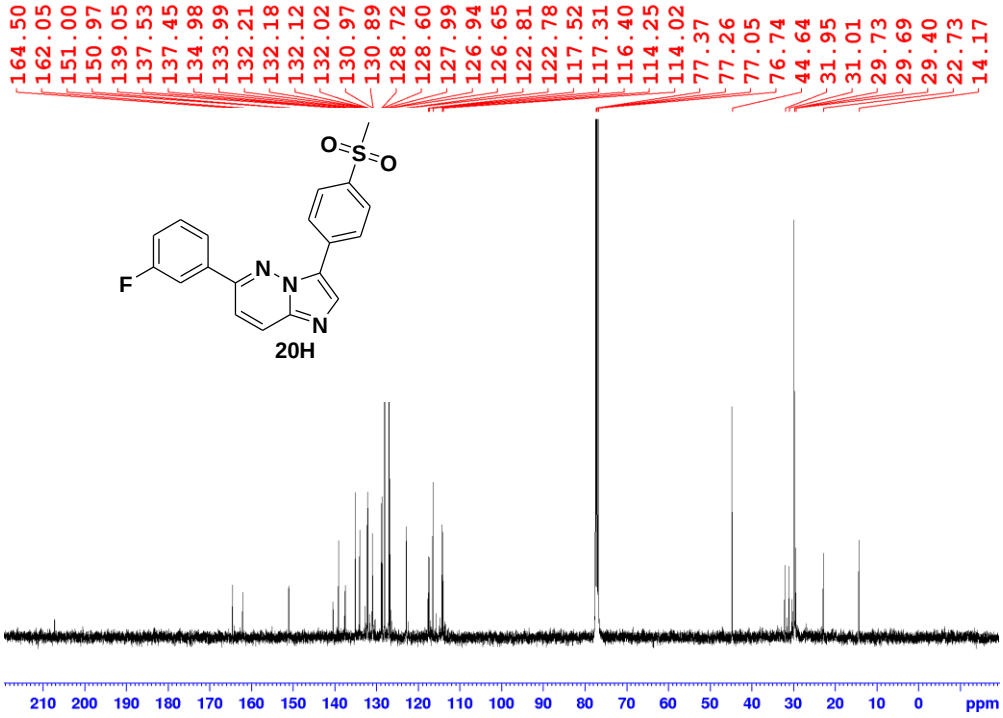

Figure 5.19: ^{13}C NMR of 6-(3-fluorophenyl)-3-(4-(methylsulfonyl)phenyl)imidazo[1,2-b]pyridazine.

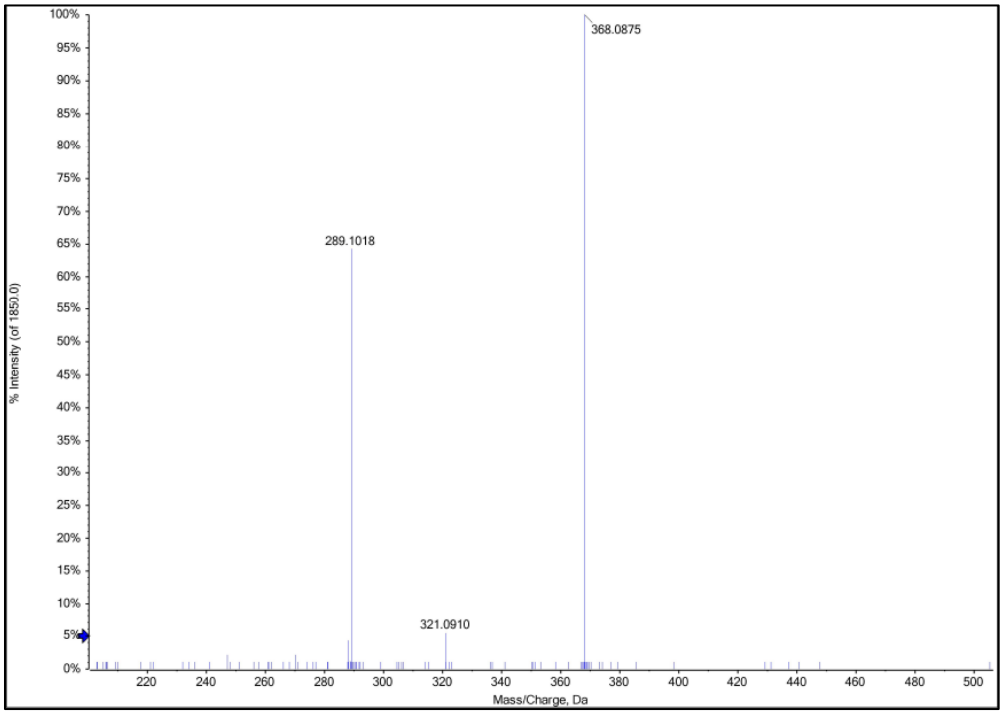

Figure 5.20: MS of 6-(3-fluorophenyl)-3-(4-(methylsulfonyl)phenyl)imidazo[1,2-b]pyridazine.

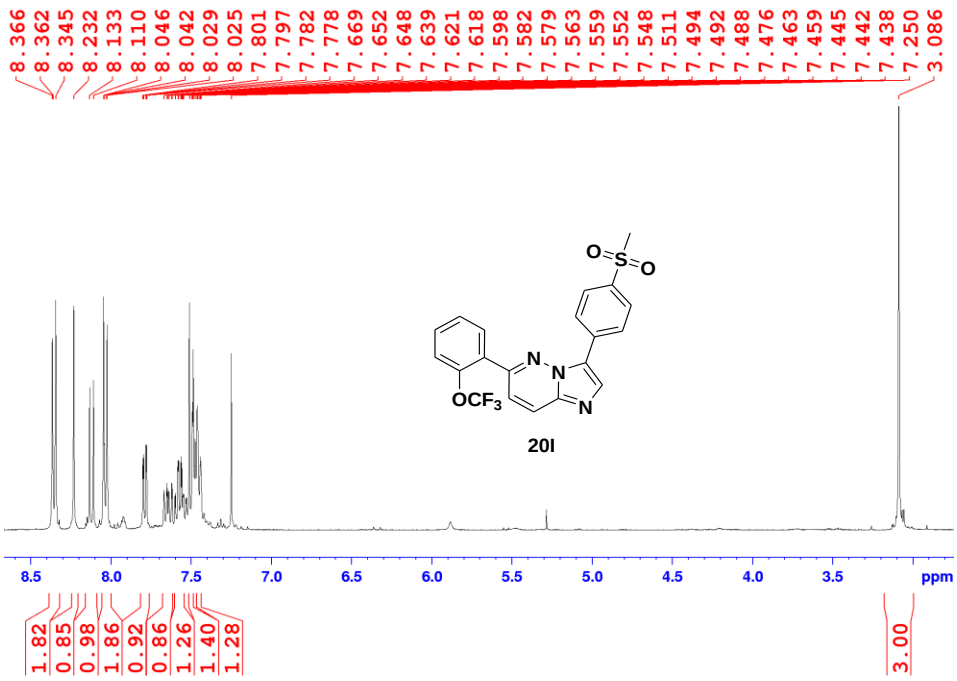

Figure 5.21: ^{1}H NMR of 3-(4-(methylsulfonyl)phenyl)-6-(2-(trifluoromethoxy)phenyl) imidazo[1,2-b] pyridazine.

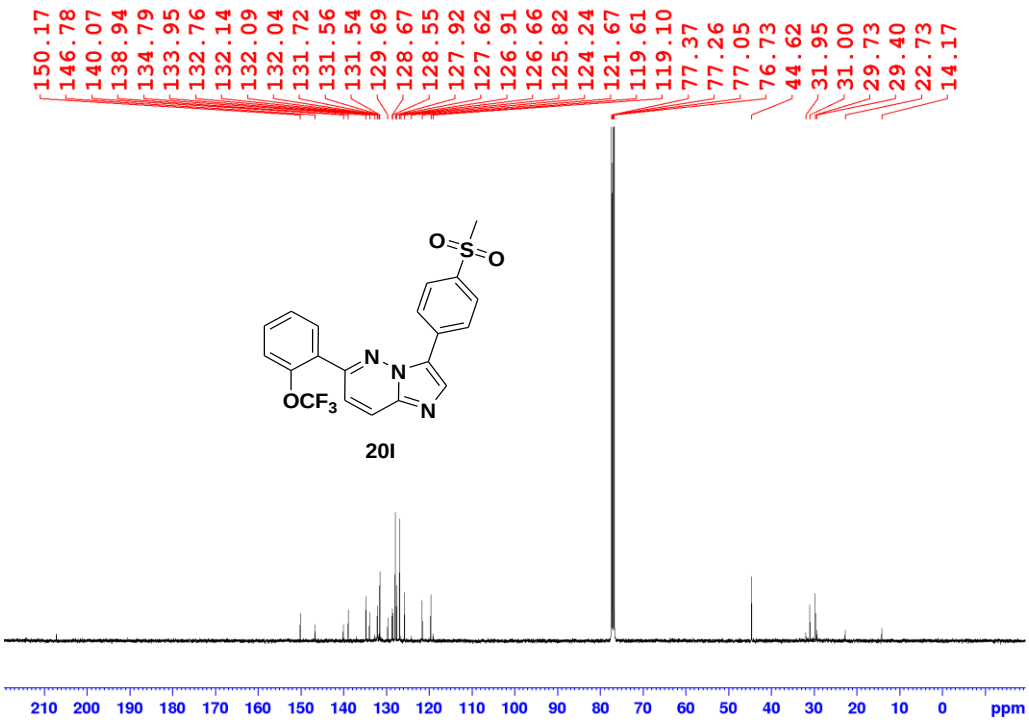

Figure 5.22: ^{13}C NMR of 3-(4-(methylsulfonyl)phenyl)-6-(2-(trifluoromethoxy)phenyl) imidazo[1,2-b] pyridazine.

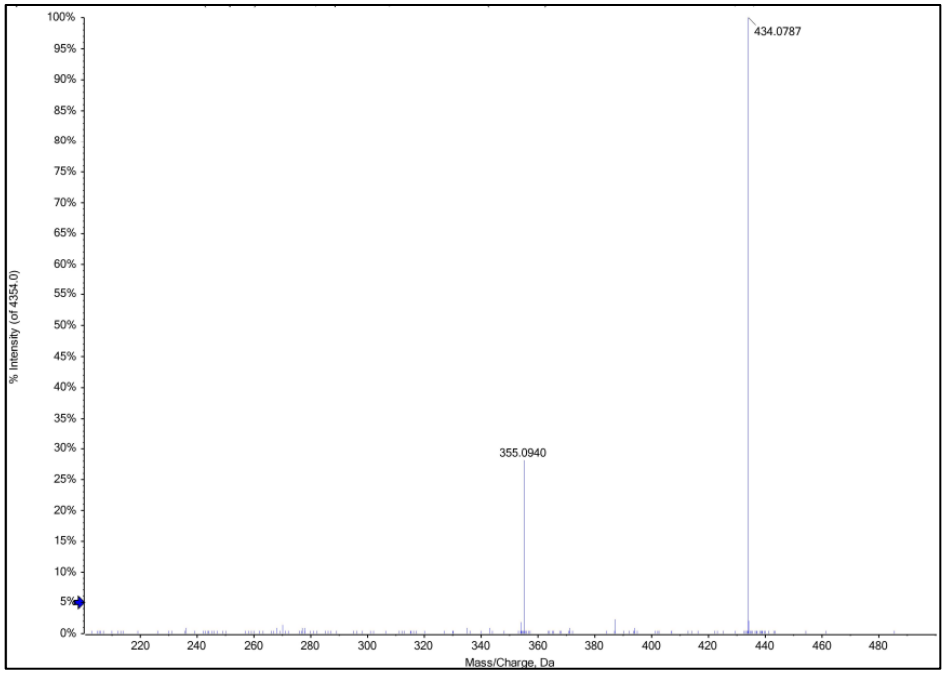

Figure 5.23: MS of 3-(4-(methylsulfonyl)phenyl)-6-(2-(trifluoromethoxy)phenyl) imidazo[1,2-b] pyridazine.

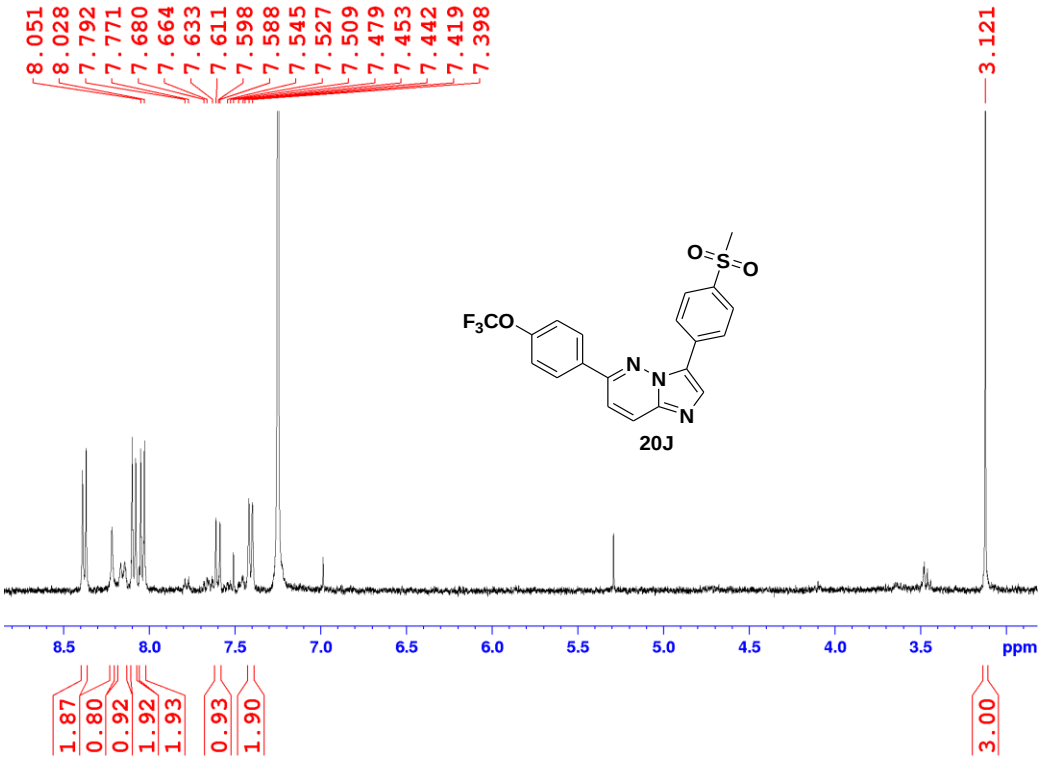

Figure 5.24: ^{1}H NMR of 3-(4-(methylsulfonyl)phenyl)-6-(4-(trifluoromethoxy)phenyl) imidazo[1,2-b] pyridazine.

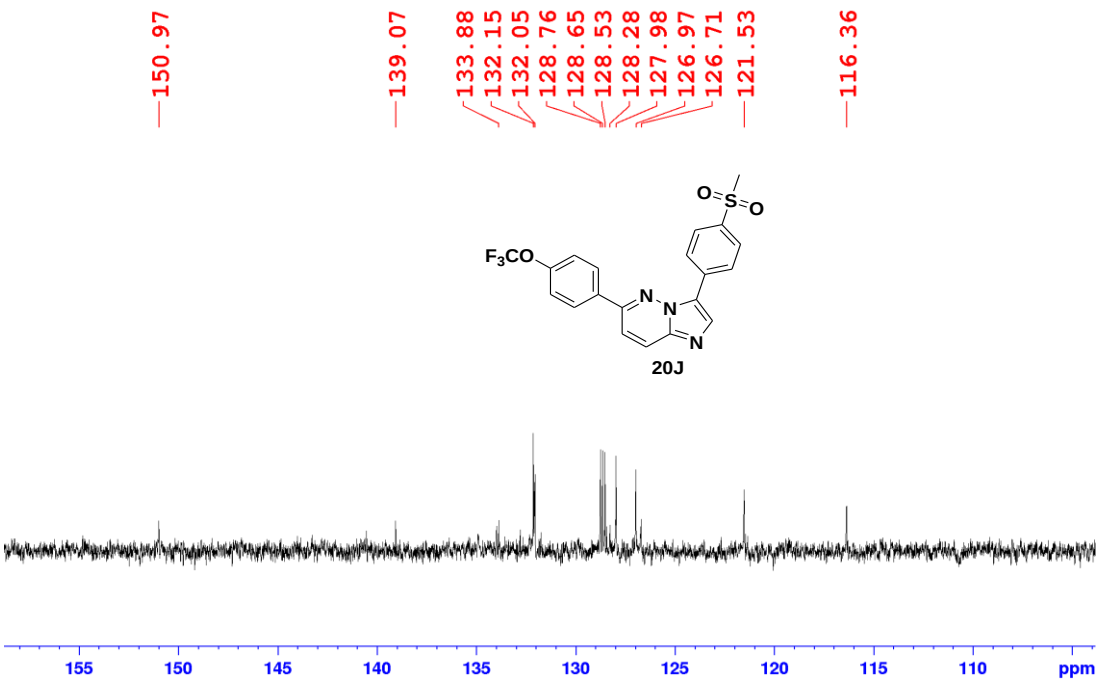

Figure 5.25: ^{13}C NMR of 3-(4-(methylsulfonyl)phenyl)-6-(4-(trifluoromethoxy)phenyl) imidazo[1,2-b] pyridazine.

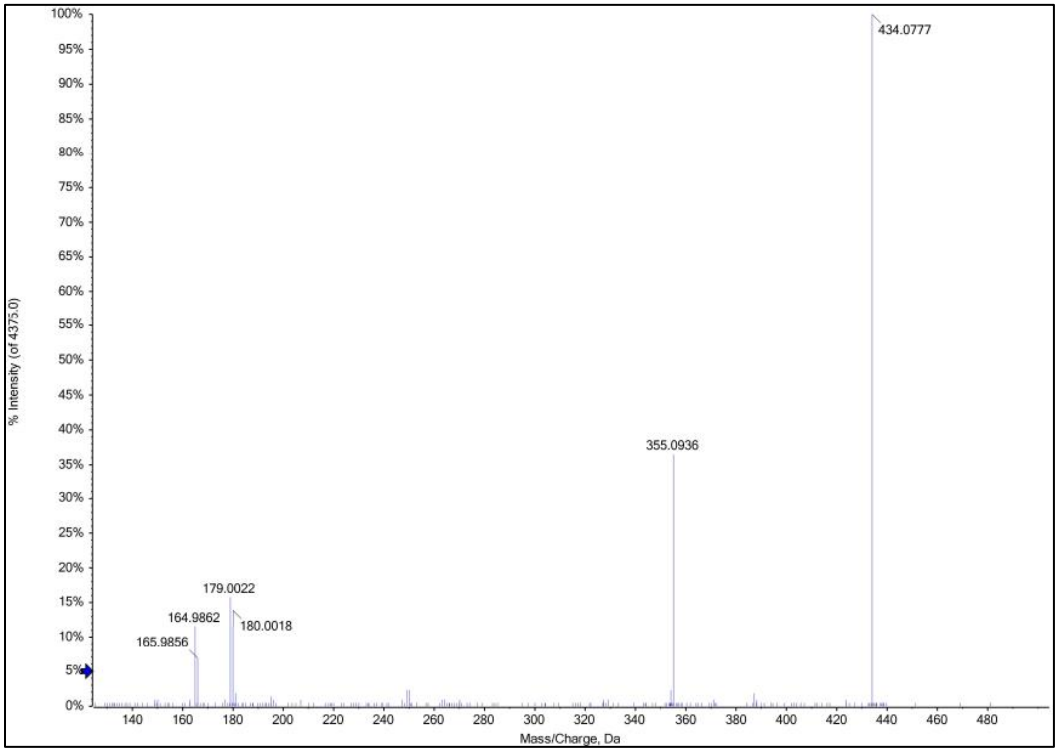

Figure 5.26: MS of 3-(4-(methylsulfonyl)phenyl)-6-(4-(trifluoromethoxy)phenyl) imidazo[1,2-b] pyridazine.

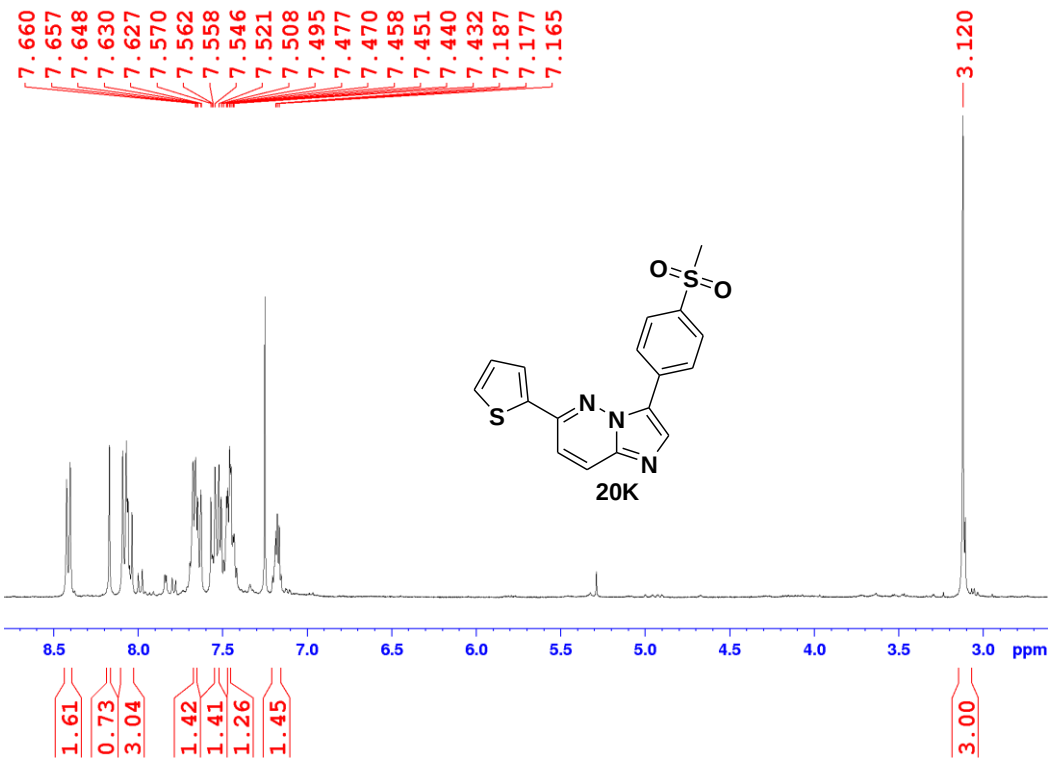

Figure 5.27: ^{1}H NMR of 3-(4-(methylsulfonyl)phenyl)-6-(thiophen-2-yl)imidazo[1,2-b]pyridazine.

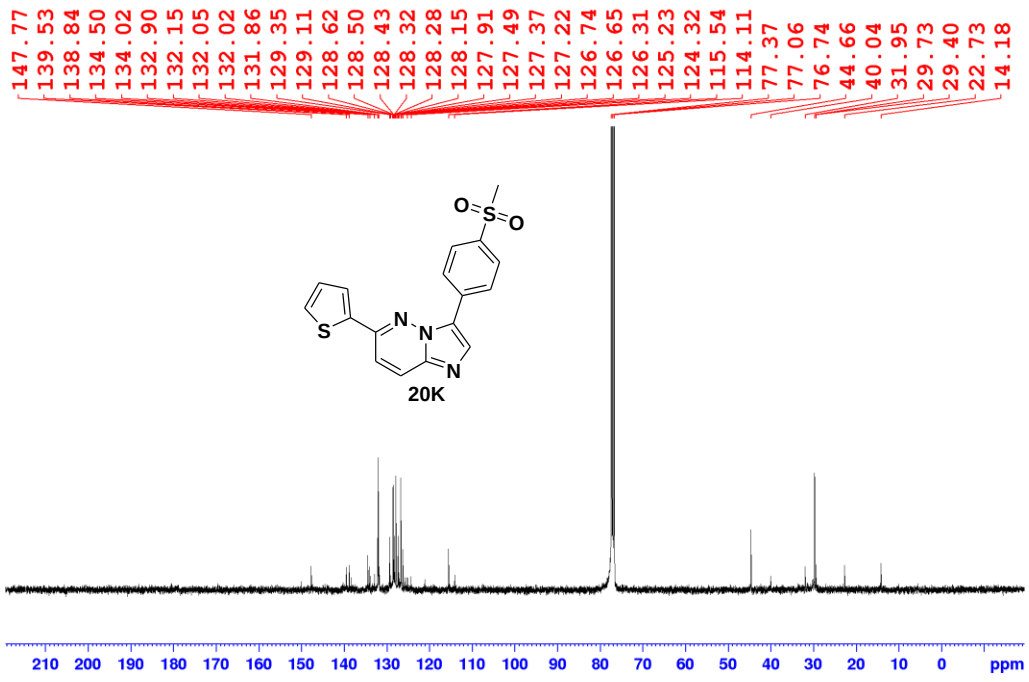

Figure 5.28: ^{13}C NMR of 3-(4-(methylsulfonyl)phenyl)-6-(thiophen-2-yl)imidazo[1,2-b]pyridazine.

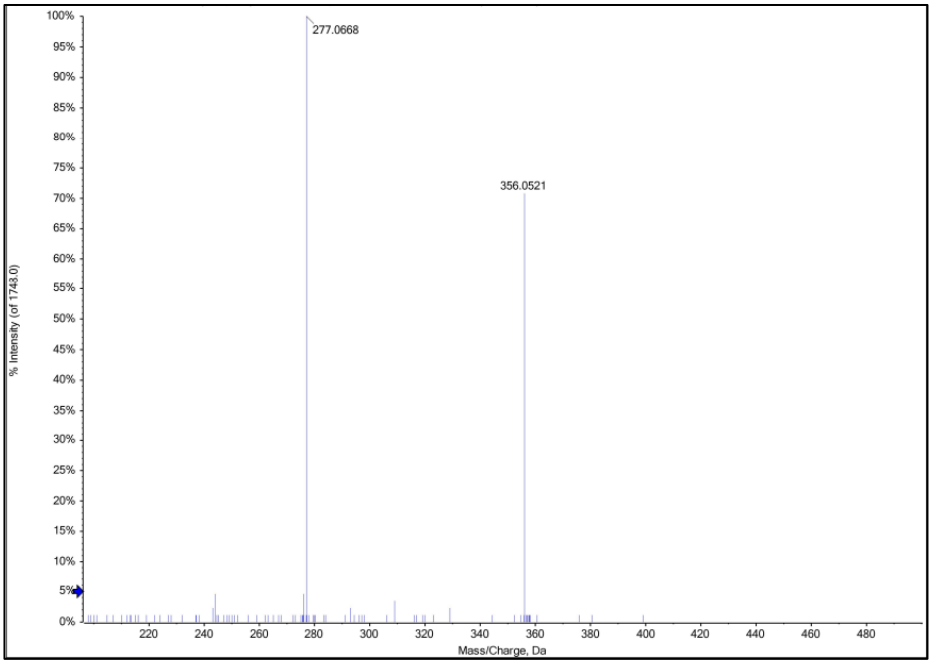

Figure 5.29: MS of 3-(4-(methylsulfonyl)phenyl)-6-(thiophen-2-yl)imidazo[1,2-b]pyridazine.

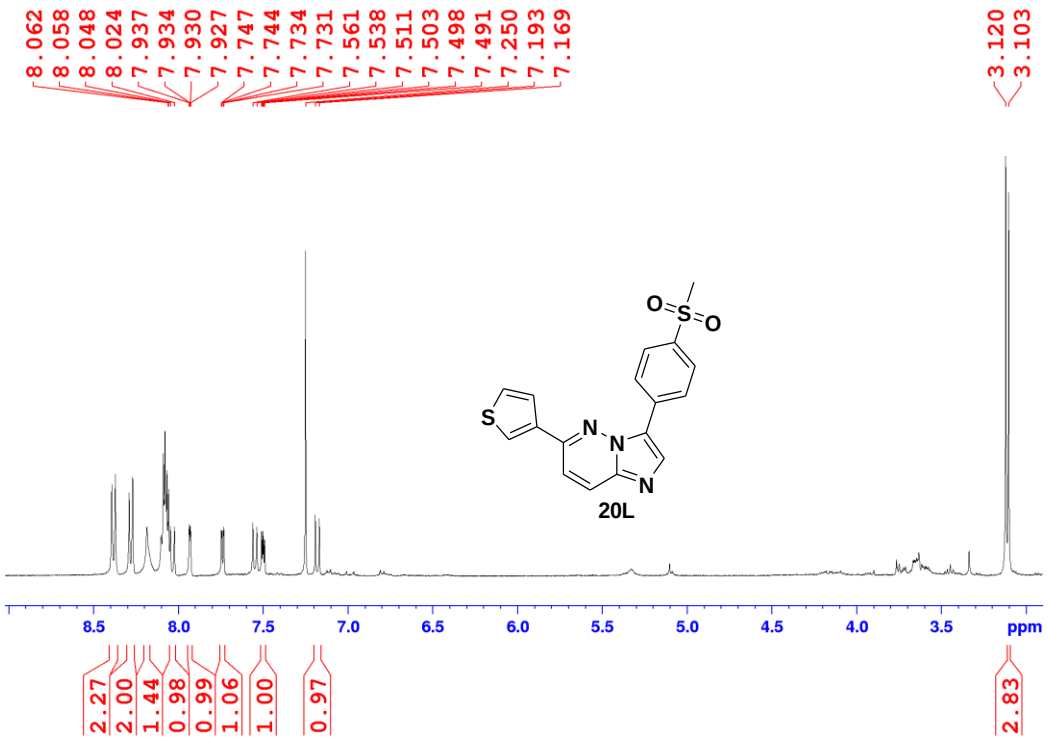

Figure 5.30: ^{1}H NMR of 3-(4-(methylsulfonyl)phenyl)-6-(thiophen-3-yl)imidazo[1,2-b]pyridazine

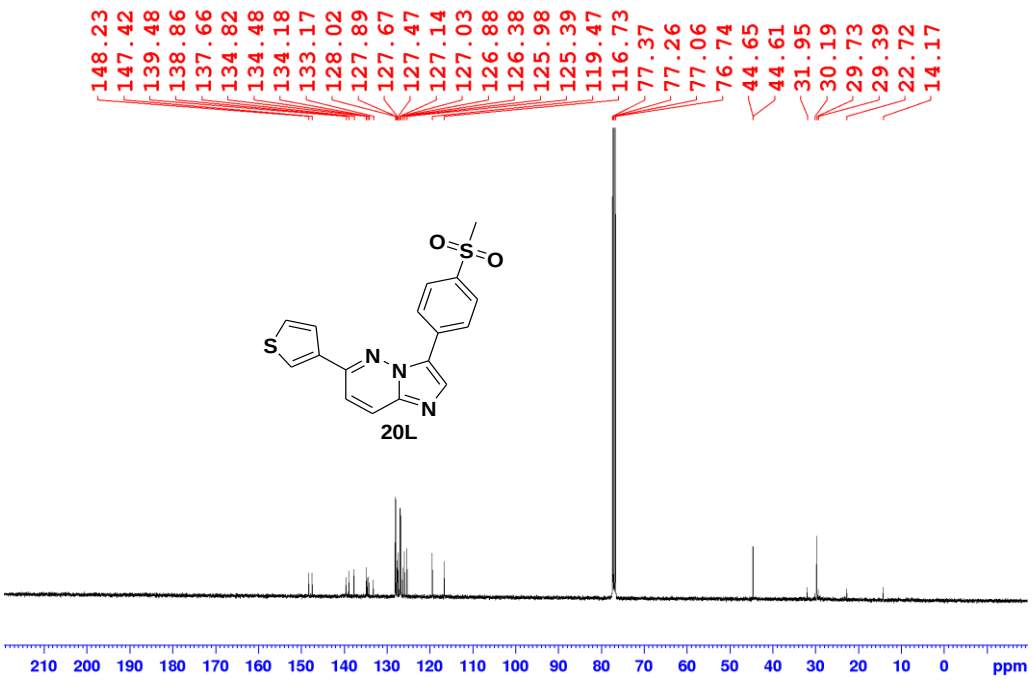

Figure 5.31: ^{13}C NMR of 3-(4-(methylsulfonyl)phenyl)-6-(thiophen-3-yl)imidazo[1,2-b]pyridazine.

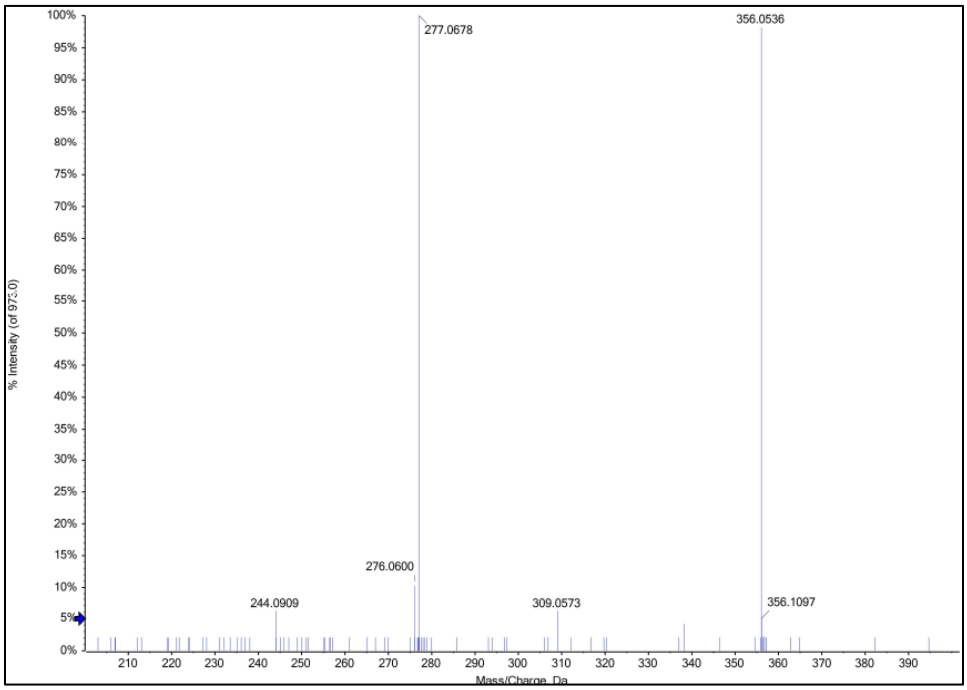

Figure 5.32: MS of 3-(4-(methylsulfonyl)phenyl)-6-(thiophen-3-yl)imidazo[1,2-b]pyridazine.

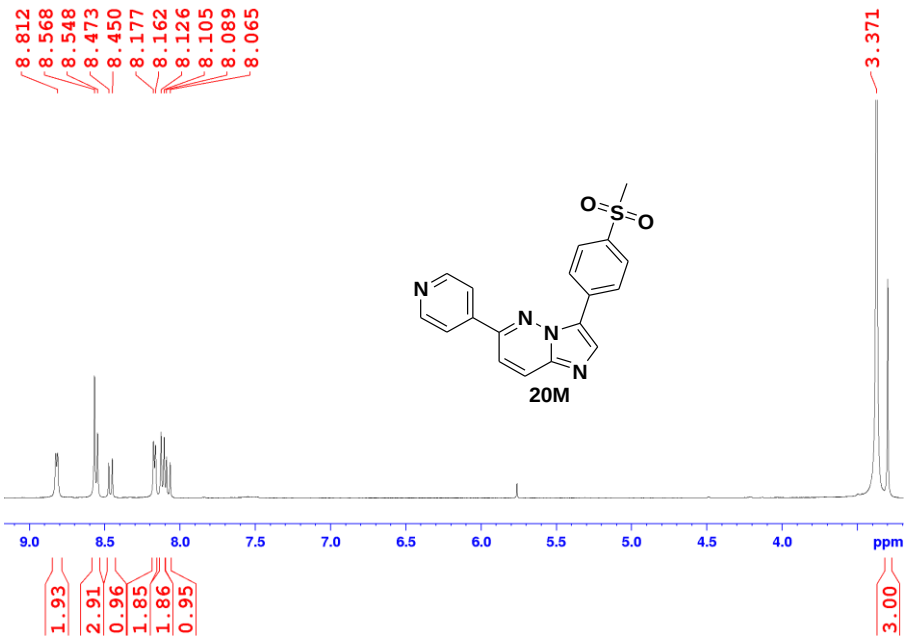

Figure 5.33: ^{1}H NMR of 3-(4-(methylsulfonyl)phenyl)-6-(pyridin-4-yl)imidazo[1,2-b]pyridazine.

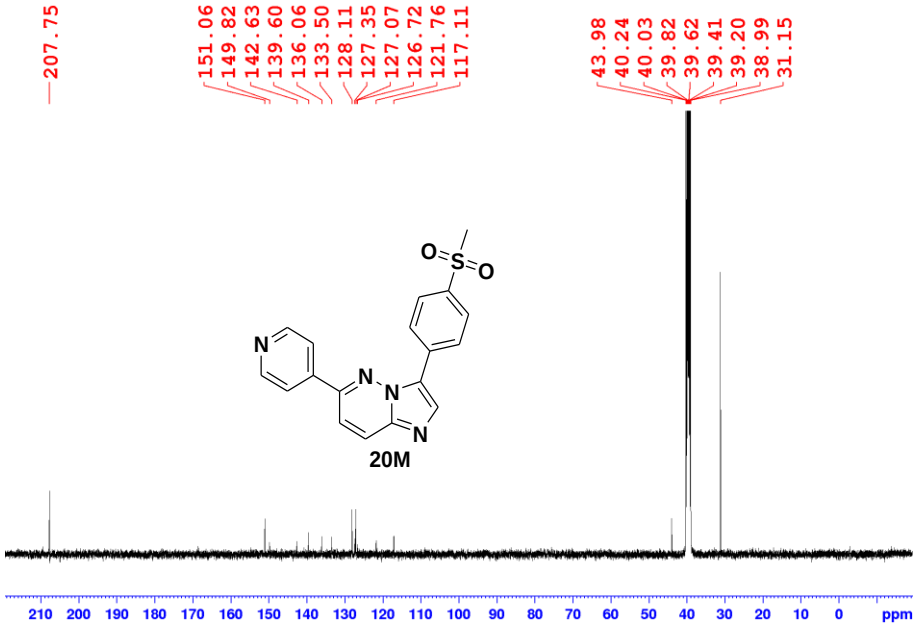

Figure 5.34: ^{13}C NMR of 3-(4-(methylsulfonyl)phenyl)-6-(pyridin-4-yl)imidazo[1,2-b]pyridazine.

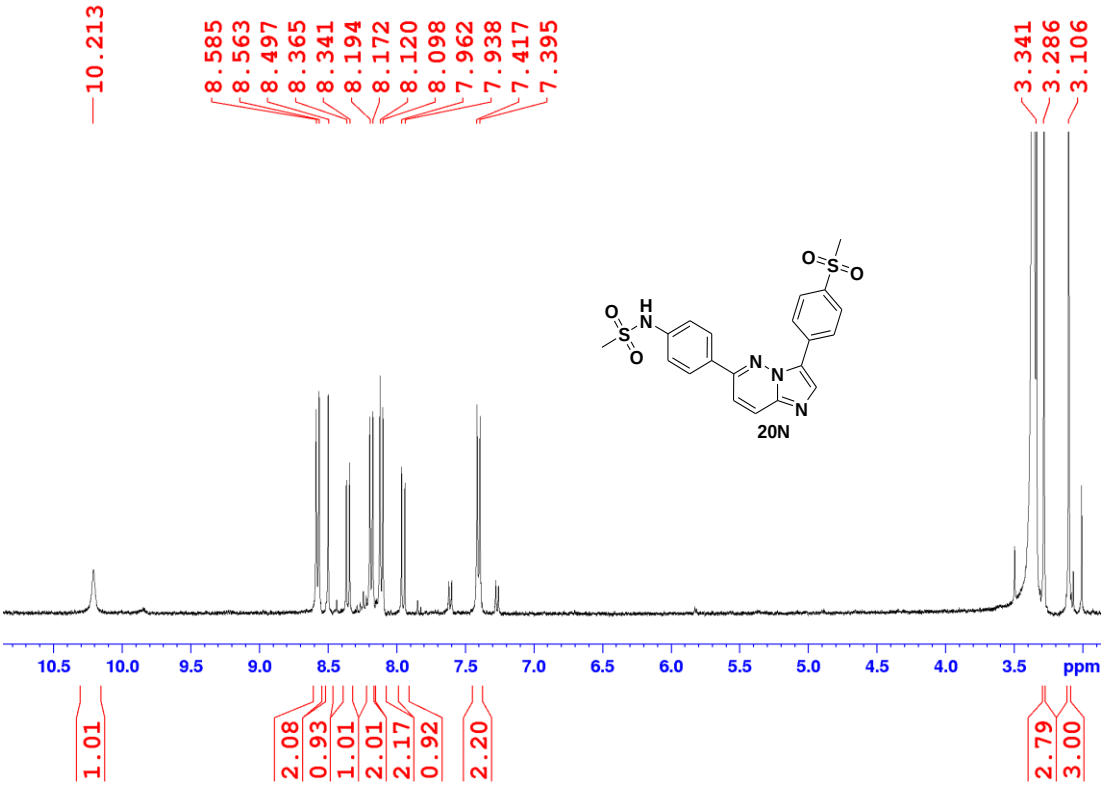

Figure 5.35: ^{1}H NMR of compound **20N**.

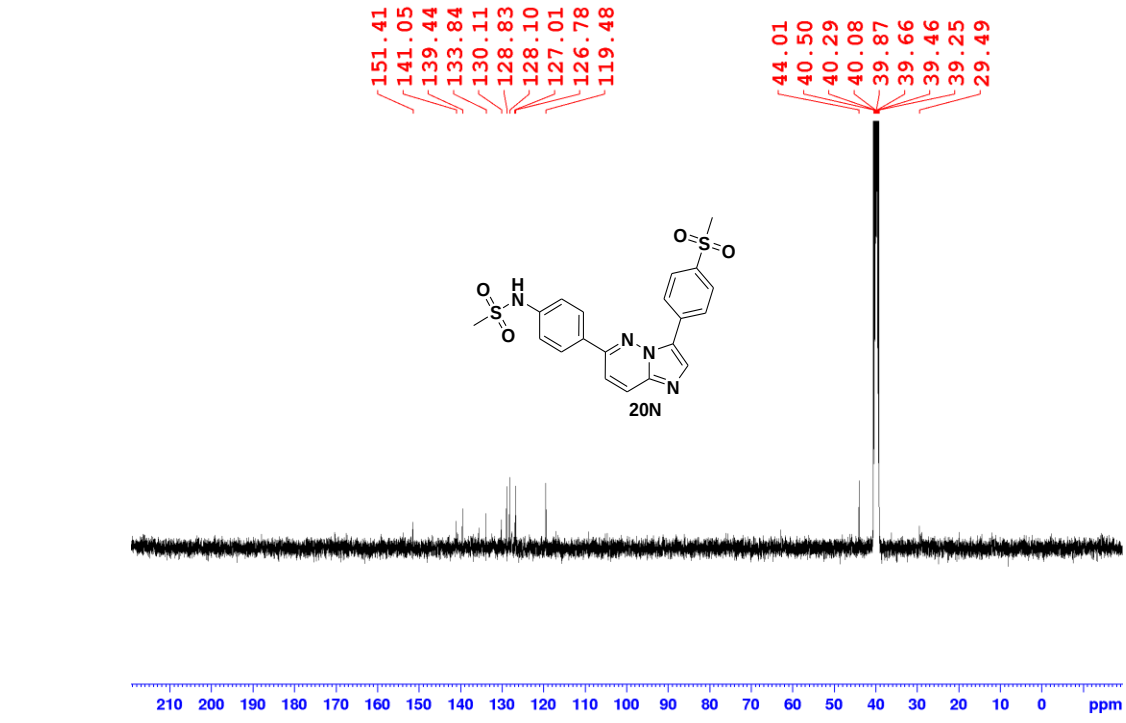

Figure 5.36: ^{13}C NMR of compound **20N**.

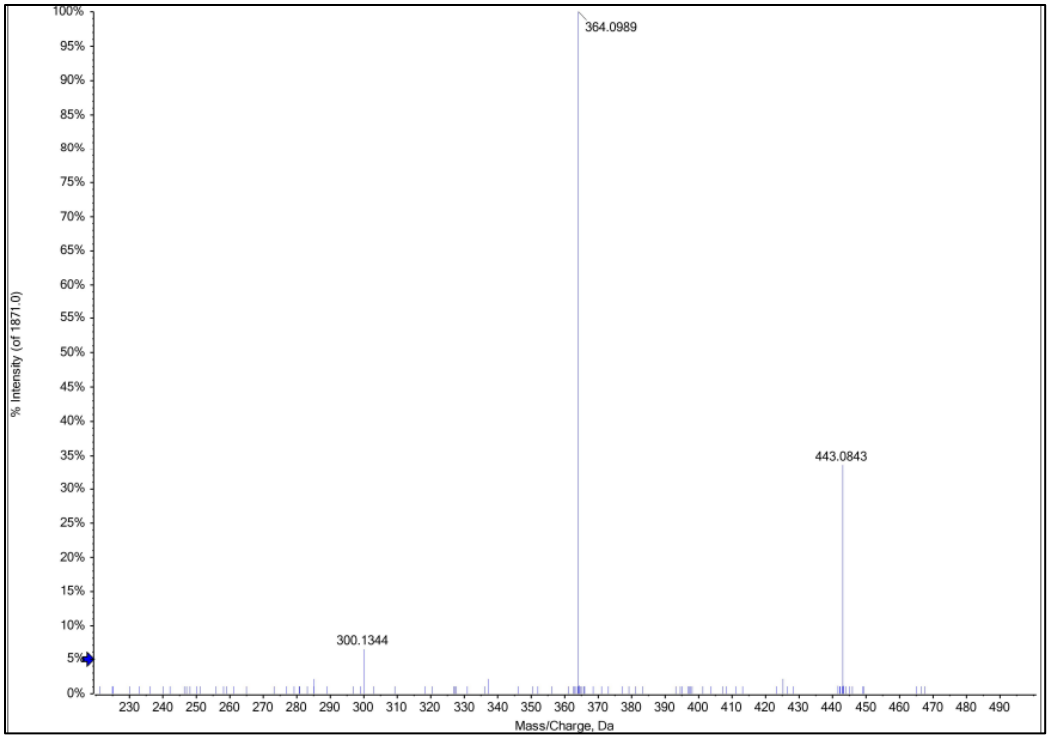

Figure 5.37: MS of compound **20N**.

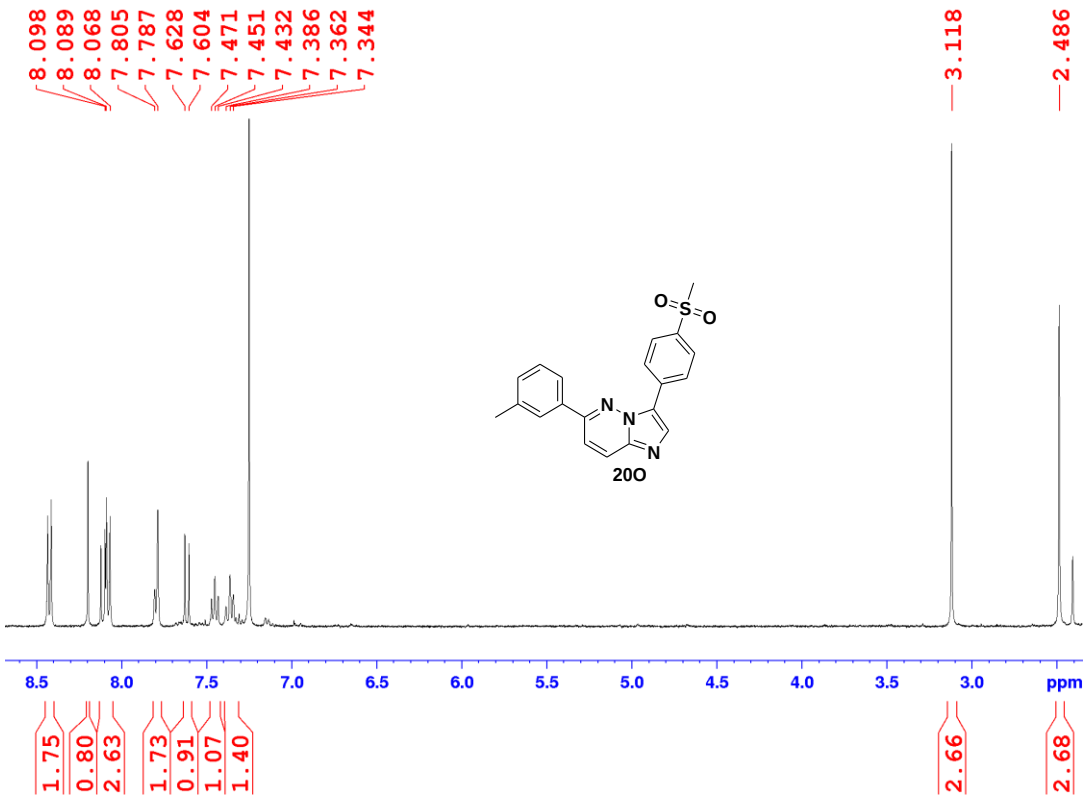

Figure 5.38: ^{1}H NMR of 3-(4-(methylsulfonyl)phenyl)-6-m-tolylimidazo[1,2-b]pyridazine.

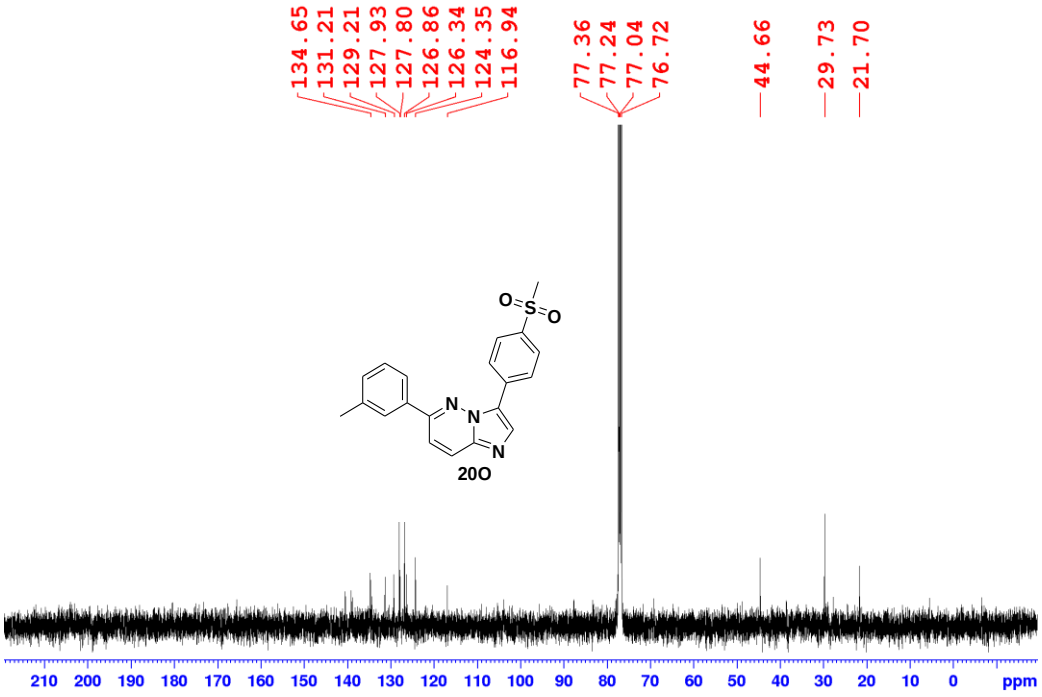

Figure 5.39: ^{13}C NMR of 3-(4-(methylsulfonyl)phenyl)-6-m-tolylimidazo[1,2-b]pyridazine.

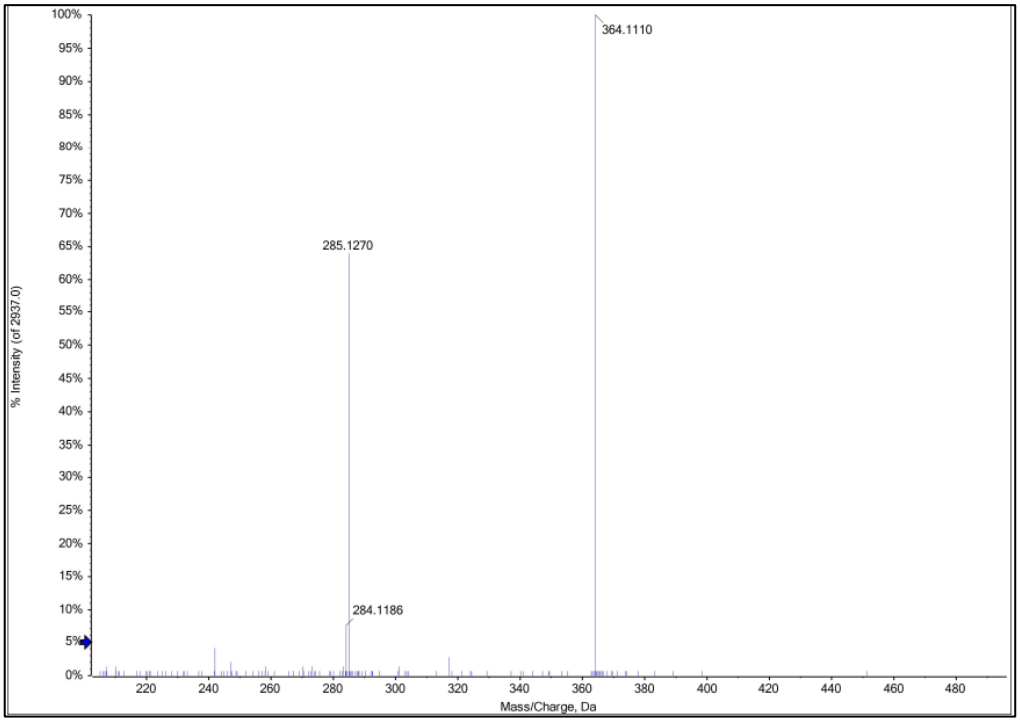

Figure 5.40: MS of 3-(4-(methylsulfonyl)phenyl)-6-m-tolylimidazo[1,2-b]pyridazine.

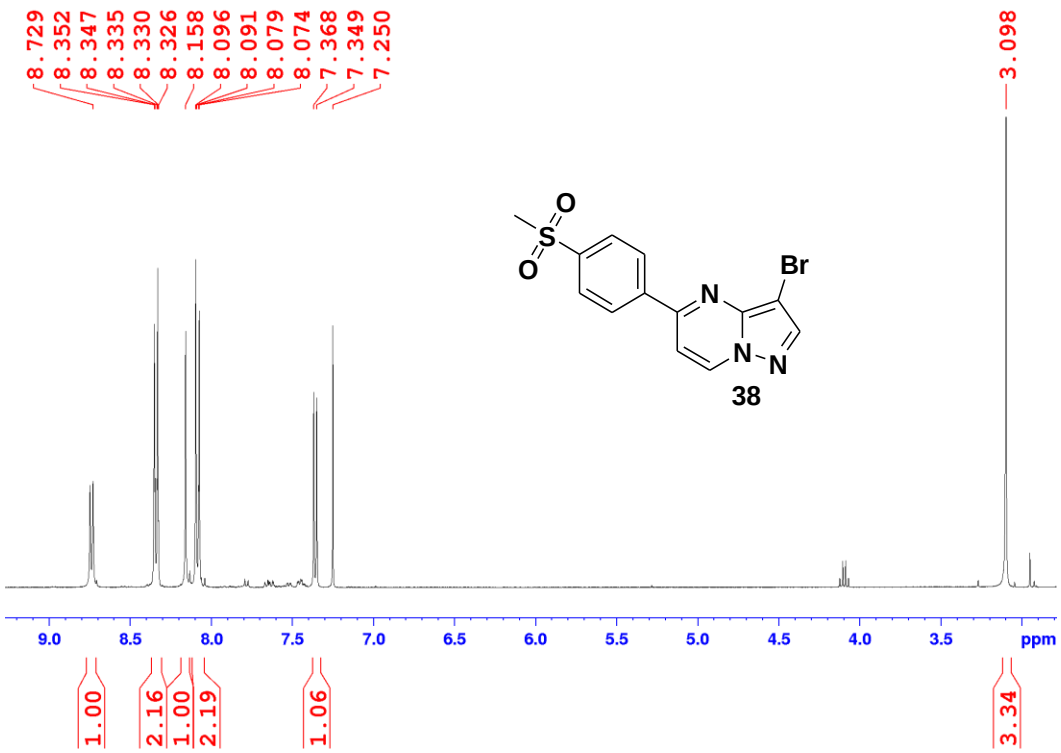

Figure 5.41: [1]H NMR of 3-bromo-5-(4-(methylsulfonyl)phenyl)pyrazolo[1,5-a]pyrimidine.

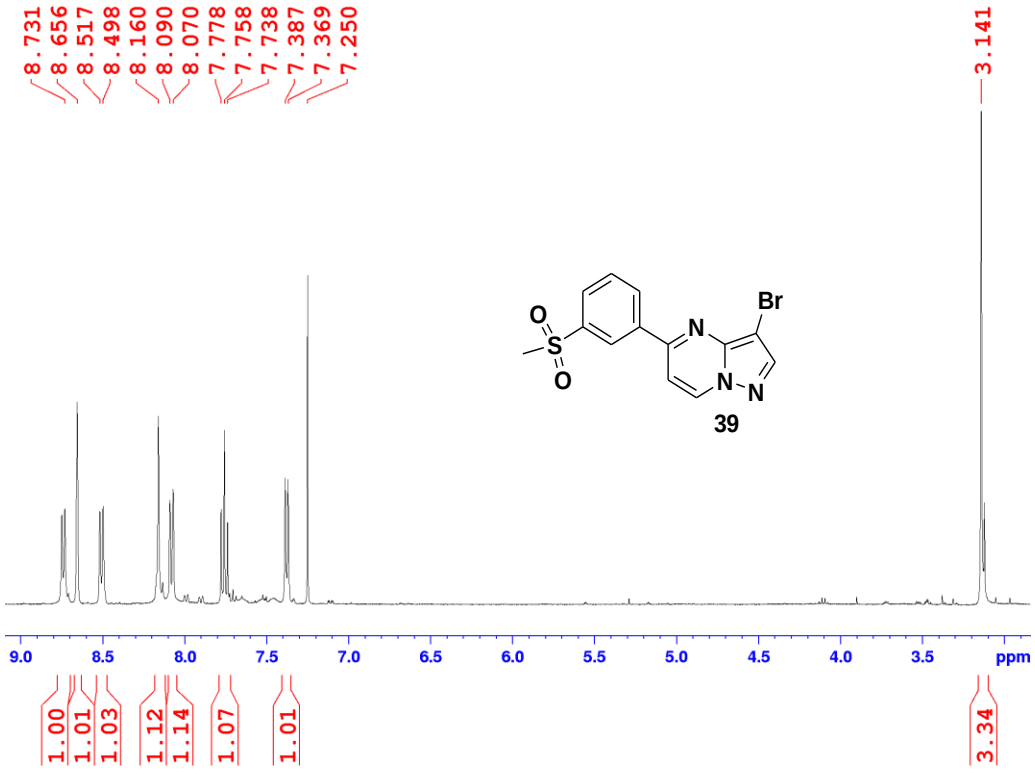

Figure 5.42: [1]H NMR of 3-bromo-5-(3-(methylsulfonyl)phenyl)pyrazolo[1,5-a]pyrimidine.

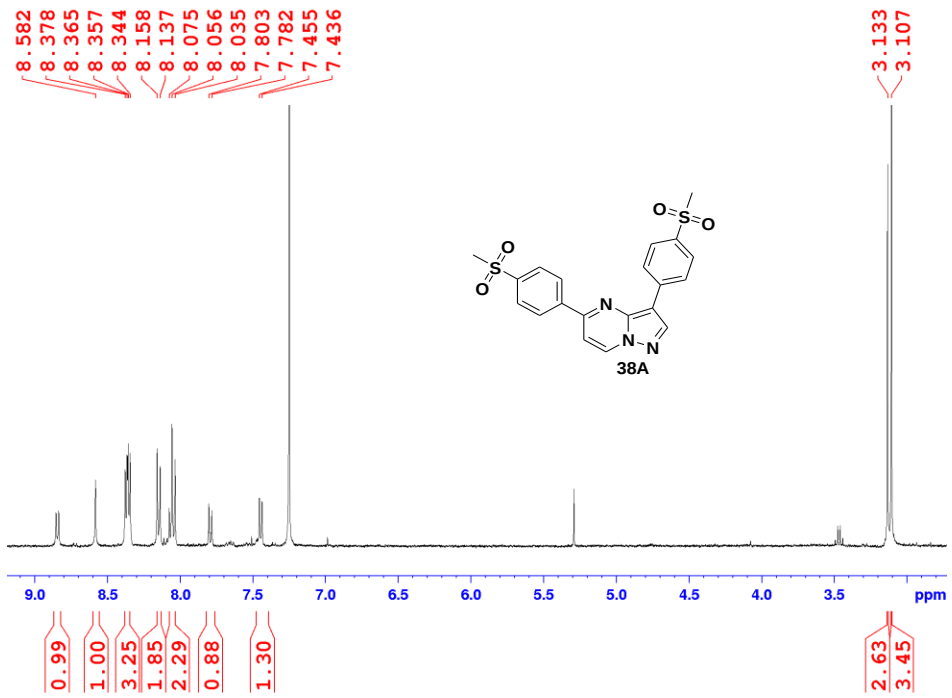

Figure 5.43: ^{1}H NMR of 3,5-bis(4-(methylsulfonyl)phenyl)pyrazolo[1,5-a]pyrimidine.

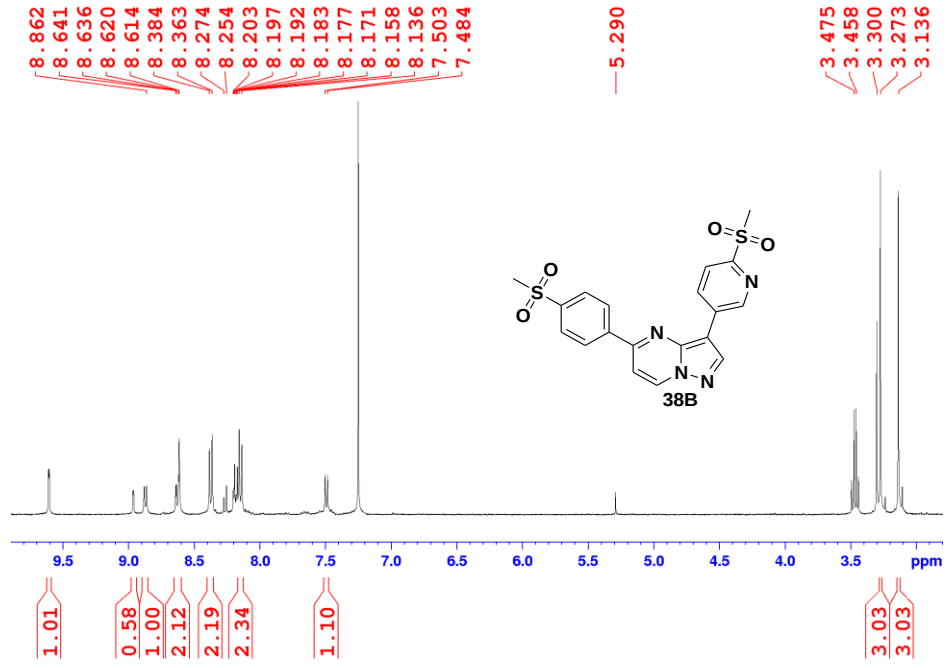

Figure 5.44: ^{1}H NMR of 5-(4-(methylsulfonyl)phenyl)-3-(6-(methylsulfonyl)pyridin-3-yl)pyrazolo[1,5-a]pyrimidine.

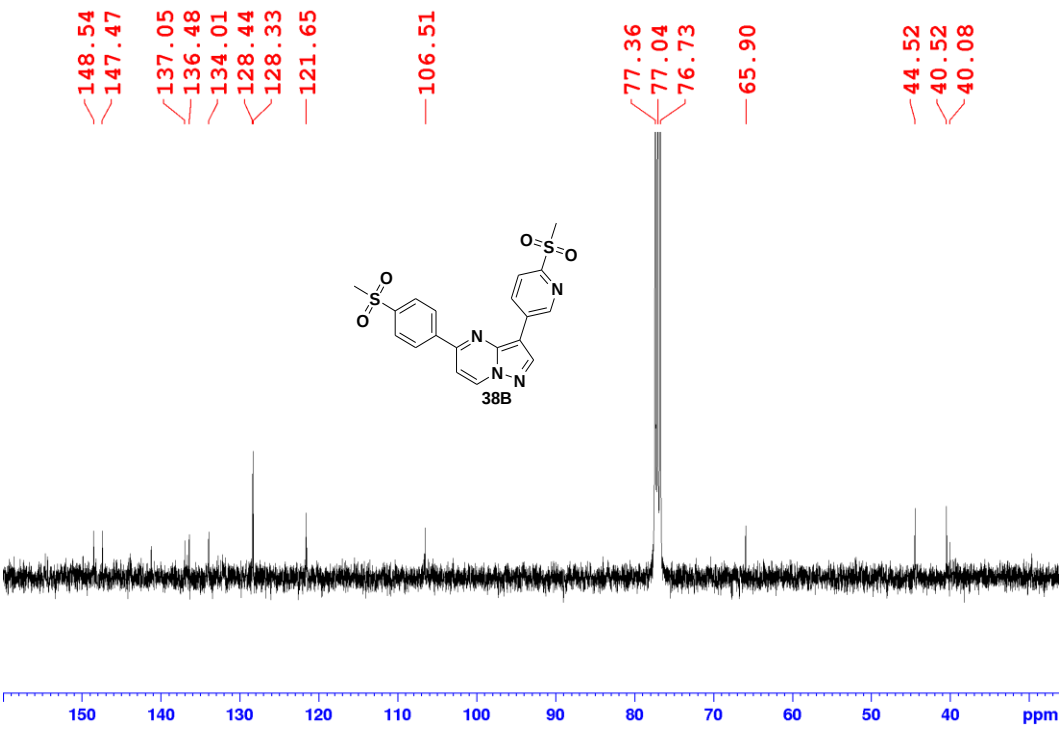

Figure 5.45: ^{13}C NMR of 5-(4-(methylsulfonyl)phenyl)-3-(6-(methylsulfonyl)pyridin-3-yl)pyrazolo[1,5-a]pyrimidine.

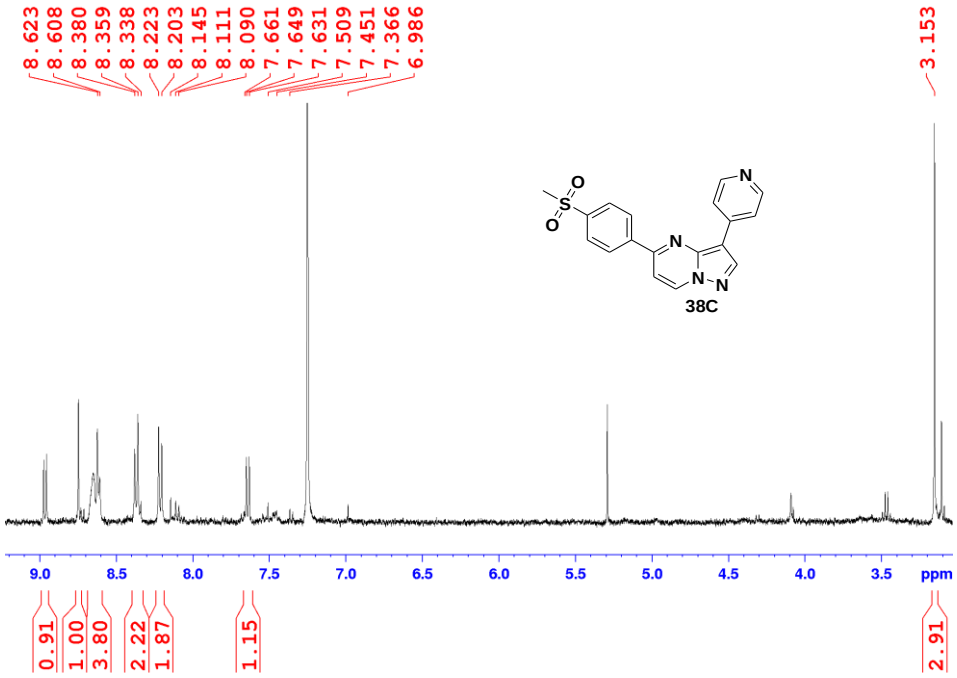

Figure 5.46: ^{1}H NMR of 5-(4-(methylsulfonyl)phenyl)-3-(pyridin-4-yl)pyrazolo[1,5-a]pyrimidine.

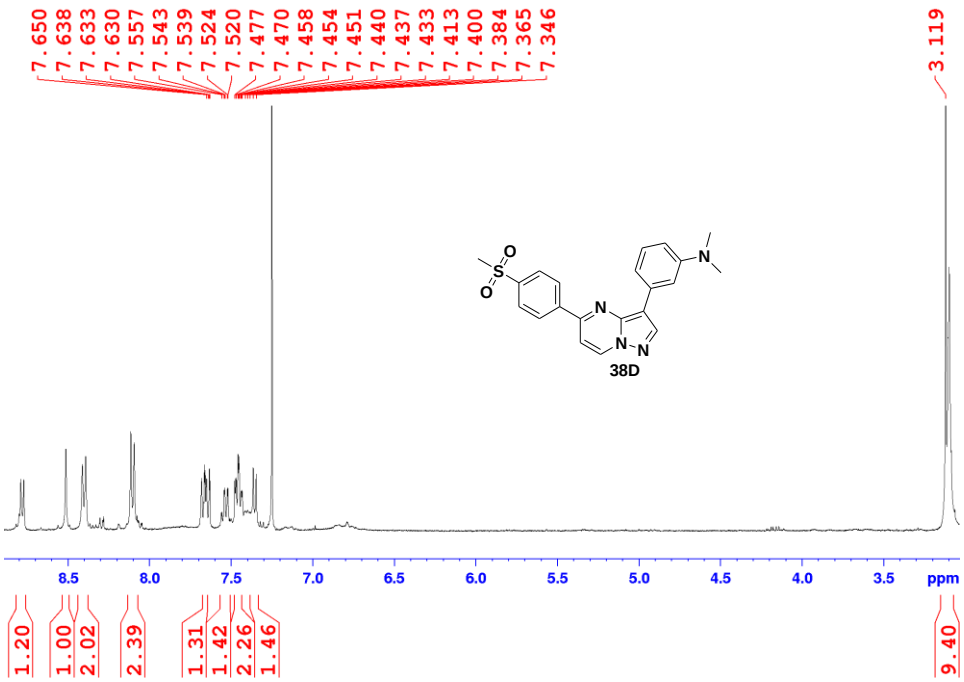

Figure 5.47: ^{1}H NMR of N,N-dimethyl-3-(5-(4-(methylsulfonyl)phenyl)pyrazolo[1,5-a]pyrimidin-3-yl)benzenamine.

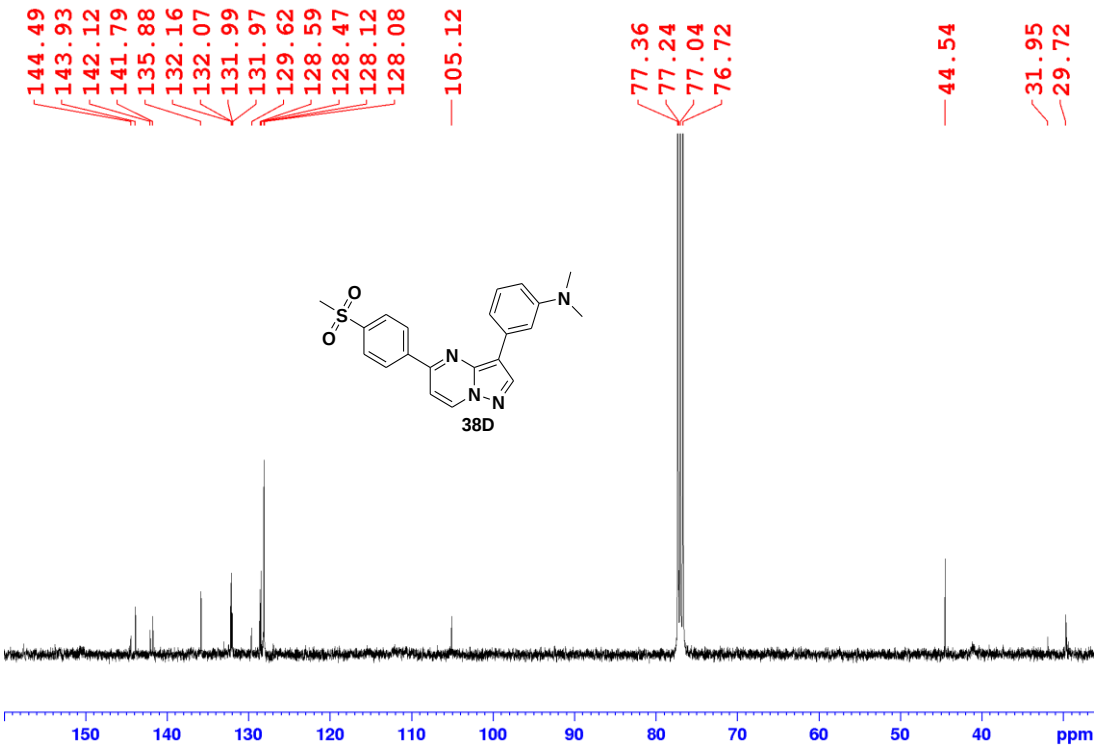

Figure 5.48: ^{13}C NMR of N,N-dimethyl-3-(5-(4-(methylsulfonyl)phenyl)pyrazolo[1,5-a]pyrimidin-3-yl)benzenamine.

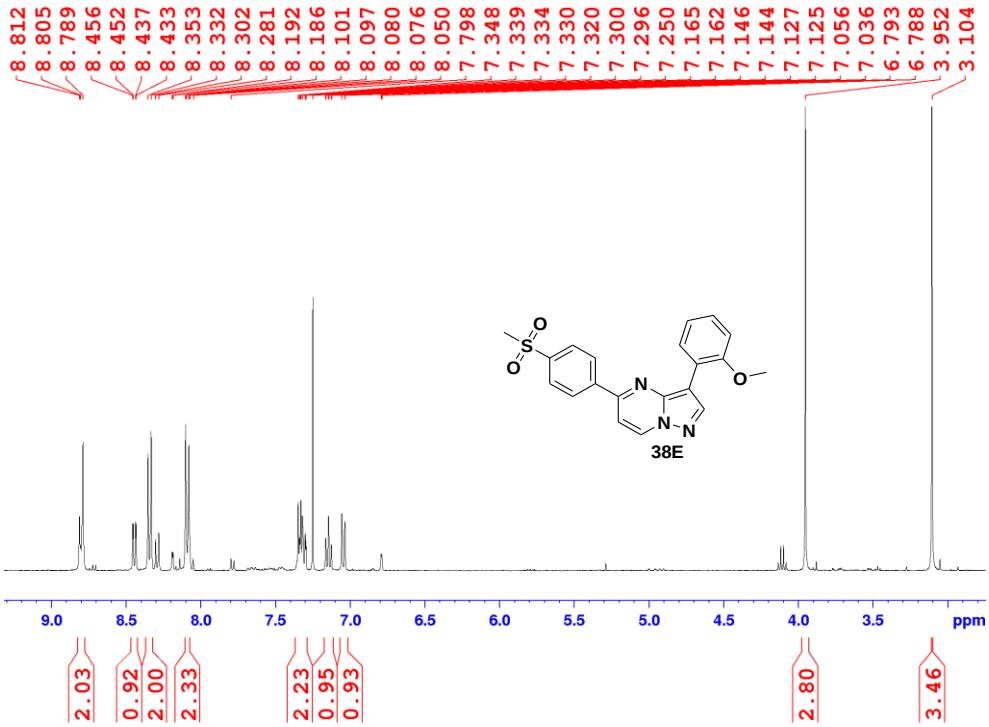

Figure 5.49: ^{1}H NMR of 3-(2-methoxyphenyl)-5-(4-(methylsulfonyl)phenyl)pyrazolo[1,5-a]pyrimidine.

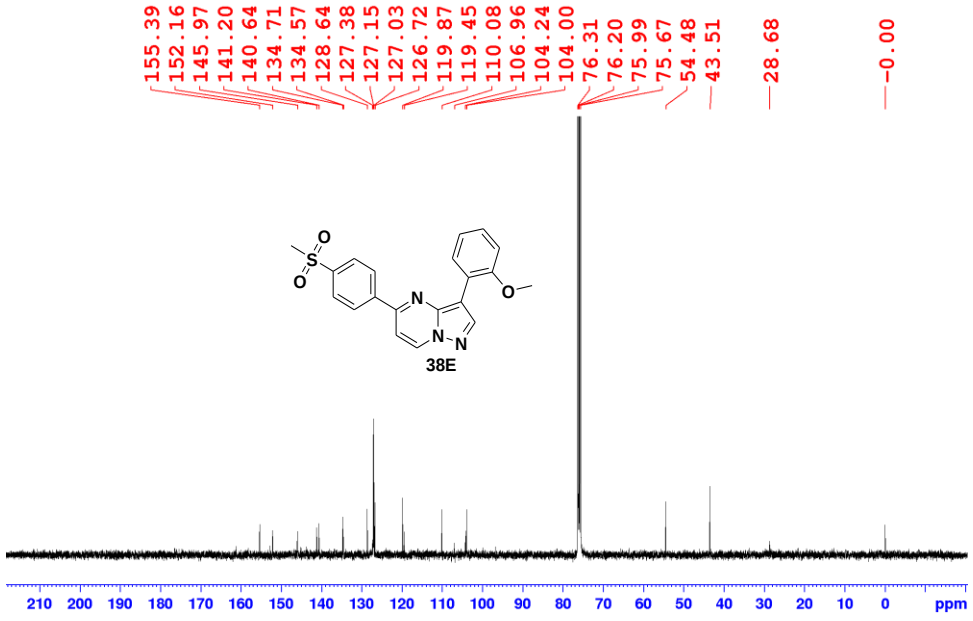

Figure 5.50: ^{13}C NMR of 3-(2-methoxyphenyl)-5-(4-(methylsulfonyl)phenyl)pyrazolo[1,5-a]pyrimidine.

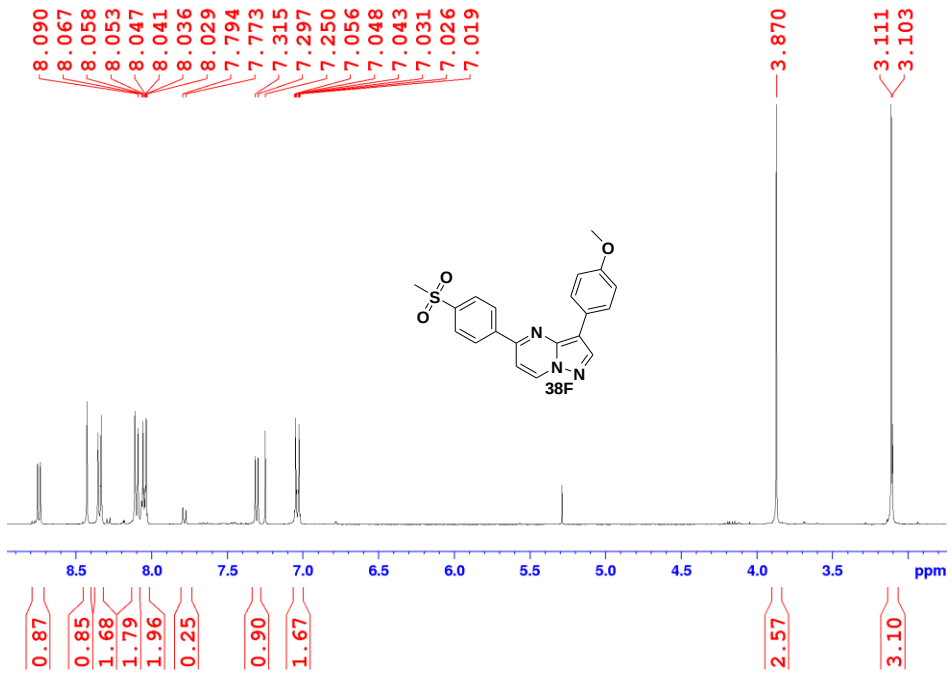

Figure 5.51: [1]H NMR of 3-(4-methoxyphenyl)-5-(4-(methylsulfonyl)phenyl)pyrazolo[1,5-a]pyrimidine.

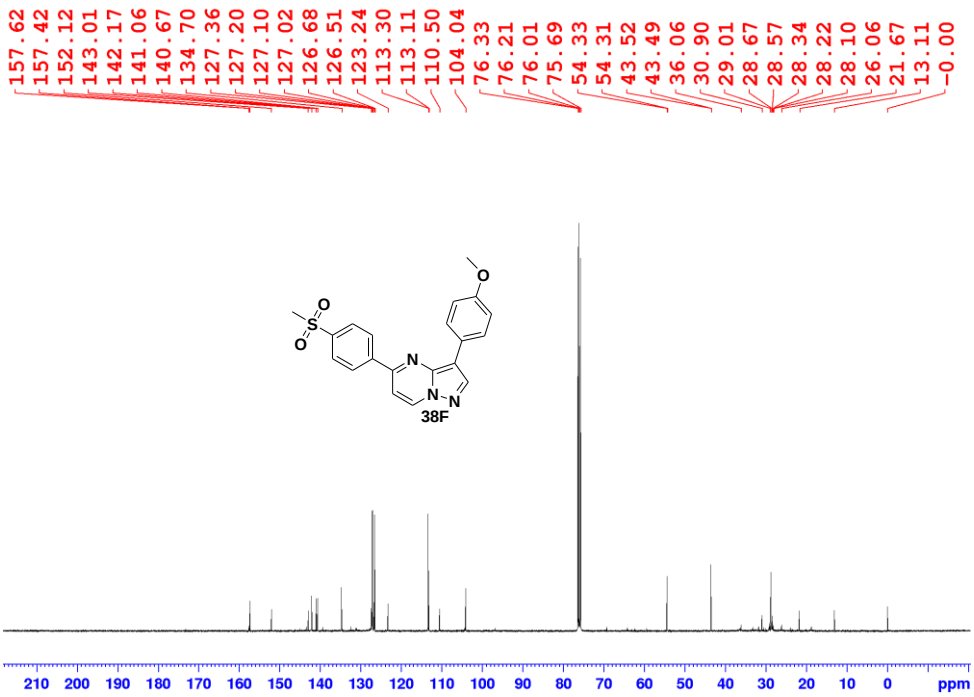

Figure 5.52: [13]C NMR of 3-(4-methoxyphenyl)-5-(4-(methylsulfonyl)phenyl)pyrazolo[1,5-a]pyrimidine.

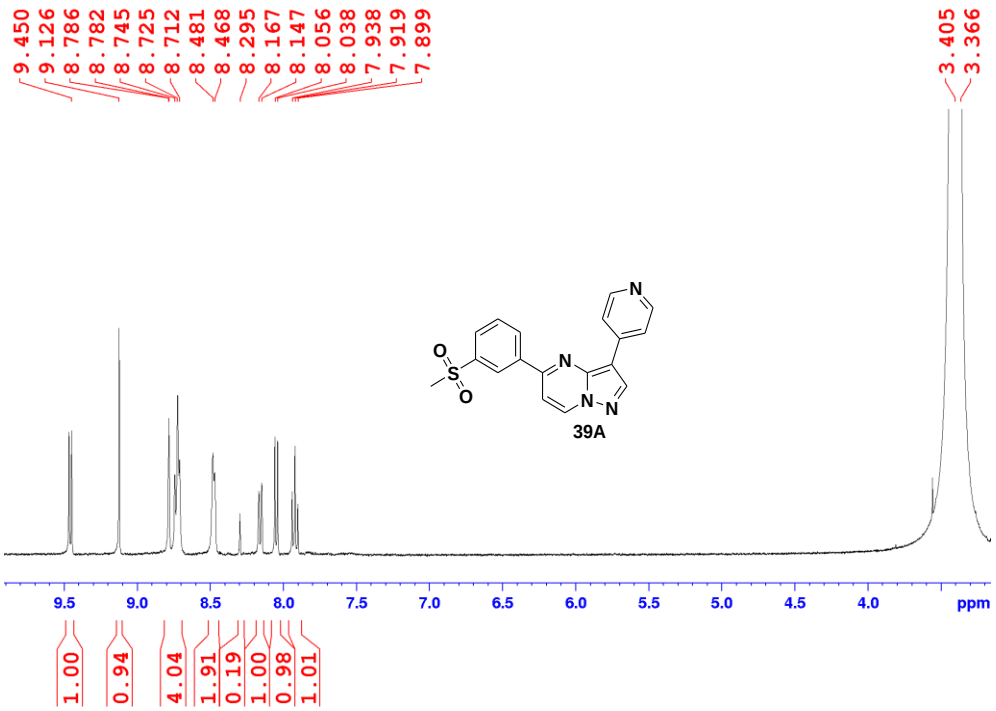

Figure 5.53: ^{1}H NMR of 5-(3-(methylsulfonyl)phenyl)-3-(pyridin-4-yl)pyrazolo[1,5-a]pyrimidine.

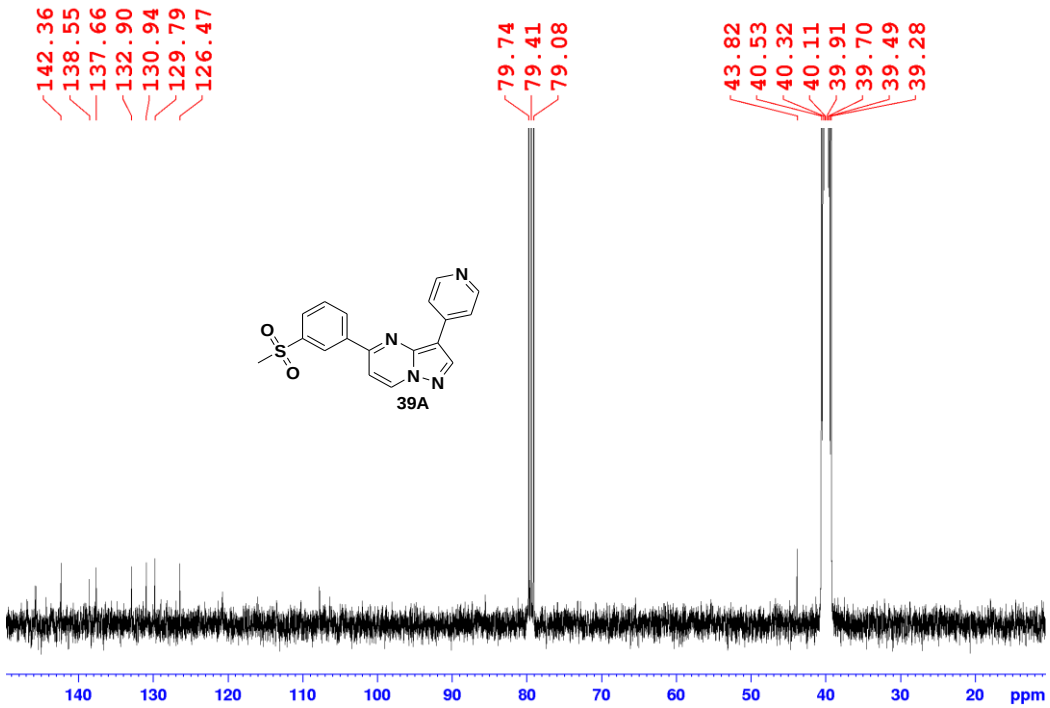

Figure 5.54: ^{1}H NMR of 5-(3-(methylsulfonyl)phenyl)-3-(pyridin-4-yl)pyrazolo[1,5-a]pyrimidine.

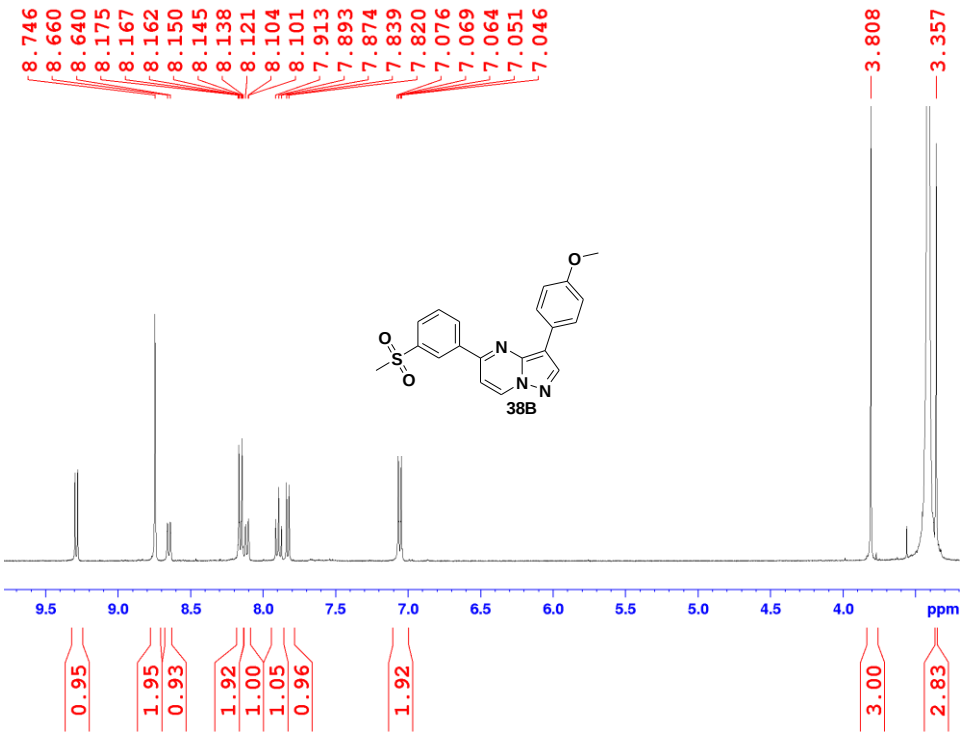

Figure 5.55: ^{1}H NMR of 3-(4-methoxyphenyl)-5-(3-(methylsulfonyl)phenyl)pyrazolo[1,5-a]pyrimidine.

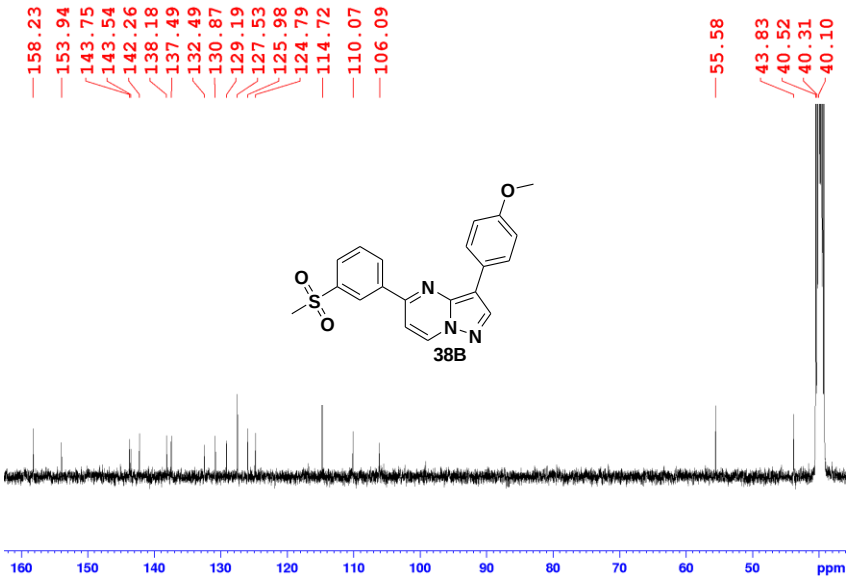

Figure 5.56: ^{13}C NMR of 3-(4-methoxyphenyl)-5-(3-(methylsulfonyl)phenyl)pyrazolo[1,5-a]pyrimidine.

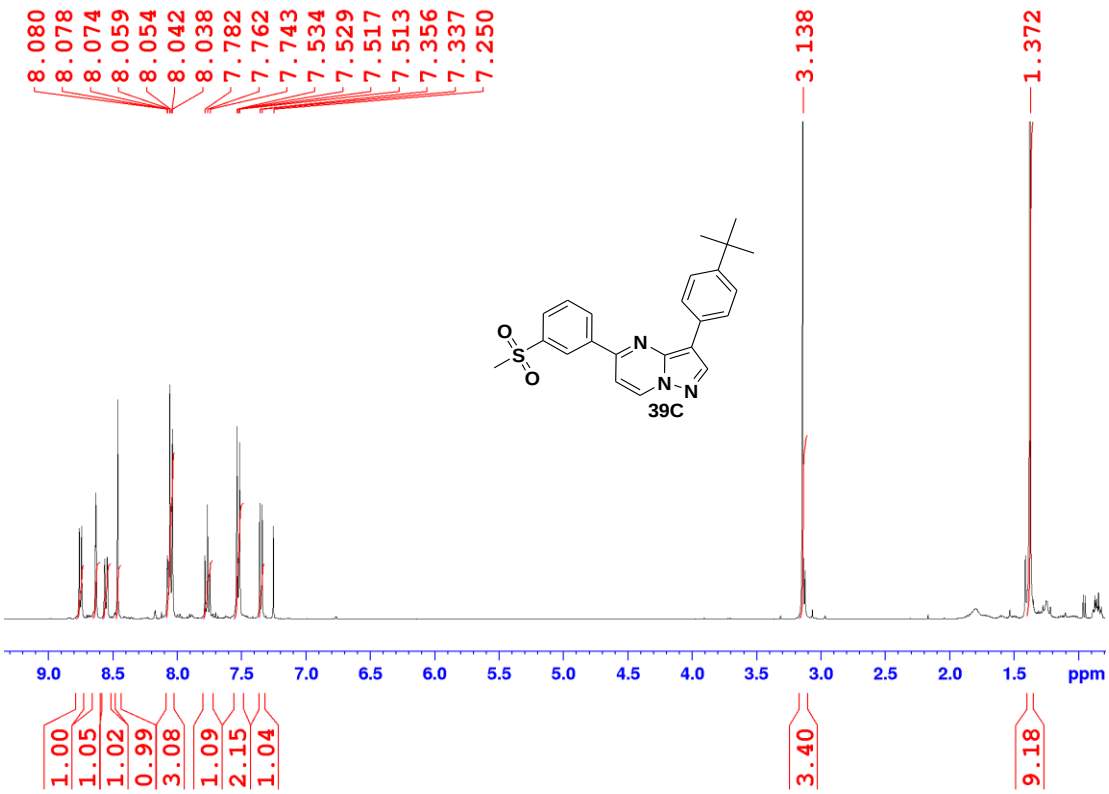

Figure 5.57: ^{1}H NMR of 3-(4-tert-butylphenyl)-5-(3-(methylsulfonyl)phenyl)pyrazolo[1,5-a]pyrimidine.

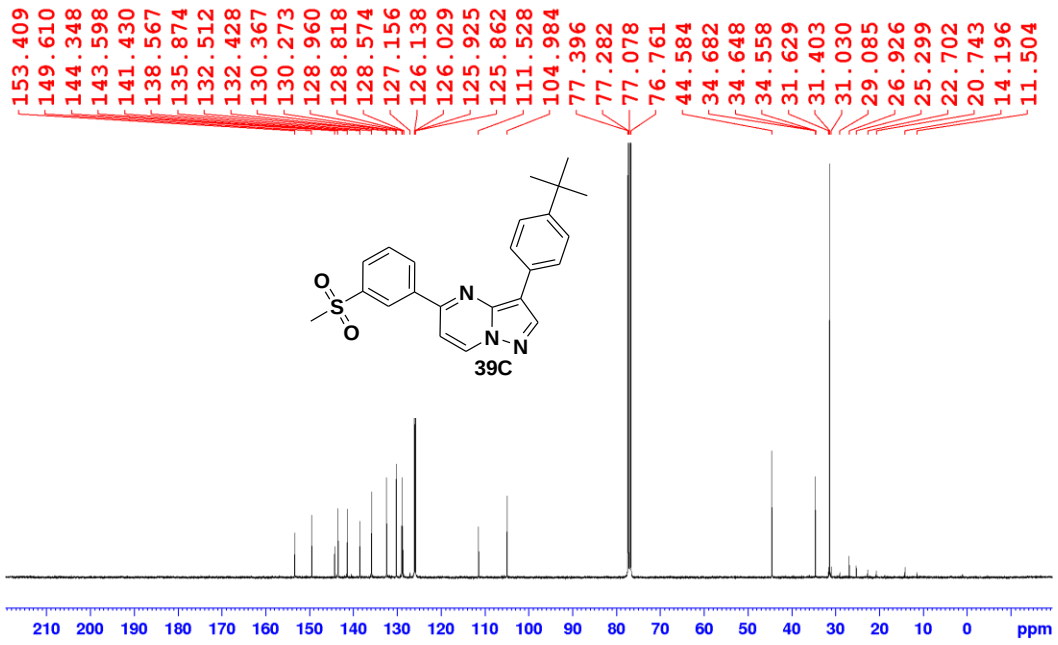

Figure 5.58: ^{13}C NMR of 3-(4-tert-butylphenyl)-5-(3-(methylsulfonyl)phenyl)pyrazolo[1,5-a]pyrimidine.

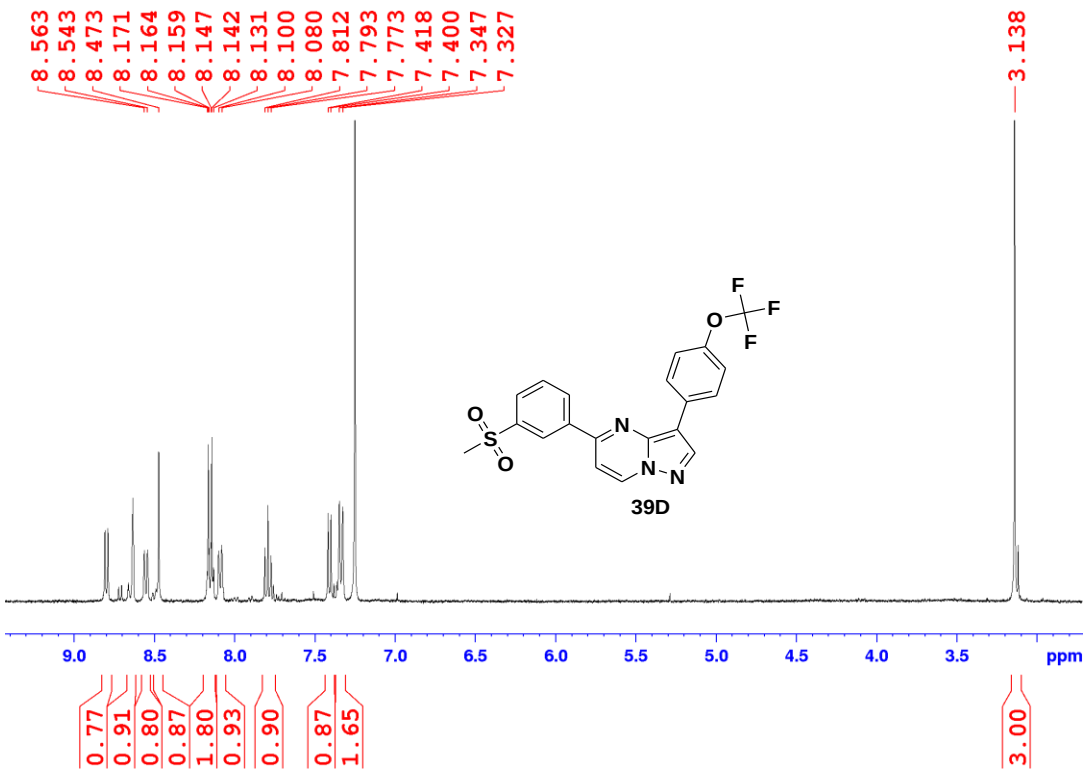

Figure 5.59: ^{1}H NMR of 5-(3-(methylsulfonyl)phenyl)-3-(4-(trifluoromethoxy)phenyl)pyrazolo[1,5-a]pyrimidine.

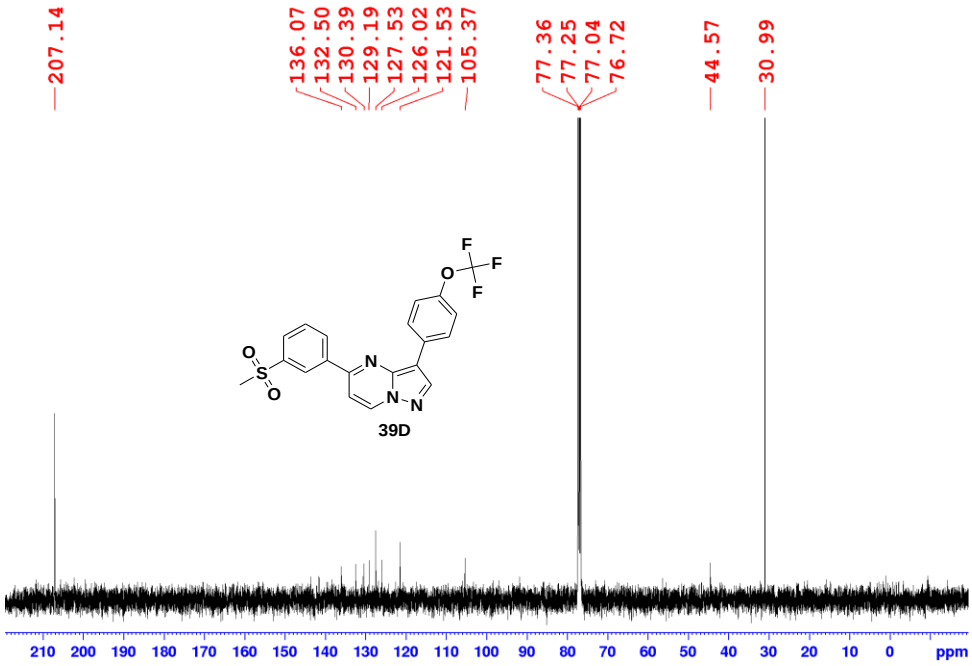

Figure 5.60: ^{1}H NMR of 5-(3-(methylsulfonyl)phenyl)-3-(4-(trifluoromethoxy)phenyl)pyrazolo[1,5-a]pyrimidine.

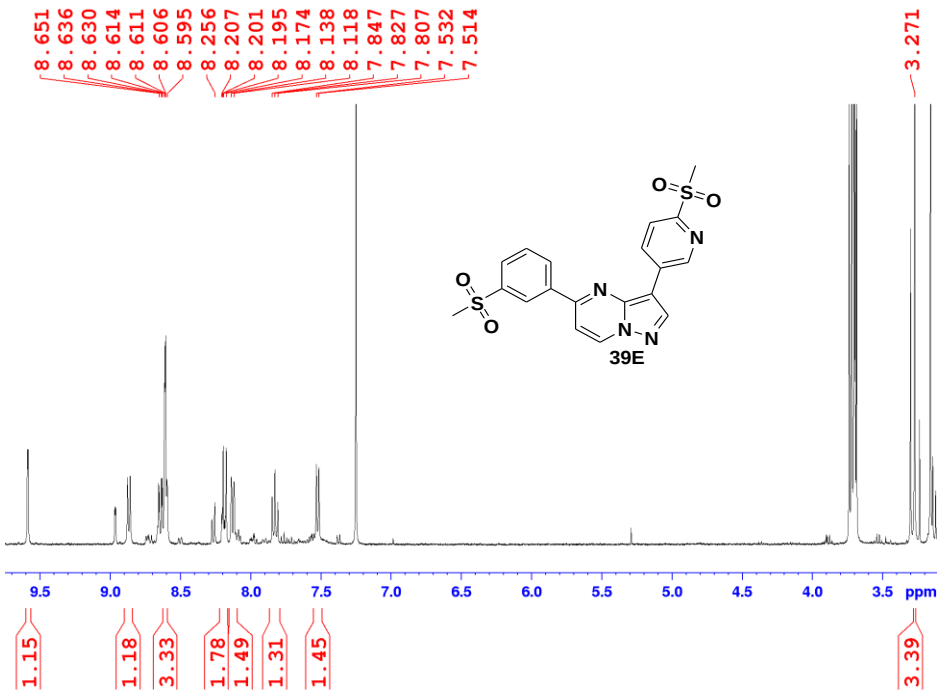

Figure 5.61: ^{1}H NMR of 5-(3-(methylsulfonyl)phenyl)-3-(6-(methylsulfonyl)pyridin-3-yl)pyrazolo[1,5-a]pyrimidine.

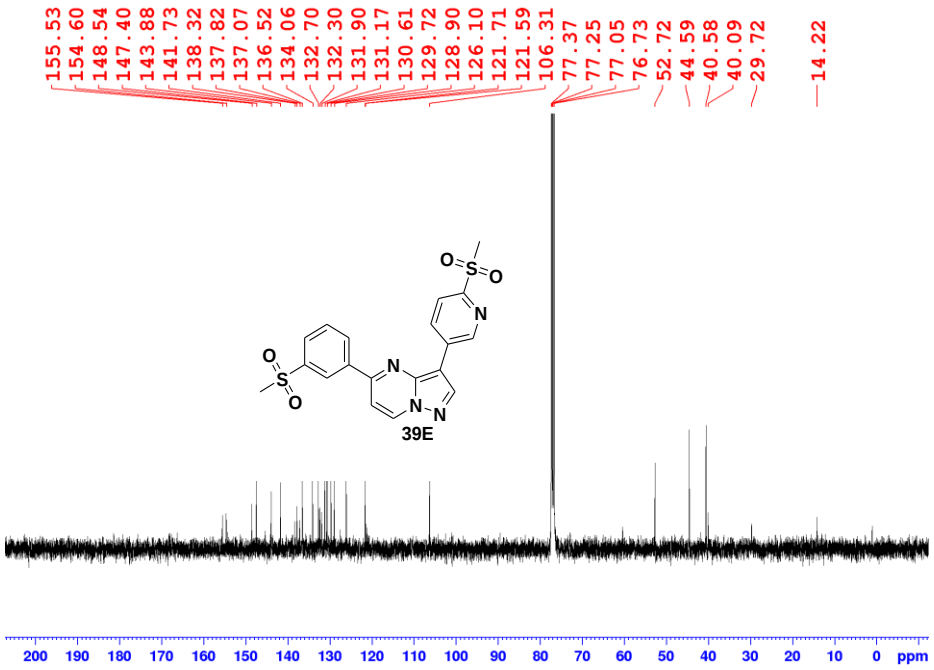

Figure 5.62: ^{13}C NMR of 5-(3-(methylsulfonyl)phenyl)-3-(6-(methylsulfonyl)pyridin-3-yl)pyrazolo[1,5-a]pyrimidine.

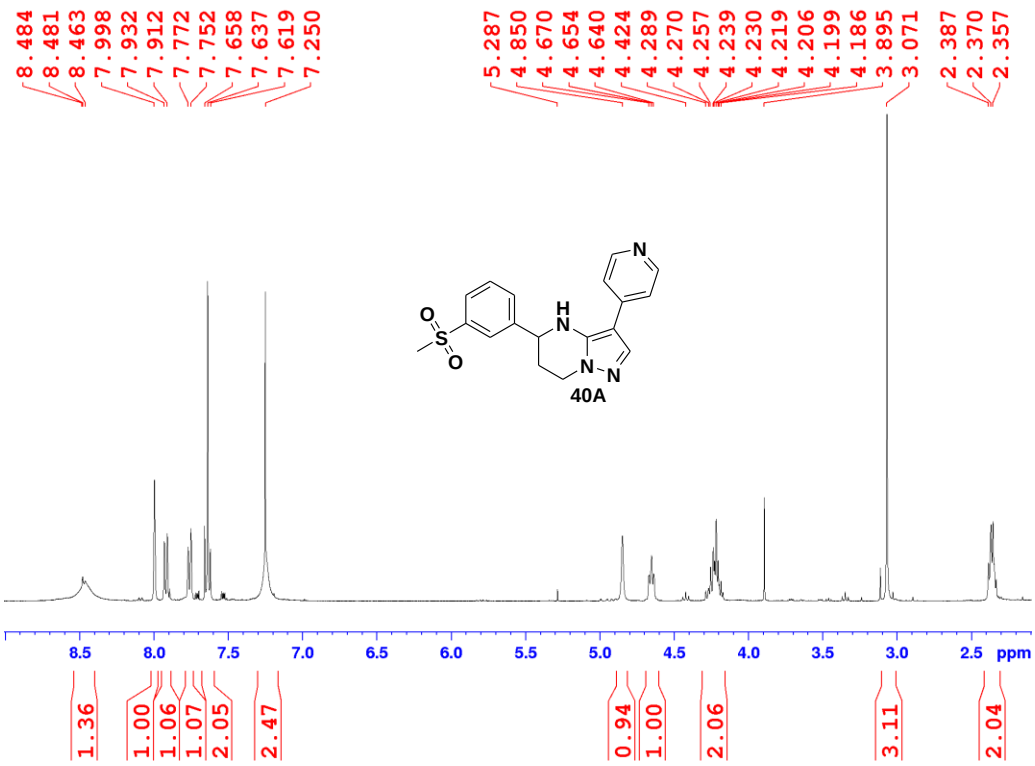

Figure 5.63: ^{1}H NMR of 5-(3-(methylsulfonyl)phenyl)-3-(pyridin-4-yl)pyrazolo[1,5-a]pyrimidine.

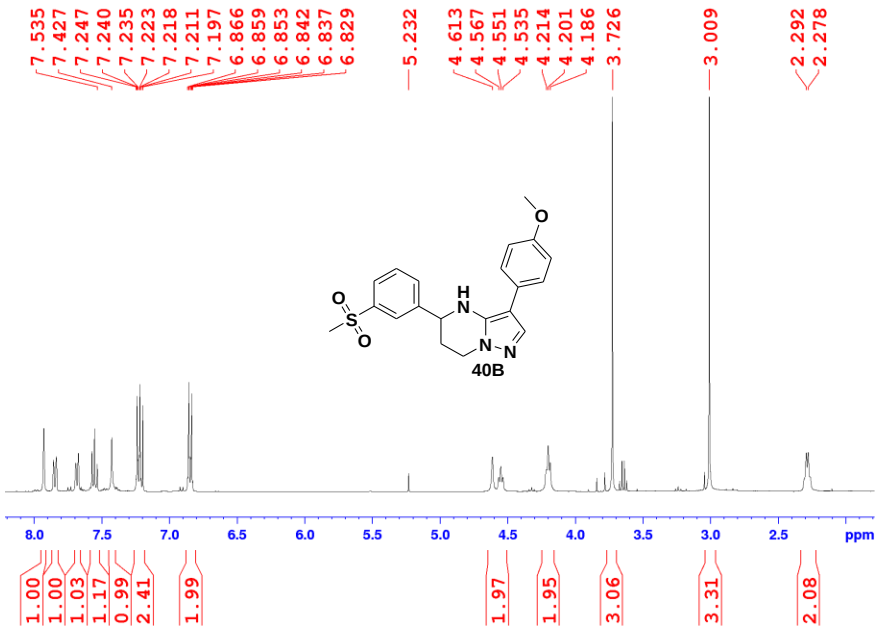

Figure 5.64: ^{1}H NMR of 4,5,6,7-tetrahydro-3-(4-methoxyphenyl)-5-(3-(methylsulfonyl) phenyl)pyrazolo[1,5-a]pyrimidine.

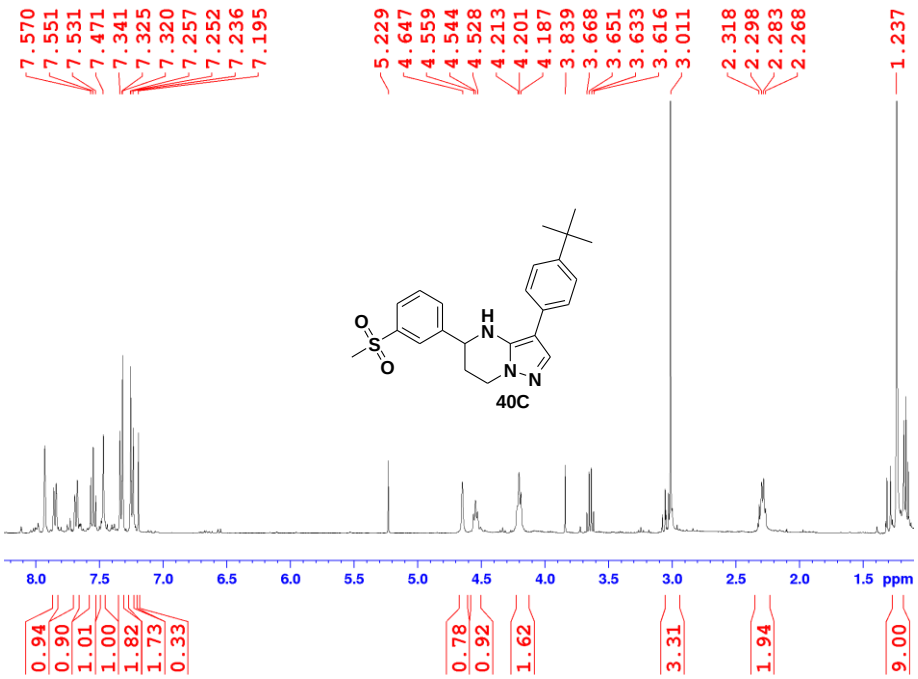

Figure 5.65: ^{1}H NMR of 3-(4-tert-butylphenyl)-4,5,6,7-tetrahydro-5-(3-(methylsulfonyl) phenyl)pyrazolo[1,5-a]pyrimidine.

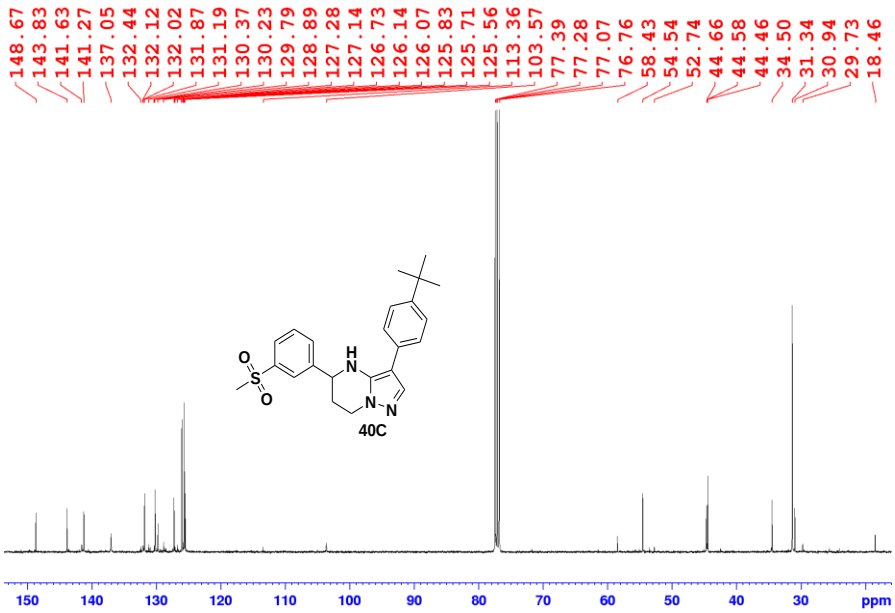

Figure 5.66: ^{13}C NMR of 3-(4-tert-butylphenyl)-4,5,6,7-tetrahydro-5-(3-(methylsulfonyl) phenyl)pyrazolo[1,5-a]pyrimidine.